Failure Analysis and Diagnosis Scheme in Distribution Systems

Bhandia, R.

DOI
10.4233/uuid:e94efb97-b56d-415f-9044-57da2cb57fb9

Publication date
2021

Document Version
Final published version

Citation (APA)
Bhandia, R. (2021). *Failure Analysis and Diagnosis Scheme in Distribution Systems*. [Dissertation (TU Delft), Delft University of Technology]. https://doi.org/10.4233/uuid:e94efb97-b56d-415f-9044-57da2cb57fb9

Failure Analysis and Diagnosis Scheme in Distribution Systems

Failure Analysis and Diagnosis Scheme in Distribution Systems

Dissertation

for the purpose of obtaining the degree of doctor
at Delft University of Technology
by the authority of the Rector Magnificus Prof.dr.ir. T.H.J.J. van der Hagen;
Chair of the Board for Doctorates
to be defended publicly on
Friday 26 February 2021 at 15:00 o'clock

by

RISHABH BHANDIA

Master of Science in Smart Grid & Buildings
Grenoble Institute of Technology, France
born in Kolkata (Calcutta), India

This dissertation has been approved by the promotors.

Composition of the doctoral committee:

Rector Magnificus	Chairperson
Prof.dr. P. Palensky	Delft University of Technology, promoter
Dr. M. Cvetkovic	Delft University of Technology, co-promoter

Independent members:

Prof.dr. S. Santoso	The University of Texas at Austin, USA
Dr.ir. M. Mousavi	Sentient Energy, USA
Ir. M. McGranaghan	Electrical Power Research Institute, USA
Prof.dr. N. Hadjsaid	Grenoble Institute of Technology, France
Prof.dr.ir P.Bauer	Delft University of Technology
Prof.dr.ir M. Zeeman	Delft University of Technology, reserve member

Keywords: Incipient failure detection, waveform analytics, intelligent grid analytics system, power system transients, situational awareness

ISBN: 978-94-6419-151-6

An electronic version of this dissertation is available at *http://repository.tudelft.nl*

Printed by Gildeprint, Enschede, the Netherlands

Dedicated to my parents for their unwavering support and love

If you want to find the secrets of this universe, think in terms of energy, frequency and vibration.

-NIKOLA TESLA

Tolerance to humor is essential for a thinking society.

-DR. A.P.J. ABDUL KALAM

It is important to keep a balance in life. Because the person who wants too much, risks losing absolutely everything. Of course, the person who wants too little from life might not get anything at all.

-ANONYMOUS

SUMMARY

Continuous and rapid technological advancements have transformed the modern day power system. Increased global interconnectivity has made reliable power supply a critical requirement. A small outage can cascade into a blackout causing great inconvenience and significant monetary damage. These concerns highlight the need of an additional layer of proactive approach in conventional protection schemes. The focus of such an approach would be to shift from *reacting* to a failure to *anticipating* a failure. Anticipating a failure gives time to better prepare and mitigate the failure by efficient allocation of resources in order to limit the negative consequences. Starting from the inception of the event causing the failure to the final occurrence of the failure, the time-period in between is termed as the pre-failure period where the signatures of the incipient failure can be observed. The availability of high-resolution devices has improved monitoring of grid operations during this pre-failure period. Improved monitoring enhances situational awareness leading to easier detection of incipient failure signatures. Research conducted in this field has led to development of few failure anticipation techniques but the application potential of some are restricted to specific equipment or phenomena while that of others are restricted by resource requirements. There is a need of addressing the research gap of a comprehensive failure anticipation technique that fulfills three major criteria of low computational burden, wide applicability in different scenarios and installation compatibility with existing grid monitoring devices for economical implementation. The research conducted in this thesis aims to address this research gap by developing a comprehensive failure anticipation technology titled *Failure Anticipation and Diagnosis Scheme* (FADS) for AC distribution systems.

FADS implementation broadly comprises of three functionalities. The *first functionality* is concerned with quick and accurate identification of incipient failure signatures. Almost all failure anticipation techniques rely on cross-referencing historical databases or identifying specific patterns in order to detect incipient failure signatures. However, incipient failure signatures seldom manifest in same patterns. Hence, FADS relies on the fundamental aspect that pure AC sinusoids are complex exponentials. Incipient failure signatures would invariably violate certain properties of complex exponentials and manifest as waveform distortions, which would be leveraged by FADS to detect the signatures. The *second functionality* involves the data processing of the distortion data. Several novel parameters are introduced in the second functionality that helps in processing the data obtained from the first functionality. The use of novel parameters helps in accurate assessment of the stress experienced by the grid operations due to the event causing distortions. Such an assessment help FADS to be robust to false positives or false negatives. Finally, the *third functionality* involves interpretation of the information obtained through data processing. The interpretation provides metrics to rank the severity of the damage the event can inflict on grid operations along with specific inputs on the event location. This interpreted and refined data helps to provide means to the Distribution System Operator (DSO) for informed decision-making and time-efficient resource allocation for failure mitigation purposes. The different FADS functionalities

work in unison to detect incipient failure signatures and extract valuable information, which can be then used to plan mitigation strategies. The different functionalities of FADS are designed to be installed in a manner such that the incremental costs of widespread FADS implementation are minimal.

The evaluation of FADS in this thesis is conducted through a series of stringent and realistic test cases. The test cases are simulated on the standard IEEE-13 and IEEE-34 node test feeders. The first set of simulation studies focusses on detecting High Impedance Faults (HIF) as conventional protection schemes mostly fail to detect it. The test cases comprise of several novel stringent scenarios to evaluate the capability of FADS to accurately distinguish and detect HIF events among multiple switching events and normal grid actions at different sections of the grid. The second set of simulation studies involves recreating transient behavior generated due to real life incipient equipment failure conditions in laboratory based simulations. Simulations are used to evaluate the ability of FADS to detect and assess the incipient failure before the equipment breakdown occurs. The next set of studies is focused on analyzing how the FADS performance in previous simulation studies could be translated to assess the improvement in major reliability indices, mainly System Average Interruption Duration Index (SAIDI). Improvement in reliability indices are a major area of concern for utilities and the results obtained from FADS implementation are further quantified to provide a range of possible improvement in SAIDI value in percentage terms. Finally, the proposed benefit of FADS is illustrated through implementation on real field data provided by the Dutch DSO, Stedin B.V. In the course of FADS implementation, few shortcomings were noticed and possibilities of further improvements were identified. The final chapters of this thesis discuss the shortcomings and recommend improvements for future research studies. The functionalities of FADS are flexible and mostly user-dependent and can be systematically improved over time to make FADS a global standard for industrial and research applications for failure anticipation in AC distribution systems.

SAMENVATTING

Voortdurende technologische ontwikkelingen zorgen voor een transformatie van het huidige energiesysteem. Door het toenemende verbruik van elektriciteit in al onze dagelijkse activiteiten en processen, is een betrouwbare stroomvoorziening een cruciale vereiste geworden. Een kleine storing in het elektriciteitssysteem kan uiteindelijk resulteren in een langdurige stroomonderbreking, wat veel ongemak en aanzienlijke financiële schade met zich meebrengt. Dit onderstreept de noodzaak om in de conventionele beveiligingssystemen een additionele ontwerp laag gebaseerd op een proactieve benadering toe te passen. In een dergelijke benadering verschuift de focus van de huidige beveiligingsschema's van reactief (reageren op een storing) naar proactief (anticiperen op een storing). Het voordeel van een proactieve benadering is dat het anticiperen op een storing tijd geeft om deze beter voor te bereiden en om de negatieve gevolgen van de storing te minimaliseren door een efficiënte toewijzing van middelen. In de proactieve benadering is de pre-failure periode cruciaal. Deze wordt gedefinieerd als het tijdsinterval vanaf het begin van de gebeurtenis die een storing veroorzaakt tot het daadwerkelijk optreden van een storing. In deze pre-failure periode kunnen karakteristieken van de beginnende storing worden waargenomen. De beschikbaarheid van geavanceerde apparaten heeft de monitoring van deze karakteristieken in de pre-failure periode aanzienlijke verbeterd. Hoe eerder de karakteristieken kunnen worden waargenomen, des te meer tijd er beschikbaar is om de gevolgen van een storing te minimaliseren. Onderzoek op dit gebied heeft geleid tot de ontwikkeling van enkele technieken om storingen te anticiperen. Een grote nadeel voor de toepassing van deze technieken is dat enkele van deze technieken beperkt zijn tot specifieke apparatuur of verschijnselen, terwijl die van andere beperkt zijn door de vereiste middelen. Als zodanig is er behoefte aan het ontwikkelen van een nieuwe techniek voor storingsanticipatie die voldoet aan drie belangrijke criteria, namelijk (i) lage rekenlast, (ii) brede toepasbaarheid in verschillende scenario's en (iii) compatibiliteit met bestaande en reeds geïnstalleerde monitoringsapparatuur. Het hoofddoel van dit proefschrift voorziet in deze behoefte door de ontwikkeling van een technologie voor het anticiperen op storingen in AC-distributiesystemen, genaamd Failure Anticipation and Diagnosis Scheme (FADS).

De implementatie van FADS omvat drie functionaliteiten. De eerste functionaliteit betreft de snelle en nauwkeurige identificatie van de karakteristieken van beginnende storingen. Vrijwel alle technieken voor het anticiperen op storingen maken gebruik van historische databases of specifieke patronen om de karakteristieken van beginnende storingen te detecteren. Echter, karakteristieken van beginnende storingen manifesteren zich zelden in dezelfde patronen. Daarom identificeert de ontwikkelde FADS de karakteristieken middels een ander concept: vanuit een fundamenteel oogpunt zijn pure AC-sinusoïden complexe exponentiële signalen. De karakteristieken van beginnende storingen zullen bepaalde eigenschappen van deze complexe exponentiële signalen schenden, welke zich manifesteren als vervormingen in de pure, complexe signalen. Deze vervormingen worden vervolgens door de FADS gebruikt om de karakteristieken van de beginnende storing te detecteren.

De tweede functionaliteit betreft de verwerking van de data welke zijn verkregen uit de eerste functionaliteit. Hiervoor worden verschillende nieuwe parameters geïntroduceerd, welke helpen bij een nauwkeurige beoordeling van de gebeurtenis die eventueel leidt tot een storing. Een dergelijke beoordeling maakt de ontwikkelde FADS robuust tegen foutpositieven en foutnegatieven.

De derde en laatste functionaliteit betreft de interpretatie van de informatie die is verkregen door de verwerking van de data. Deze functionaliteit geeft (i) indices die de ernst van de schade die een storing kan toebrengen kwantificeert en (ii) specifieke input met betrekking tot de locatie van de storing. Deze informatie assisteert de bedrijfsvoerder in het besluitvormingsproces voor het efficiënt toewijzen van middelen ten einde de negatieve gevolgen van storingen te minimaliseren.

De drie FADS-functionaliteiten werken samen om de karakteristieken van beginnende storingen te detecteren en nuttige informatie af te leiden, die vervolgens kan worden gebruikt om schadebeperkende maatregelen te plannen. Het ontwerp van de verschillende functionaliteiten van FADS faciliteert dat de incrementele kosten voor een wijd verspreide FADS-implementatie minimaal zijn.

De evaluatie van FADS in dit proefschrift wordt uitgevoerd aan de hand van simulaties van een reeks van realistische testcases. De testcases worden gesimuleerd op de bestaande IEEE-13 en IEEE-34 netwerkmodellen. De eerste reeks simulaties is gericht op het detecteren van High Impedance Faults (HIF), aangezien conventionele beveiligingsschema's deze meestal niet detecteren. De testcases omvatten verschillende scenario's om het vermogen van FADS te evalueren om nauwkeurig HIF-gebeurtenissen te onderscheiden en te detecteren tussen meerdere schakel- en normale gebeurtenissen in verschillende secties van het net. In de tweede reeks simulaties zijn relevante historische gebeurtenissen nagebootst in simulaties. Deze simulaties worden gebruikt om het vermogen van FADS (om beginnende storingen te detecteren en te beoordelen) te evalueren op basis van daadwerkelijk opgetreden storingen in het elektriciteitsnetwerk. Verbetering in de betrouwbaarheid van de elektriciteitsvoorziening is een belangrijk aandachtspunt voor nutsbedrijven. De volgende reeks onderzoeken is daarom gericht op het analyseren van hoe de FADS-prestaties in de hierboven genoemde simulaties kan worden vertaald naar een verbetering in deze betrouwbaarheid. In dit onderzoek wordt de System Average Interruption Duration Index gebruikt om de betrouwbaarheid te kwantificeren. Ten slotte worden de voordelen van de ontwikkelde FADS geïllustreerd door het gebruik van daadwerkelijke gebeurtenissen, verkregen van de Nederlandse distributie netbeheerder Stedin B.V.

De functionaliteiten van FADS zijn flexibel en grotendeels gebruikersafhankelijk en kunnen in de loop van de tijd systematisch worden verbeterd om van FADS een wereldwijde standaard te maken voor industriële en onderzoek toepassingen voor het anticiperen op storingen in AC-distributiesystemen. Tijdens de ontwikkeling van FADS werden enkele tekortkomingen in en mogelijkheden voor verdere verbeteringen van de FADS geïdentificeerd. Deze worden besproken in de laatste hoofdstukken van dit proefschrift.

CONTENTS

CHAPTER 1

INTRODUCTION

1.1 BACKGROUND

Present day power systems as seen as a generic representation in Figure 1.1 have transformed significantly compared to that of older times. Emergence of new technologies has led to shift of generation from conventional sources to renewable energy resources like wind and solar energy. The renewable sources however are quite different in their characteristics. Renewable generation is uncertain, volatile an intermittent. Renewable sources also require advanced power electronic converters to harness their energy. Hence, increased reliance on renewables has led to decentralized energy generation along with implementation of advanced components and control techniques. Additionally, due to decentralized energy generation, the flow of electricity has become two-way. The consumer at the end of the supply chain has itself become a producer; supplying electricity back to the grid, thus turning into a *prosumer*. These developments have made the current power grid more complex in structure and more difficult to operate safely and reliably.

The complexity of this power system is amplified by the fact that today's world has become increasingly inter-connected and interdependent. Reliable power supply has become the heartbeat of the modern world. All major technology related systems ranging from flight departures to bank transactions to medical procedures are heavily reliant on reliable power supply. Our technological world has become deeply dependent upon the continuous availability of electrical power and any outage or blackout or even a load shedding of a few minutes can lead to massive loss of productivity. The ageing electrical grid and implementation of new technologies have further complicated grid operations. A study in U.S. by Electrical Power Research Institute (EPRI) has shown that industrial and digital business firms are losing $45.7 billion per year due to power interruptions with another $15 billion to $24 billion lost due to all other power quality problems [1]. Long-term power interruptions are usually caused due to cascading blackouts. These cascading blackouts are generally the result of a combination of unanticipated sequence of several small disturbances in the grid. Some of the major cascading blackouts of recent times include the blackout in India in 2012 where almost 700 million residents were affected for several hours [2]. In 2003, several US states and Canada were affected by a blackout [3-4], where an estimated 50 million people were without electricity. Other major blackouts reported were in the Swedish-Danish system [5] and the Italian-Swiss grid [6-7]. The blackout in Bangladesh in 2014 had the highest duration at 24 hours [8]. The recent blackout in Brazil in 2018 affected close to 10 million consumers [9]. A major blackout in January 2017 during morning rush hour in Amsterdam, the Netherlands,

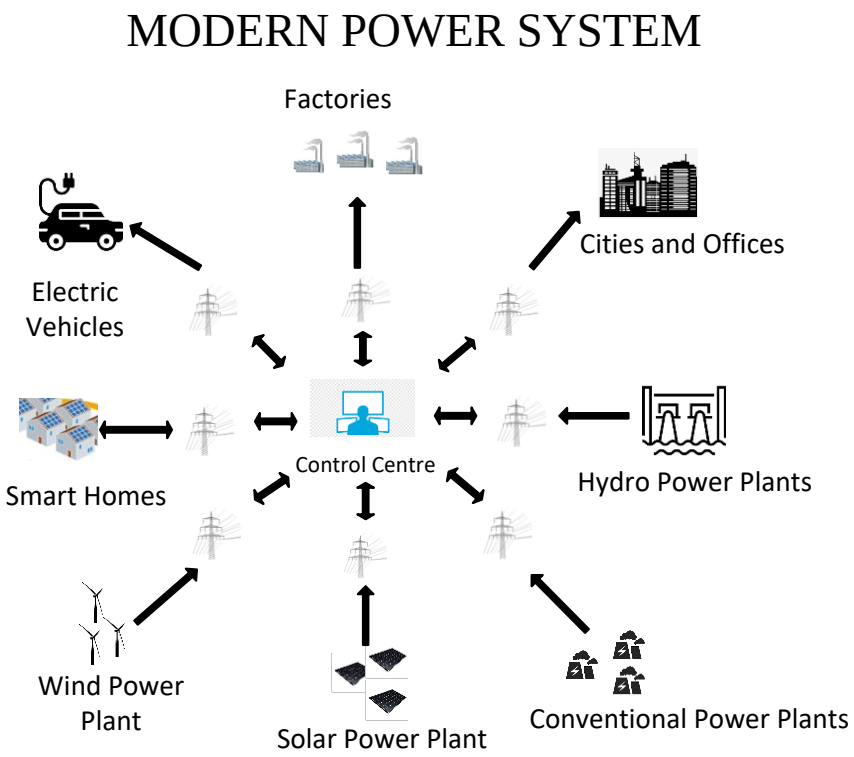

Figure 1.1: Generic representation of modern day power system

affected 360 thousand households and completely halted train traffic. The main cause as per the report by the Transmission System Operator (TSO) was the cascading effect of a component failure [10]. All these blackouts were associated with millions in damages. Power blackouts also cause tremendous inconvenience for consumers and can have social, economic and political impact on human activities [11]. A comprehensive summary of blackouts all over the world is well documented in [12].

A common element in all major blackouts is that they are usually a result of the cascading effect of a small failure or fault somewhere in the power grid. The analysis of blackouts from 2011 to 2019 indicate that close to 80% of them occurred due to cascading effect of a failure initially caused by an adverse weather effect, degrading equipment or a simple human error [12]. The key to avoid such cascading failures would be to control and localize the impact of the failure. The current protection schemes mostly employed by grid operators at DSO level to avoid cascading failures are Under Frequency Load Shedding (UFLS) and Under Voltage Load Shedding (UVLS). However due to increasing energy demand, the modern power systems are already operating very close to the steady state stability margins, which leaves grid operators with a very small time-window to implement restorative actions to prevent cascading failures [13-14]. Utilities also carry out periodic maintenance to improve situational awareness and prevent outage due to

failing equipment. However, the maintenance approach of the utilities are to prioritize inspection of mostly critical and costly components like transformers, circuit-breakers etc. [15]. Such an approach is inadequate as power grid contains thousands of small components spread over vast geographic areas, which cannot be covered by the periodic maintenance. Hence, there is an urgent need for new solutions for improved power system monitoring, which can identify incipient failure conditions giving operators enough time for judicious decision-making and ensure the reliability of grid operations. These technologies are implemented mostly in the distribution systems since they serve as the final link between utilities and customers. It has been documented that that 74% of the customer minutes lost due to power interruptions in U.S. has been in 11 kV network [16]. Hence, in the work done in this thesis focusses exclusively on AC distributions systems.

1.1.1 EMERGING TECHNOLOGIES AND CHALLENGES

One of the emerging technologies to improve power grid monitoring is the use of wide area monitoring based methods. These methods utilize the Wide Area Measurement System (WAMS) platform [17-18]. WAMS platform based tools focus on online coordinated monitoring of power grid operations enhancing the observability of the grid helping to detect mal-operations quickly. The main objective of most of the WAMS based tools is to use selected local data information to counteract the propagation of large disturbances and prevent blackouts [19-20]. WAMS based tools require synchronized data from Phasor Measurement Unit (PMU) for their decision-making. Several WAMS based tools are in different stages of development and experimental implementation with varying degree of success and in future help in improving reliability and energy production [21]. WAMS based tools focus primarily on restricting propagation of the failure after its occurrence rather than failure anticipation.

Another interesting research work conducted in the field of designing a self-healing grid has led to development of Fault Detection, Isolation and Restoration (FDIR) techniques. FDIR implementation aims for a fast detection and location of a failure event so that the corresponding area can be quickly isolated and power restored such that the outage duration is minimum [22]. FDIR based techniques are being increasingly adopted by utilities to improve reliability indices like SAIDI, SAIFI and CAIDI. FDIR techniques often use complex statistical techniques for their decision making process [23]. These statistical techniques are very reliable but at the same time, their complexity usually implies higher resource consumption.

Extensive research, cost-efficient technologies and increased concerns of climate change will further drive the penetration of renewable sources in the current energy mix adding to the complexity of grid operations. This additional complexity and stress on the grid provides fertile ground for unexpected and unwanted failures, especially in the distribution grid. Proper compliance to grid codes and regulatory norms is also a necessity with many external players now entering the electricity distribution market. The evolving and expanding grid with changing topologies, load-levels and other operational complexities has created new issues for the grid [20]. The focus of newer technologies should be to protect the power system from extreme contingencies. WAMS, FDIR and other related techniques encapsulate the research done to improve the situational awareness of the power grid and address such issues. Academic research has been

focusing on developing newer and efficient techniques in collaboration with electrical utilities but often the innovations are not shared in public domain and access is highly restricted. The development of these techniques is a result of normal technological progression in the field of protection of electrical systems. However, in an era where both reliability of power systems and time taken to fix failures are of utmost importance, there can be minimal compromise between the two. There is a need of a comprehensive, accurate and proactive technology, which is low on resource consumption, easily implementable and widely applicable. Hence, in this thesis, the research work has tried to identify and fulfill the research gap of a comprehensive and proactive protection technology. In order to achieve the research objectives ahead of the normal technological progression, there is a need of a technological jump.

1.1.2 TECHNOLOGICAL JUMP

The contribution of this thesis is to present and discuss the theoretical aspects and implementation results of the proposed technological jump. Figure 1.2 gives an insight into this concept. It shows the average value of the unplanned System Average Interruption Duration Index (SAIDI) values over the years for European countries. The data has been compiled from the 6th Benchmarking Report on the Quality of Electricity Supply by Council of European Energy Regulators (CEER) [24]. The values are until the year 2016 and the dashed blue line in the figure further shows how natural technological progression in future would lead to progressive reduction in SAIDI values as per current trends. The dashed red line shows how the proposed technological jump would probably lead to a steeper decline in SAIDI values leading to reliable power delivery.

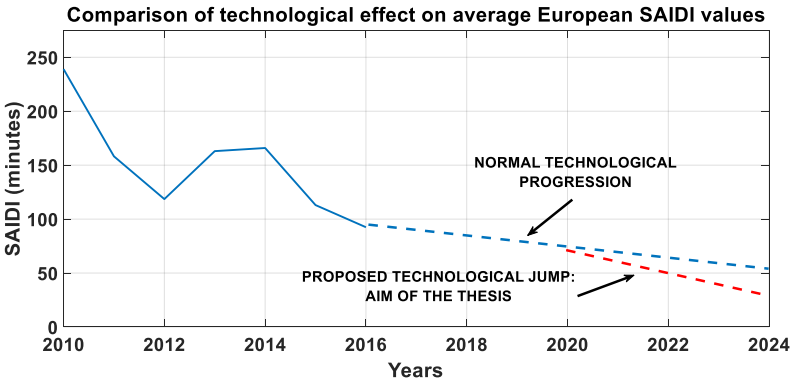

Figure 1.2: Effect on average European SAIDI values (Normal Technological Progression v/s Proposed Technological Jump)

In order to achieve this technological jump, there is a need of a systematic, well-defined analytical approach. Such an approach should be broadly divided into three stages of operation, namely, data acquisition, data processing and data interpretation. Data acquisition is an important first step. Low-resolution data has earlier hindered development of analytical methods to improve grid reliability. However, advancements in technology has led to the development of high fidelity Intelligent Electronic Devices (IEDs) which have made it possible to record waveforms with greater precision and higher sampling rates in real-time. The second process concerned with data processing should be based on solid fundamental mathematical approaches. Data processing

techniques are very crucial since they have to strike a fine balance with accuracy and time consumption. Accurate performance requires minute understanding of grid operations but at the same time, it will lead to generation of huge volumes of data by IEDs. Hence, the challenge is to formulate a method to efficiently process such raw datasets and extract useful information from it in a time-efficient manner. The final stage of data interpretation helps us to draw useful conclusions. Data interpretation will need to compare the results of data processing against certain parameters like threshold violations, impact indicators etc. to accurately gauge the severity of the event affecting grid operations. The next part for this well-defined analytical approach would be to validate its performance in different scenarios. After fulfillment of all these requirements can any approach/algorithm or technology be ready for field deployment and a meaningful technological jump achieved. This technological jump would benefit producers, consumers, system operators alike since the overall reliability of the power grid will be improved.

This thesis proposes the Failure Anticipation and Diagnosis Scheme (FADS) for distribution systems. FADS is meant to be a small stepping-stone in facilitating the above-discussed technological jump. FADS, as explained in future chapters, is designed to be a lightweight yet effective early warning system for incipient failures in power distribution system.

1.2 PROBLEM DEFINITION

The conventional protection schemes are reactionary in nature. They perform an excellent job in dealing with conventional failures like overvoltage or overcurrent situations but they react after a fault or failure has occurred. A white paper from EPRI [25] states that prevention or anticipation of a failure is one of the most important elements of a resilient power distribution system. As documented in numerous articles, incipient failures have high level of diversity in context of time-scales and waveform patterns [26-30]. Hence, in order to anticipate failures, a more proactive approach is required compared to conventional protection schemes.

1.2.1 PRE-FAILURE PERIOD

Real-time monitoring of power systems by IEDs provides us the opportunity to anticipate certain failures. As explained in [15], there typically exists a *pre-failure period* which is the intermediate period between the normal operation and an outage. The concept is illustrated in Figure 1.3. Certain power system failures ranging from incipient failures, equipment damage or adverse weather related effects generate from a small event, deteriorate over time (pre-failure period) and the full impact is felt only after a while. By the time the full impact is felt, it might be too late to react. The time scale of such a pre - failure period can range from few seconds to weeks to months. During this time, the normal grid operations come under stress and the grid starts to lose slowly its stability, eventually leading to a full-scale outage. However, the signatures of the grid enduring stress are often reflected in the electrical waveforms (current and voltage) during the pre-failure period in form of some minute deviations from fundamental properties of the waveforms. These waveforms can be recorded by the IEDs in high resolution, which gives us a better observability to the minute deviations. Such signatures in the electrical waveforms are collectively referred as incipient failure signatures. However, fast

detection and processing of such incipient failure signatures is needed to extract useful information. This extracted information will improve the situational awareness of the stability of grid operations, helping to anticipate a failure and plan corrective actions to limit the impact to minimum.

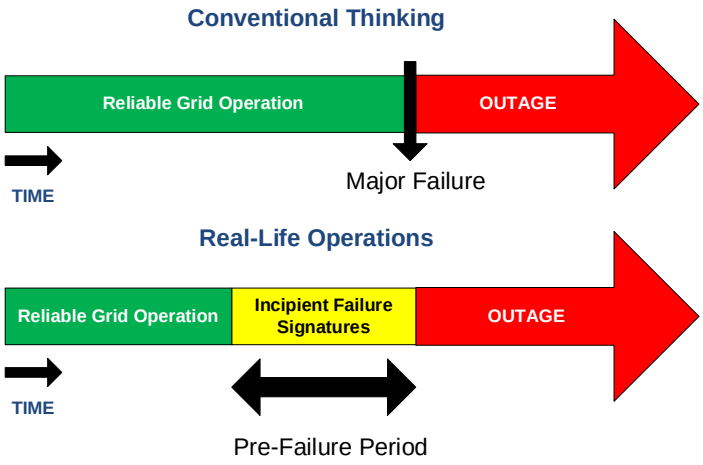

Figure 1.3: The different paradigms of grid operating conditions (*adapted from [15]*)

FADS intends to utilize this pre-failure period for anticipating failures. FADS is intended to be implemented online and engage in real-time monitoring of electrical waveforms via IEDs. In order to process the incoming raw data in a fast and efficient manner to gain knowledge about grid operations, FADS relies on application of mathematical techniques. These techniques help to identify minute deviations of fundamental properties or abnormalities in electrical waveforms. The application of these mathematical techniques is collectively referred as Waveform Analytics. In the study conducted in this thesis, waveform analytics application will be implemented for voltage and current waveforms collectively referred as electrical waveforms. Apart from application related to failure anticipation, FADS application will also be used to detect failures where conventional protection schemes underperform such as High Impedance Faults (HIF). A detailed literature survey on failure anticipation techniques and the structure of FADS and various stages of its implementation are explained in detail in Chapter 2.

1.2.2 WAVEFORM DISTORTIONS

Waveform distortions as per IEEE Power and Energy Society (PES) Technical Report-73 can be defined as a transient or persistent deviation from the sinusoidal voltage or current waveforms [31]. Waveforms distortions are also referred as waveform disturbances or waveform abnormalities but in this thesis, the terminology of waveform distortions will be used. Leveraging waveform distortions for situational awareness comes under the broader umbrella of waveform analytics based approaches. Some of the other waveform analytics based approaches include use of harmonics, wavelets, transient characteristics etc. Exhaustive list of such techniques with references have been discussed

in chapter 2. Analysis of waveform distortions has emerged as a major research field in recent years and is included in the domain of Power Quality (PQ) data analytics [32]. The waveform distortions are utilized as the main signatures of incipient failures in this dissertation. Considerable amount of research has been done to analyze and classify such distortions, which would be presented in detail in chapter 2. A major section of that research work aims to classify waveform distortions as one of the several PQ disturbances as defined in [31]. However as mentioned in [26], incipient power system failures would not always manifest as a specific PQ disturbance. In [26], [31] and [32], it has also been clearly acknowledged that there is a lack of a comprehensive and holistic yet fast and easy approach to implement failure anticipation technique. Hence, the approach to classify the waveform distortions from the PQ disturbances perspective may not be sufficient and limited in practical application. There is a need for alternative approaches. These alternative approaches maybe implemented independently or complement strategies and techniques based on PQ data monitoring. The ultimate goal will always be to improve grid reliability.

In order to develop alternative approaches, there is need of a more mathematical and fundamental understanding of the waveform distortions. In this thesis, when a reference to electrical waveform is made, it is implied that the waveform in question is a pure sinusoid AC current or voltage waveform. These sinusoid waveforms adhere to certain fundamental mathematical properties. Waveform distortions, irrespective of the event causing the distortions or whether those distortions fall in the ambit of the definition of PQ disturbances, would invariably lead to violation of certain fundamental mathematical properties of sinusoids. FADS intends to utilize waveform analytics to identify such violations. Hence, FADS developed in this thesis focusses on leveraging fundamental aspects of waveform distortions in order to be more comprehensive in its application. The detailed explanation and mathematical formulations on the detection of waveform distortions is presented in chapter 2.

Before, the research objectives and approach are explained in detail, it is very important to define failure in the context of this thesis. Failure has been defined in different ways in literature keeping the essence of the meaning same. In some literature, failure and fault are used invariably for each other. However, in the context of this thesis, failure can be defined as:

Disruption to normal grid operations caused by unplanned or exceptional events will be termed as failure. A conventional single-phase or three-phase fault event can also be termed as failure. However, a blackout caused by adverse weather event would be referred as a failure and not as a fault in this thesis.

1.3 RESEARCH OBJECTIVE AND QUESTIONS

The focus of the thesis is to develop a comprehensive failure anticipation technology in distribution systems. Hence, the main research objective of this thesis can be encapsulated as:

Creation of a failure anticipation and diagnosis scheme in distribution systems, which will utilize waveform analytics based techniques in real-time during the pre-failure period to quickly detect incipient fault signatures, process the data from waveform deviations in a time-efficient manner and accurately interpret the results such that the grid operators have enough time and information to plan and implement mitigation strategies.

The three main properties of such a failure anticipation technology should be:

- Low computational burden implying faster decision-making and minimal resource cost.
- Wide application in different cases in real-life situations ranging from slowly degrading equipment to different scenarios where conventional protection systems are not sufficient.
- Installation compatibility with present-day IEDs for minimizing implementation costs and eliminating the need of additional measurement devices.

The research questions related to the research objectives are:

1. *Would a shift towards development of innovative, intelligent and proactive protection schemes to anticipate failures lead to improvement in reliability of power supply?*
2. *Can incipient failures be accurately detected in distribution grids in real time by applying waveform analytics in pre-failure period?*
3. *Which parameters, thresholds or ratings should waveform analytics leverage for a fast and accurate detection and economical implementation?*
4. *Can such a failure anticipation technology help also to locate the event area for quicker response and subsequent improvement in reliability indices?*
5. *Can such a failure anticipation technology be validated across different test cases so that it can be adopted as a novel and comprehensive protection scheme to complement the conventional protection schemes?*

1.4 RESEARCH APPROACH

In order to achieve the research objectives and answer the research question, there is a need of a well-defined research structure. Hence, the research structure would be broadly

divided in two parts. The first part would focus on developing the FADS scheme, while the second part will highlight the application of such a scheme in different scenarios and evaluate the performance.

The first part involves the development of FADS. The theoretical aspects of waveform distortion detection are explained and the mathematical formulations to support the theoretical aspects are presented in detail. Waveform distortion detection becomes the primary indicator of a possible incipient failure event in the grid. Subsequently, various parameters are introduced to process effectively the distortion detection data in order to extract useful information. The functionality of each parameter, their position in the data processing hierarchy and their specific technical contribution to FADS's working are explained in detail. Finally, the metrics are created to interpret the extracted useful information and analyze the severity of the event causing distortions. In summary, the first part of research approach deals with building the small functionality blocks and then linking them together to create the comprehensive Failure Anticipation and Diagnosis Scheme while preserving time and resource efficiency.

The second part of the research approach involves the validation of the FADS scheme in a number of different failure scenarios using real-time simulation. Conventional protection schemes' involving digital protection relays are adept in detecting overload conditions, short-circuit and other faults. These protection schemes are time tested and are in wide use. FADS does not intend to replace them, rather complement the working of conventional protection schemes during events where they are insufficient. Similarly, other upcoming incipient failure technologies can be implemented in parallel with FADS to complement each other's working. The test cases for evaluating FADS performance range from HIFs to equipment damage to real-field data analysis. The objective for such varied types of test cases is to display FADS's efficacy in wide range of scenarios and that FADS application is not restricted only to a certain type of failures. Appropriate conclusions are drawn from the FADS performance and an analysis of the observed advantages and perceived shortcomings of FADS are documented in the final chapter of this thesis.

1.5 THESIS OUTLINE

The thesis outline can be seen in Figure 1.4. The structure of the outline shows how the different chapters are linked and provides a coherent structure to this thesis.

Chapter 1, Introduction, presents the background relating to protection concerns related to the modern power grid. The background is used to motivate the need of the technological jump in the field of protection systems to facilitate innovation and a shift towards development of protection schemes related to anticipation of incipient failures. The research objectives and the associated research questions to facilitate such a technological jump and develop a comprehensive failure anticipation technology are discussed and listed. The research approach to be taken to answer the research questions are discussed briefly. Finally, the thesis outline and the distribution of different chapters are presented.

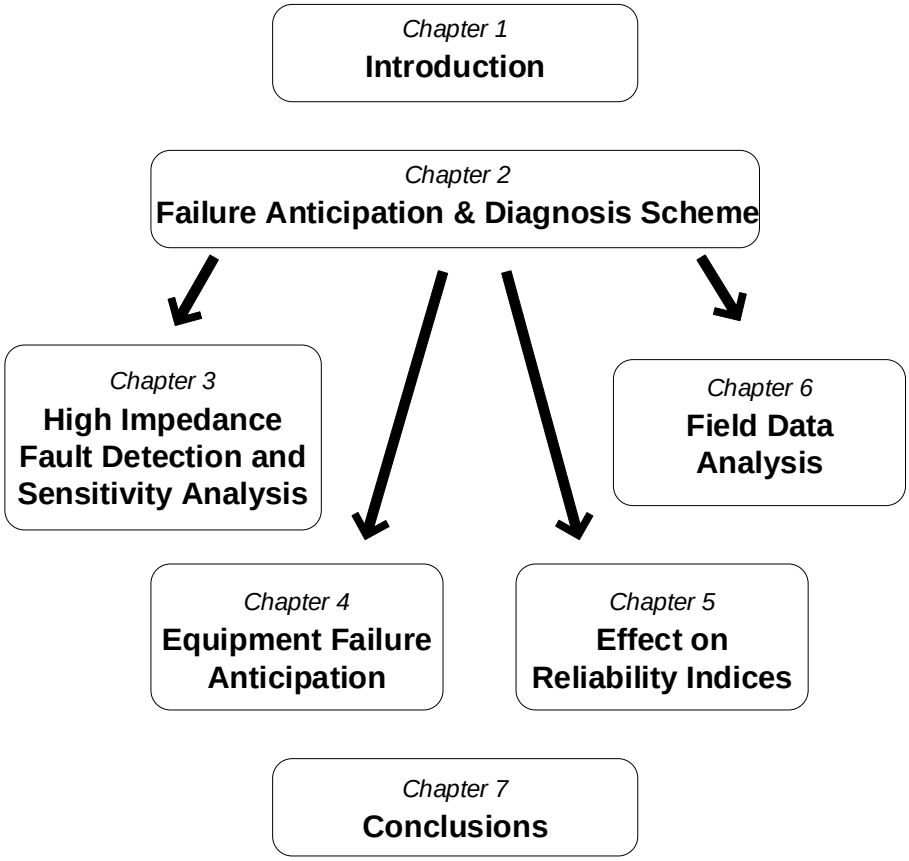

Figure 1.4: The thesis outline flowchart

Chapter 2 presents the fundamentals of the novel FADS scheme. The various stages of FADS implementation are presented in detail. The choice of test systems is also motivated. The rationale behind leveraging certain fundamental properties of electrical waveforms via waveform analytics based approach to anticipate failures are explained further. The mathematical formulations and associated proofs governing the waveform analytics is presented in detail. Then the various stages of the FADS scheme implementation starting from acquisition of raw data from IEDs to extraction of useful information to facilitate informed decision-making for grid operators are presented systematically. The choice and determination of parameters, thresholds, tools or metrics associated with every stage of FADS implementation are discussed. The different characteristics and functionalities, which make FADS a comprehensive failure anticipation technology, are highlighted and the real field implementation protocols are discussed.

Chapter 3 presents the FADS application for detection of HIF in distribution systems. Conventional protection schemes often fail to detect HIF due to its unpredictable nature

and low fault current. Hence, there is a lack of a comprehensive HIF detection method. In this thesis, standard HIF model are used to simulate HIF and FADS is implemented to detect and locate HIF across different simulation cases and scenarios. Several novel and complex simulation scenarios are designed to conduct a stringent test of FADS capabilities. A sensitivity analysis is also conducted to evaluate FADS performance for HIF occurrence from different surfaces. FADS evaluation results are analyzed and presented in detail. The apparent advantages of FADS over other existing HIF techniques are also presented.

Chapter 4 presents the FADS application for anticipating equipment failures. The case studies in this chapter are inspired from real-field events and are designed to mimic closely the transient behavior as observed in field recordings. In the real-field cases, the non-detection of incipient failure signatures leads to no action from utilities until the incipient failure develops into a permanent fault. FADS implementation results and observation indicate how the equipment failure signatures would have been detected in time along with actionable input on the location of the event.

Chapter 5 presents the effect on reliability indices by FADS implementation. The event location input from the test cases of previous chapter are used to analyze and quantify the possible improvement of reliability indices. In order to preserve the realism, novel concepts are introduced to translate FADS implementation results to realistic savings. The results obtained from the analysis show the positive effect on improvement of reliability indices.

Chapter 6 presents the results of FADS implementation on field data obtained from a Dutch DSO and highlights FADS effectiveness in real-field implementation.

Chapter 7 presents a summary of the conclusions related to this thesis, highlights the scientific contributions by emphasizing how the different research questions were answered. The chapter also identifies remaining research gaps and provides recommendations for future research.

REFERENCES

[1] D. Lineweber, and S. McNulty. (2001, Jun.). The Cost of Power Disturbances to Industrial and Digital Economy Companies. Electrical Power Research Institute (EPRI), USA. [Online]. Available: https://www.epri.com/#/pages/product/3002000476/

[2] J. J. Romero, "Blackouts illuminate India's power problems," in *IEEE Spectrum*, vol. 49, no. 10, pp. 11-12, October 2012.

[3] A. Muir, and J. Lopatto. (2004, Apr.). Final report on the August 14, 2003 blackout in the United States and Canada : causes and recommendations. US-Canada Power System Outage Task Force, Ottawa, Canada. [Online]. Available: https://www.osti.gov/etdeweb/biblio/20461178

[4] G. Andersson et al., "Causes of the 2003 major grid blackouts in North America and Europe, and recommended means to improve system dynamic performance," in *IEEE Transactions on Power Systems*, vol. 20, no. 4, pp. 1922-1928, Nov. 2005.

[5] S. Larsson and A. Danell, "The black-out in southern Sweden and eastern Denmark, September 23, 2003.," 2006 *IEEE PES Power Systems Conference and Exposition*, Atlanta, GA, 2006, pp. 309-313.

[6] S. Corsi and C. Sabelli, "General blackout in Italy Sunday September 28, 2003, h. 03:28:00," *IEEE Power Engineering Society General Meeting*, 2004., Denver, CO, 2004, pp. 1691-1702 .

[7] A. Berizzi, "The Italian 2003 blackout," IEEE Power Engineering Society General Meeting, 2004., Denver, CO, 2004, pp. 1673-1679 Vol.2.

[8] M. A. Kabir, M. M. H. Sajeeb, M. N. Islam and A. H. Chowdhury, "Frequency transient analysis of countrywide blackout of Bangladesh Power System on 1st November, 2014," *2015 International Conference on Advances in Electrical Engineering (ICAEE)*, Dhaka, 2015, pp. 267-270.

[9] B. Chen and H. Chen, "Impact of Cyber System Failure on Cascading Blackout of Power Grid," *2018 2nd IEEE Conference on Energy Internet and Energy System Integration (EI2)*, Beijing, 2018, pp. 1-5.

[10] Integrated Annual Report 2017. TenneT Holding B.V. 2017. [Online]. Available: https://annualreport.tennet.eu/2017/annualreport

[11] S. Joo, J. Kim and C. Liu, "Empirical Analysis of the Impact of 2003 Blackout on Security Values of U.S. Utilities and Electrical Equipment Manufacturing Firms," in *IEEE Transactions on Power Systems*, vol. 22, no. 3, pp. 1012-1018, Aug. 2007.

[12] H. Haes Alhelou, M. Hamedani-Golshan, T. Njenda, and P. Siano, “A Survey on Power System Blackout and Cascading Events: Research Motivations and Challenges,” *Energies*, vol. 12, no. 4, p. 682, Feb. 2019.

[13] H. Wang and J. S. Thorp, "Optimal locations for protection system enhancement: a simulation of cascading outages," in *IEEE Transactions on Power Delivery*, vol. 16, no. 4, pp. 528-533, Oct. 2001.

[14] M. Hajiakbari Fini, G. R. Yousefi and H. Haes Alhelou, "Comparative study on the performance of many-objective and single-objective optimisation algorithms in tuning load frequency controllers of multi-area power systems," in *IET Generation, Transmission & Distribution*, vol. 10, no. 12, pp. 2915-2923, 2 9 2016.

[15] J. A. Wischkaemper, C. L. Benner, B. D. Russell and K. Manivannan, "Application of Waveform Analytics for Improved Situational Awareness of Electric Distribution Feeders," in *IEEE Transactions on Smart Grid*, vol. 6, no. 4, pp. 2041-2049, July 2015.

[16] A. Kavousi-Fard and T. Niknam, "Optimal Distribution Feeder Reconfiguration for Reliability Improvement Considering Uncertainty," in *IEEE Transactions on Power Delivery*, vol. 29, no. 3, pp. 1344-1353, June 2014.

[17] A.G.Phadke, T. Bi, Phasor measurement units, WAMS, and their applications in protection and control of power systems. J. Mod. Power Syst. Clean Energy 6, 619–629 (2018).

[18] K.Sun. WAMS-Based Controlled System Separation to Mitigate Cascading Failures in Smart Grid. In Smart Grid Control; Springer: New York, NY, USA, 2019; pp. 185–195.

[19] V. Terzija *et al*., "Wide-Area Monitoring, Protection, and Control of Future Electric Power Networks," in *Proceedings of the IEEE*, vol. 99, no. 1, pp. 80-93, Jan. 2011.

[20] P. Zhang, F. Li and N. Bhatt, "Next-Generation Monitoring, Analysis, and Control for the Future Smart Control Center," in *IEEE Transactions on Smart Grid*, vol. 1, no. 2, pp. 186-192, Sept. 2010.

[21] V. Terzija *et al*., "Flexible Wide Area Monitoring, Protection and Control applications in future power networks," *10th IET International Conference on Developments in Power System Protection (DPSP 2010). Managing the Change*, Manchester, 2010, pp. 1-5

[22] A. Zidan et al., "Fault Detection, Isolation, and Service Restoration in Distribution Systems: State-of-the-Art and Future Trends," in *IEEE Transactions on Smart Grid*, vol. 8, no. 5, pp. 2170-2185, Sept. 2017.

[23] I. Hwang, S. Kim, Y. Kim and C. E. Seah, "A Survey of Fault Detection, Isolation, and Reconfiguration Methods," in *IEEE Transactions on Control Systems Technology*, vol. 18, no. 3, pp. 636-653, May 2010.

[24] 6th CEER Benchmarking Report on the Quality of Electricity and Gas. Supply Ref: C16-EQS-72–03 CEER Brussels July 2016. [Online]. Available: https://www.ceer.eu/eer_publications/annual_reports

[25] M. McGranaghan, M. Olearczyk and C. Gellings. (2013, Jan.). Enhancing Distribution Resiliency. Electrical Power Research Institute (EPRI), USA. [Online]. Available https://www.epri.com/#/pages/product/1026889/

[26] B. Li, Y. Jing and W. Xu, "A Generic Waveform Abnormality Detection Method for Utility Equipment Condition Monitoring," in IEEE Transactions on Power Delivery, vol. 32, no. 1, pp. 162-171, Feb. 2017.

[27] P. Dutta, A. Esmaeilian and M. Kezunovic, "Transmission-Line Fault Analysis Using Synchronized Sampling," in *IEEE Transactions on Power Delivery*, vol. 29, no. 2, pp. 942-950, April 2014.

[28] S. Kulkarni, S. Santoso and T. A. Short, "Incipient Fault Location Algorithm for Underground Cables," in *IEEE Transactions on Smart Grid*, vol. 5, no. 3, pp. 1165-1174, May 2014.

[29] S. Santoso and D. D. Sabin, "Power quality data analytics: Tracking, interpreting, and predicting performance," *2012 IEEE Power and Energy Society General Meeting*, San Diego, CA, 2012, pp. 1-7.

[30] L. A. Irwin, "Real experience using power quality data to improve power distribution reliability," *Proceedings of 14th International Conference on Harmonics and Quality of Power - ICHQP 2010*, Bergamo, 2010, pp. 1-4.

[31] IEEE Working Group on Power Quality Data Analytics, Tech. Rep. 73: Electrical signatures of power equipment failures. Dec 2019. [online] Available: http://grouper.ieee.org/groups/td/pq/data/.

[32] G. W. Chang, Y. Hong and G. Li, "A Hybrid Intelligent Approach for Classification of Incipient Faults in Transmission Network," in *IEEE Transactions on Power Delivery*, vol. 34, no. 4, pp. 1785-1794, Aug. 2019.

CHAPTER 2

FAILURE ANALYSIS AND DIAGNOSIS SCHEME

2.1 INTRODUCTION

This chapter lays the foundation of FADS. FADS operates in real-time and acquires data from IEDs continuously monitoring the grid. FADS as mentioned and motivated in Chapter 1 is supposed to be implemented for AC distribution systems. The data FADS operates with are the voltage and current waveforms. FADS scans the continuous incoming electrical waveforms to detect any possible electrical waveform distortions and then analyzing the extent of distortions against a defined set of thresholds and indicators, a conclusion is reached whether the event causing the waveform distortions threatens the stability of the grid. The research approach of FADS is broadly divided in two parts. The first part deals with the detection of electrical waveform distortions. The mathematical principle of such distortion detection is based on leveraging the violation of certain fundamental properties of AC sinusoidal waveforms. In the second part, the data collected from waveform distortion detection goes through the process of data analysis. A severity scale is then used to rank the severity of the negative impact of the event on the grid operations and an estimate of location of the event is provided. This working of FADS has been divided in different stages of data handling. These different stages of FADS including the mathematical formulation, estimation and calculation of various parameters and interpretation of the extracted useful information are explained and presented in detail in this chapter.

In order to fulfill the research objectives, FADS has been developed such that it always achieves two important features of any novel technology, namely, *Operational Efficiency* and *Ease of Implementation*. The operational efficiency of FADS can be better gauged when FADS is applied in different failure scenarios and an evaluation is made on results obtained. The FADS application in different failure scenarios are presented in subsequent chapters. Regarding ease of implementation, as the different aspects of FADS are explained in detail in the course of this chapter, special care has been taken to emphasize how the FADS is designed to be simple, effective and easy to implement.

Parts of this chapter have been published in IEEE Transactions on Power Delivery journal [68], Innovative Smart Grid Technologies Europe (ISGT 2018) conference [69] and IEEE International Conference on Industrial Electronics, Control and Instrumentation (IECON 2018) [70].

2.2 STATE-OF-THE-ART

The following section documents the current technological advances in the field of failure anticipation or similar technologies. Incipient failures are random and do not leave a specific trace or signature. This makes it difficult for traditional feature analysis and classification techniques to anticipate failures [1]. Failure anticipation and related work is relatively new field in electrical protection systems and hence compared to conventional protection systems, considerable new research work will follow in years to come. However, the field has recently gained a lot of traction and attention leading to development of innovate techniques and algorithms.

Majority of work done in failure anticipation field is focused towards anticipating specific equipment damage related issues. Such a focus is expected since equipment damage issues are a major source of incipient failures. Incipient failure techniques to have been used in [2-3] anticipate underground cable damage via wavelet transform. Wavelet transform along with Self Organizing Map (SOM) technology has been used in [4] for anticipating failures in underground cables. Wavelet transforms have been used to analyze the transient behavior in time and frequency domains in underground cables to detect incipient failures [5-6]. Wavelet based techniques have been also developed for incipient fault detection in induction machines [7-9] and transformers [10]. One of the crucial parameters in determining the success of wavelet based techniques is the accurate choice of the mother wavelet. Fourier transform based techniques have also been used for detecting incipient failures in underground cables [11-12] and in medium voltage circuits [13]. High-Frequency signal based techniques have been used to detect incipient failures in insulators [14]. Other failure anticipation techniques based on different technological approaches include terminal-voltage measurement based technique [15], coil-current signature [16], dielectric characterization [17], harmonic analysis [18], Hilbert-Huang transformation [19], cumulative sum approach in underground cables [20], identification of sub-synchronous resonance [21], parameter estimation approach [22] and high-voltage arc in underground cables [23] . Dissolved Gas Analysis (DGA) of transformer oil has been used to detect incipient failures in transformers in combination with neural networks in [24] and with hidden Markov model in [25]. DGA based methods to anticipate failure has also been used in [26-27]. Kalman filter based technique is used to anticipate failures in [28]. S-transform along with vector regression approach to anticipate failure in underground cables has been used in [29]. Artificial Neural Network (ANN) based failure anticipation techniques has been used in [30-32] and deep learning based technique has been used in [33].

In the domain of PQ data analytics, the incoming PQ disturbance data from Power Quality Monitors (PQM) installed in the distribution grid is used to detect incipient failures, mostly equipment damage. The classification guideline of PQ disturbance is laid down in the IEEE standard in [34]. Some techniques aim to classify incipient failure in PQ disturbance categories while some techniques utilize the abnormal current and voltage data from PQM to further process and identify incipient failures. The approach of classifying incipient failures as PQ disturbances in not widely applicable, as incipient failures will not always manifest as PQ disturbances [35]. In [36], PQ data is used to detect pre-insertion impedance switch malfunction for capacitor banks. PQ data has been

used to detect incipient failures and to improve grid reliability in [37-38]. A comprehensive technical report on application of different mathematical approaches for analysis of the power equipment failure signatures and the subsequent comparison of results is well documented in [39].

The above-discussed techniques are restricted in their universal implementation due to their single application characteristic i.e. they work for either underground cables or capacitor banks or transformers etc. Recent efforts have been made in addressing this challenge. Recent research work in [35] and [40] also acknowledge this challenge and try to create a universal failure anticipation technique. Research work in [35] focusses on developing a waveform abnormality detection method for any type of utility equipment condition monitoring. In [35], the steady state components of normal waveforms are modelled as Gaussian samples. During equipment damage conditions, the abnormal waveforms will lead to huge deviation in Gaussian samples. Kullback-Leibler Divergence (KLD) is then used to quantify such deviations and help in the process of detecting incipient equipment failure. In [40], the authors adopt KLD and other waveform abnormality detection parameters like energy, entropy, average values etc. to identify distinct features of an incipient failure. A Support Vector Machine (SVM) is then used as a classifier. The application of the hybrid intelligent technique developed in [40] is broader as it aims to classify incipient failures in an entire transmission network. Hydro Quebec researchers have developed a waveform analysis based intelligent power line maintenance prototype called MILE [41]. In addition to improving the reliability of power supply, MILE can give an accurate indication of failure location. Significant work in developing holistic failure anticipation technology has been done by researchers in Texas A&M University in collaboration with EPRI. The work has led to development of a waveform analytics system called Distribution Fault Anticipation (DFA) technology that is used to analyze the incipient failure signatures [42-44]. DFA technology has been implemented in real-field in collaboration with many utilities in U.S. and Canada. DFA functions by cross-referencing massive databases of failure and fault signatures recorded by the utilities over several years. Whenever DFA detects a waveform abnormality patterns or traits similar to a recorded historical incipient failure signature, an analysis report is generated and transmitted to grid operator. The results of DFA implementation in various scenarios are well documented in several articles and journals [45-54].

The state of art shows that failure anticipation and related field has been identified by researchers as the future area of focus for electrical protection systems. The main requirement for failure anticipation based techniques is enhanced situational awareness, which will require intelligent data processing. The techniques discussed in this section focus on it for extracting knowledge. Some of these techniques are restricted in their comprehensiveness by limited applicability; some are restricted by their comparatively high resource consumption and some by initial startup requirements. Even though the emergence of newer failure anticipation techniques are getting more comprehensive and efficient day by day, there is still a huge research gap which can be filled by a simple yet effective and comprehensive failure anticipation technique. FADS discussed in detail in subsequent sections aims to fill this gap.

2.3 BENCHMARK TEST SYSTEMS

Before FADS is discussed in detail, it is important to discuss the benchmark test systems on which the test cases would be modelled, simulations conducted and FADS would be validated. As mentioned in chapter 1, majority of the faults occur in distribution system. Hence, in this thesis, the FADS is implemented and validated in distribution systems. Different distribution systems consist of different voltage ratings, feeder lengths and load profiles. Hence, it is difficult to model every type and category of distribution system present in the world. In this thesis, two popular benchmark distribution systems provided by IEEE are used, namely IEEE-13 bus node feeder and IEEE-34 bus node feeder system [55]. These test feeders have been developed by the Test Feeder Working Group of the Distribution System Analysis Subcommittee of IEEE PES section. The test feeders have been extensively used by electrical engineers to validate their algorithms and techniques and the results obtained have worldwide credibility and acceptability.

The basic layout of IEEE-13 and IEEE-34 node feeders can be seen in Figure 2.1 and Figure 2.2 respectively. The test feeders were chosen as such, in order to have a comprehensive approach in validation of FADS. The different properties of these two

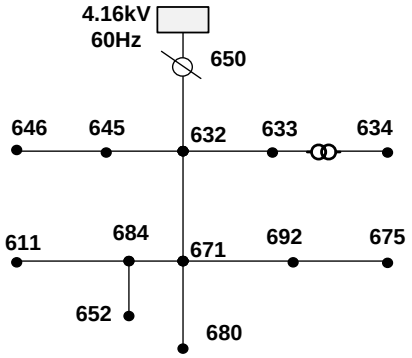

Figure 2.1: IEEE-13 Node Test Feeder System

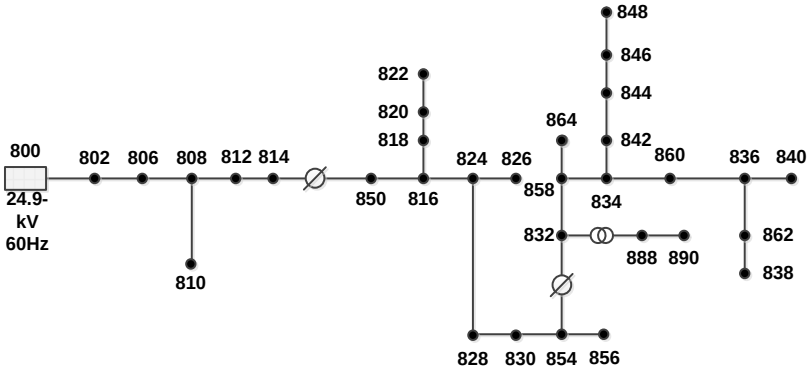

Figure 2.2: IEEE-34 Node Test Feeder System

benchmark systems encapsulate very well the wide variety of designs, the associated analytic challenges and different characteristics of any distribution system. IEEE-13 node feeder is a short, highly loaded and unbalanced distribution system. It comprises of a single voltage regulator, a mix of overhead and underground lines, a shunt capacitor and two in-line regulators. The operating voltage level is at 4.16kV. IEEE-34 node feeder is a representation of the feeder in Arizona, U.S. The nominal voltage level is 24.9kV. The feeder is long and lightly loaded with two in-line regulators. A small 4.16kV section is connected to the main feeder via an in-line transformer. There is also presence of shunt capacitors. A more comprehensive and robust evaluation of FADS in future can be conducted in detailed models like IEEE 8500 node test case. The CIGRE LV benchmark system widely used in Europe is also an important model for future FADS evaluation.

The test feeder systems were implemented and used for simulations in Real Time Digital Simulator (RTDS) system [56], so that the performance of the FADS can be observed and validated in real-time. The real-time approach was deemed necessary so that near field like conditions can be replicated in a laboratory environment. Performance evaluation in such a setup gives a far better idea of operational deficiencies, perceived shortcomings and probable challenges associated with online deployment of the FADS compared to an ideal lab setup.

2.4 Failure Anticipation and Diagnosis Scheme

FADS is a data analytics based approach which starts with acquiring raw data from grid measurements and ends with extraction of useful information from the raw data regarding incipient failures. The FADS implementation comprises of three stages. An overview of the FADS scheme can be seen in Figure 2.3. The details of the stages and steps involved are as follow:

A. Stage A

Stage A of FADS deals with the two important aspects of raw data acquisition and detection of distortion in waveforms. The raw data is acquired from IEDs already present in the distribution system. IEDs are not just measurement instruments but they also possess the capability to conduct waveform analysis of low-computational burden. The advantage of tuning the IEDs to conduct some pre-processing of incoming grid data is manifold. The first major advantage is the time saved in comparison to transmitting all of the recorded data to a central processing unit. The time saved is critical as the failure can be anticipated faster. Since IEDs generally produce huge volume of grid data at every step, pre-processing helps in decentralized use of computing power leading to better utilization of resources. Such decentralization approach will also help in improving the scalability when FADS is implemented in larger systems. Hence, stage A of FADS is supposed to be implemented in the IEDs themselves. The details of stage A are explained next.

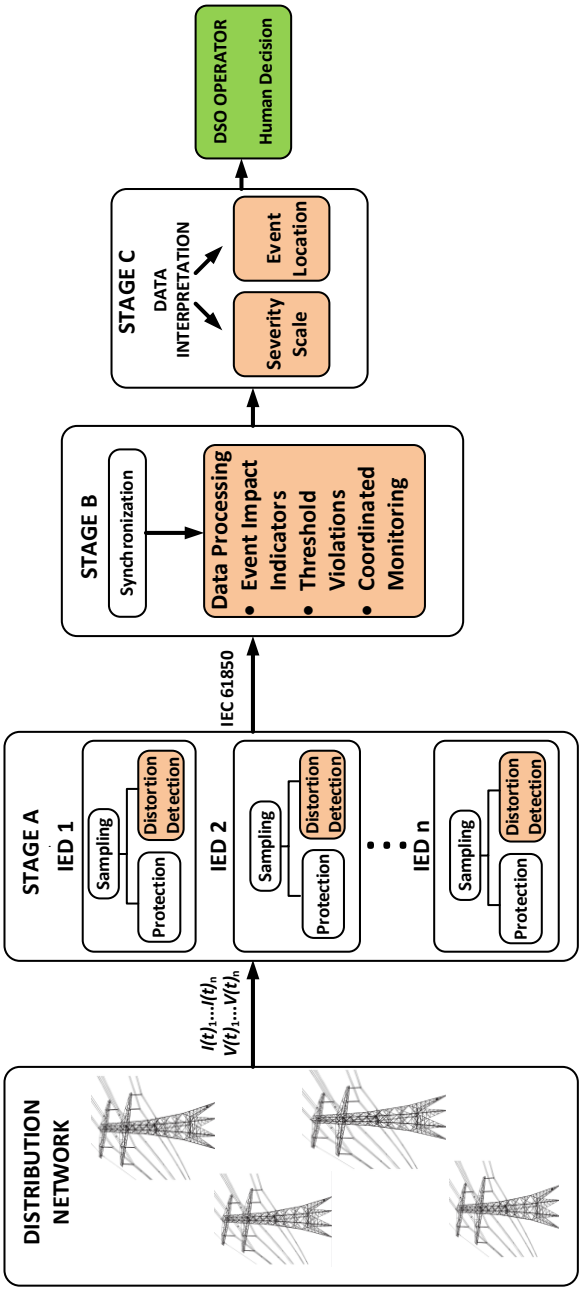

Figure 2.3: Failure Anticipation and Diagnosis Scheme (FADS) Implementation Overview

1) RAW DATA ACQUISITION

The raw data required by FADS are time-stamped sampled voltage and current waveforms from every phase. Higher sampling rate will lead to high-resolution data. Such a high-resolution data is generally desired as it captures even the smallest of deviations in the waveforms leading to better situational awareness. However, processing high-resolution data will require high processing power. Since providing such high processing power may not be economical, the standard sampling rates of IEDs are also sufficient for FADS analysis.

This initial raw data is collected individually from each IED monitoring the grid. This raw data contains information as to which sections of grid were in normal state and which sections of the grid were enduring stress. The data processing conducted in latter stages of FADS helps us to extract this information from raw data. Electrical noise in power distribution network usually ranges from 5 kHz to 100 kHz [57], which can be effectively filtered out by inbuilt low pass filters of IEDs. Due to this functionality of IEDs, the impact of noise on FADS operation would be minimal. An advanced analysis of noise effects however is outside the scope of thesis. In summary, FADS does not have any other extensive requirements for deployment of additional devices or measurement instruments, which might call for additional investment and expenditure.

2) DISTORTION DETECTION

Waveform distortion detection is the heart of FADS since a mistake in detection will lead to erroneous results. It is important on how to define a distortion. The definition should be such that the incipient failure signature are detected accurately and false flag detection is avoided. In addition, the definition should allow for the functionality of the distortion detection process to have low computational burden, so that the distortion detection functionality can be easily implemented in the IEDs. In order to achieve such an accurate yet resource-efficient technique, the FADS relies on using basic mathematical approaches to identify deviations from fundamental properties of the waveforms. The subsection is divided in two parts, the concept, where the basic idea of waveform distortions is explained and defined in the context of this thesis and the mathematical formulation, which gives a mathematical structure to the concept.

2.1) CONCEPT

The underlying concept behind FADS is that in an ideal grid operating conditions in an AC distribution system, unaffected by any external source of disturbance irrespective of its nature and source, the voltage and current waveforms would always be a pure sinusoid in nature. These pure sinusoids in mathematical terms are complex exponential functions as defined by the remarkable Euler's formula [58-60]. The complex exponential functions have some unique and fundamental properties, which would be highlighted in the next subsection. When affected by external disturbance, the waveforms will deviate from their sinusoidal nature. As at the instant of disturbance affecting the waveform, the waveform is no longer a pure sinusoid. These deviations, in the context of this thesis, constitute a *distortion*. Such distortions are usually the first signatures of incipient failures. These distortions can be a result of normal switching event, a PQ disturbance, combination of different PQ disturbances or an unexplained behavior or pattern.

Irrespective of category in which the deviations can be classified, the deviations will undoubtedly result in temporary deviation from the unique properties of the complex exponentials. At that instant, the waveform will deviate from an ideal sinusoid waveform to a distorted waveform. FADS leverages this change in properties to detect waveform distortions. Accurate identification of such distortions is the first step towards anticipating failure. The next subsection presents the mathematical formulation of the concept explained here.

2.2) MATHEMATICAL FORMULATION

The main objective is to differentiate between distorted waveforms and ideal sinusoids i.e. detecting distortions. The ideal sinusoids can be mathematically represented as complex exponentials. As seen in eqn. (2.1), Euler's formula helps us to represent a complex exponential as the sum of two trigonometric functions.

$$e^{j\omega t} = \cos \omega t + j \sin \omega t \tag{2.1}$$

Here

- e is the base of the natural logarithm
- ω is the angular frequency (*in radians per second*)
- t is the time (*seconds*)
- j is the imaginary unit.

Complex exponentials have certain unique properties. A complex exponential function unlike a real exponential function is a bounded function and does not increase or decrease in value infinitely. Complex exponential continuously rotate around the unit circle in the complex plane as seen in Figure 2.4. The figure shows the trace of $e^{j\omega t}$ around the unit circle. From the trace, one can infer that the real part of a complex exponential function starts to move from zero to peak and back. The function then moves to negative peak and after coming back to zero, it moves again to positive peak and the entire circular motion keeps repeating. Hence, it can be concluded that the real value of a complex exponential will never cross the peak and function would remain range-bound. In FADS analysis of distortion detection, the real value of the complex exponential is taken into account.

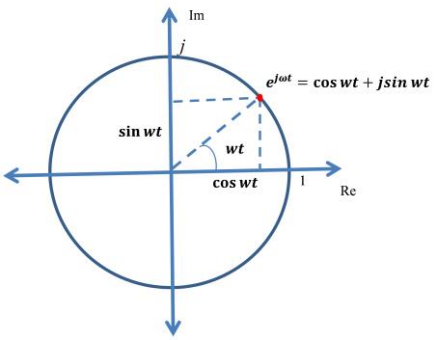

Figure 2.4: Trace of e^{jwt} around the unit circle in the complex plane

Secondly, the real value of complex exponentials does not increase or decrease linearly with time. The rate of increase or decrease of the function is directly proportional to the value of the function at that instant. Ideally, the sinusoid function decelerates from zero to peak and accelerates from peak to zero. When dealing with discrete samples, such as our case, it can be deduced that if the sinusoid is accelerating or decelerating at time t by looking at its value at the previous time instant $(t-1)$. Any change in the normal acceleration or deceleration will indicate influence of external disturbances like incipient failures. A violation of either of the above-discussed unique properties will constitute a distortion in the otherwise ideal sinusoid waveform.

A pure sine-wave can be considered as the real part of a complex exponential with phase $-\pi/4$. In order to illustrate in terms of equations, a sampled pure sine wave function, $f[k]$, as shown in Figure 2.5 is considered. It is a general representation of any voltage or current signal measured from the grid. Considering that, the signal is a sine wave of period T, which can be sampled at N samples per cycle, the total samples can be denoted as: $(n \dots k-1, k, k+1 \dots n+N)$. For simplicity, it is assumed samples are equally spaced in time at an interval of length h, such that:

$$T = h \cdot N \tag{2.2}$$

Hence, the time instants of the samples collected can be denoted as $(t_n \dots (t_k - h),\ t_k, (t_k + h) \dots t_{n+N})$.

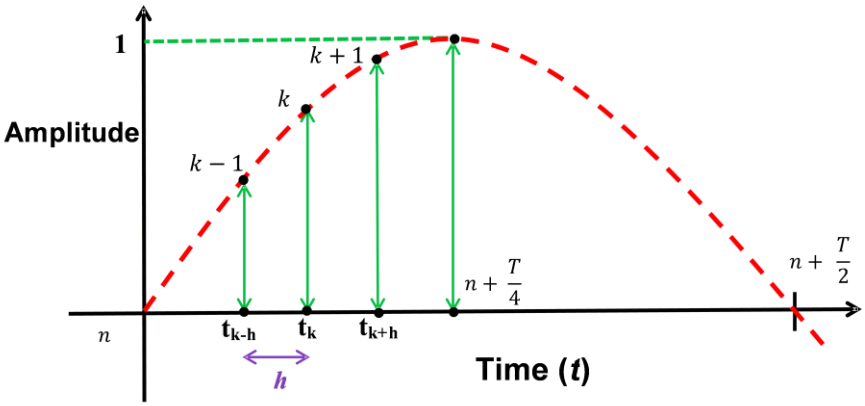

Figure 2.5: Sampled pure sinusoid signal $f[k]$

As per eqn. (2.1), the samples $(k-1, k, k+1)$ at the time instants of $(t_k - h),\ t_k, (t_k + h)$ can be mathematically represented as $(e^{j\omega(t_k-h)},\ e^{j\omega(t_k)},\ e^{j\omega(t_k+h)})$ respectively.

Considering $g[k]$ as the difference of the sampled values for samples at k and $k+1$, we can write in the interval $k \in \{n, n + \frac{T}{4}\}$:

$$g[k] = \text{Re}(e^{j\omega(t_k+h)} - e^{j\omega(t_k)}) \quad (2.3)$$

Simplifying (2.3), we get:

$$g[k] = \text{Re}(e^{j\omega t_k}(e^{j\omega h} - 1)) \quad (2.4)$$

Substituting $e^{j\omega t_k}(e^{j\omega h} - 1)$ as $\boldsymbol{A}$, we get:

$$g[k] = \text{Re}(\boldsymbol{A}) \quad (2.5)$$

Similarly, we can also write:

$$g[k-1] = \text{Re}(e^{j\omega(t_k)} - e^{j\omega(t_k-h)}) \quad (2.6)$$

Simplifying (2.6), we get:

$$g[k-1] = \text{Re}\left(\frac{e^{j\omega t_k}(e^{j\omega h}-1)}{e^{j\omega h}}\right) \quad (2.7)$$

Substituting $e^{j\omega t_k}(e^{j\omega h} - 1)$ as in (2.5), we get:

$$g[k-1] = \text{Re}\left(\frac{\boldsymbol{A}}{e^{j\omega h}}\right) \quad (2.8)$$

Since, $e^{j\omega h}$ is a complex exponential, it will rotate around the unit circle and the value would be in the range $\{-1,1\}$. In the interval of $\{n, n+\frac{T}{4}\}$, $e^{j\omega h}$ will decelerate to the positive peak value of one. In that interval since deceleration takes place, the value of $g[k-1]$would be greater than the value of $g[k]$. Subsequently, $e^{j\omega h}$ will accelerate from the positive peak value of one to zero in the interval of $\{n+\frac{T}{4}, n+\frac{T}{2}\}$. In this interval, the value of $g[k]$ would be greater than $g[k-1]$. Similarly the phenomenon will reverse in the other half cycle where the sinusoid will move from zero to negative peak and from negative peak back to zero.

In order to summarize, we can write that for any pure sinusoid for a full cycle of period T, eqns. (2.9) and (2.10) will always hold true.

$$\boldsymbol{g[k-1] > g[k], k \in \left\{n, n+\frac{T}{4}\right\} \cup \left\{n+\frac{T}{2}, n+\frac{3T}{4}\right\}} \quad (2.9)$$

$$\boldsymbol{g[k-1] < g[k], k \in \left\{n+\frac{T}{4}, n+\frac{T}{2}\right\} \cup \left\{n+\frac{3T}{4}, n+T\right\}} \quad (2.10)$$

During the positive or negative peak and zero-crossing, the value of $g[k-1]$ will be equal to value of $g[k]$. Such equality would indicate a peak or a zero crossing. At such an instant the transition of sine wave from one time interval to the other time interval occurs. As a result, the equation tracking the sinusoid for detecting distortions will also alternate. For example, the sinusoid function in the time interval of $\{n+\frac{T}{2},\ n+\frac{3T}{4}\}$ will be tracked by the eqn. (2.9). The function will reach its negative peak and then accelerate towards zero. Once the negative peak is reached, the time interval of the sinusoid function shifts to $\{n+\frac{3T}{4}, n+\ T\}$ and the equation tracking the function for distortion detection will change to eqn. (2.10). Hence, violation of eqn. (2.9) and/or eqn. (2.10) would constitute a distortion in FADS implementation context. To illustrate an example, in the interval $\{n, n+\frac{T}{4}\}$, if $\boldsymbol{g[k-1] > g[k]}$ is violated, then the sample k would be considered as distorted and a distortion would be reported.

ALTERNATE PROOF:

Considering the sampled pure sinusoid signal $f[k]$ from a different mathematical viewpoint and provide alternate proof of eqns. (2.9) and (2.10), we refer to the same pure sinusoid signal in Figure 2.5.

Expanding $e^{j\omega t}$ as per eqn. (2.1), we can write that for time instants of $(t_k - h), t_k, (t_k + h)$, the samples $(k-1, k, k+1)$ can be expressed as $\sin(\omega t_k - \omega h)$, $\sin(\omega t_k)$ and $\sin(\omega t_k + \omega h)$.

Then $g[k]$ of eqn. (2.3) can be represented as:

$$g[k] = \sin(\omega t_k + \omega h) - \sin(\omega t_k) \tag{2.11}$$

Expanding the terms, we get:

$$g[k] = \{\sin(\omega t_k)\cos(\omega h) + \cos(\omega t_k)\sin(\omega h)\} - \sin(\omega t_k) \tag{2.12}$$

Simplifying (2.12), we obtain:

$$g[k] = -\sin(\omega t_k)\{1 - \cos(\omega h)\} + \cos(\omega t_k)\sin(\omega h) \tag{2.13}$$

Considering $\cos(\omega t_k)\sin(\omega h)$ as $\boldsymbol{B}$ and $\sin(\omega t_k)\{1-\cos(\omega h)\}$ as $\boldsymbol{C}$, we can write:

$$g[k] = -\boldsymbol{C} + \boldsymbol{B} \tag{2.14}$$

Similarly, we can also re-write eqn. (2.6) as:

$$g[k-1] = \sin(\omega t_k) - \sin(\omega t_k - \omega h) \tag{2.15}$$

Expanding the terms, we get:

$$g[k-1] = \sin(\omega t_k) - \{\sin(\omega t_k)\cos(\omega h) - \cos(\omega t_k)\sin(\omega h)\} \tag{2.16}$$

Simplifying (2.16), we get:

$$g[k-1] = \sin(\omega t_k)\{1 - \cos(\omega h)\} + \cos(\omega t_k)\sin(\omega h) \tag{2.17}$$

As per our previous considerations, we can re-write eqn. (2.17) as:

$$g[k-1] = \boldsymbol{C} + \boldsymbol{B} \tag{2.18}$$

Comparing eqns. (2.14) and (2.18), we can deduce that $g[k-1] > g[k]$ when $\boldsymbol{C} > 0$ and $g[k-1] > g[k]$ when $\boldsymbol{C} < 0$.

$\boldsymbol{C}$ is composed of the product of two terms, one of which,$\{1 - \cos(\omega h)\}$, is always positive due to the cosine co-domain. Thus, $\boldsymbol{C}$ is positive when the first term, $\sin(\omega t_k)$ is positive.

So, we can infer that:

$$\boldsymbol{g[k-1] > g[k], k \in \left\{n, n + \frac{T}{4}\right\} \cup \left\{n + \frac{T}{2}, n + \frac{3T}{4}\right\}} \tag{2.19}$$

Similarly:

$$\boldsymbol{g[k-1] < g[k], k \in \left\{n + \frac{T}{4}, n + \frac{T}{2}\right\} \cup \left\{n + \frac{3T}{4}, n + T\right\}} \tag{2.20}$$

Eqns. (2.19) and (2.20) are same as eqns. (2.9) and (2.10). Similarly, when the value of the equations are same, the value of $\boldsymbol{C}$ is zero, which indicates a peak or zero crossing of the sinusoid.

Hence, the unique properties of the complex sinusoids have been illustrated through the mathematical formulations with two different approaches. The next subsection contains the discussion on how the mathematical formulation would be implemented in IEDs.

2.3) IMPLEMENTATION

As stated in previous subsection, the violations of eqns. (2.9) and/or (2.10) constitute a distortion. The low computational burden and minimal memory requirements of these equations make it relatively fast and easy to implement on the IEDs. In FADS application, the IEDs would be programmed with the mathematical formulation discussed above. Such a programmed IED can continuously check for waveform distortions in real-time. Distortions detected by the IEDs would be stored in a tuple (d, t) where d indicates the occurrence of the distortion at time t. One can define d as, $d = 1$ if a distortion is detected and $d = 0$, if a distortion is not detected. The distortions detected need to be stored in temporary datasets of small time frames of a specified length so that they can be time-synchronized and meaningful information can be extracted before moving to analyze the next dataset of distortions. The time frames of these datasets are flexible and user dependent. If there exists m IEDs in a network, such that $r = 1,2,3 \ldots m$, then the

dataset S_r containing information distortion detection data about the r^{th} IED with starting time instant of a_r and end time instant of b_r can be represented as:

$$S_r = \{(d_k, t_k) | \mathrm{d}_k \in \{0,1\}, \mathrm{t}_k \in (a_r, b_r), k = (1,2,3 \ldots)\} \qquad (2.21)$$

Here, d_k indicates the distortion detection occurrence value for k^{th} sample and t_k indicates the time stamp of the k^{th} sample. The dataset S_r from each of the m IEDs containing information about the occurrences of distortions comprises the final output of stage A and the initial input to stage B.

To summarize, the discussion on stage A implementation explains how raw data is acquired and pre-processed in the IEDs themselves. The most important element of waveform distortion definition and its detection is explained via mathematical formulation and the perceived advantages are highlighted.

B. STAGE B

Stage B is concerned with aggregating and processing the incoming distortion data collected from different IEDs in stage A. The control room is used to effectively process and store the large incoming data from stage A of different IEDs. The aggregated distortion data in itself is not granular enough for informed decision-making. A waveform distortion can be a result of common grid events like load switching, capacitor switching, feeder energization etc. These events are mostly planned and as such do not possess any danger to normal grid operations. Hence, further data processing is needed to be able to identify the harmful events. The details of stage B elements are:

1) SYNCHRONIZATION

It is very important to synchronize the data coming from different IEDs. Without data synchronization, it would be very difficult to estimate as to how a particular grid event is affecting grid operations at different locations at the same time. The MILE prototype developed by Hydro Quebec uses a similar approach before the analysis is conducted. It is desired that the IEDs have same sampling rate. However, there might be a situation where the devices will have different sampling rates. In such a situation, the device with the highest sampling rate will have the greatest resolution and the smallest time frame needed for the IED dataset S_r. This smallest time-frame for the dataset becomes the base window for synchronization. Base window A can be represented as:

$$A = (a_{base}, b_{base}) = \bigcap_{r=1}^{n} (a_r, b_r) \qquad (2.22)$$

The curtailed dataset $\widetilde{S_r}$ within the size limits of the base window can be represented as:

$$\widetilde{S_r} = \left\{ S_r = (d_k, t_k) \middle| S_r \; and \; t_k \in (a_{base}, b_{base}) and \; d_k \in \{0,1\} \right\} \quad (2.23)$$

The last processing step is to sum the values of all the distortion occurrences d_k recorded in the curtailed memory buffer $\widetilde{S_r}$ for the r^{th} IED in a data container C_r as seen in eqn. (2.24):

$$C_r = \sum_{p=1}^{|\widetilde{S_r}|} d_p \tag{2.24}$$

These synchronized datasets of fixed time frames containing distortion detection data from each of the different IEDs are then utilized for further data processing.

2) EVENT IMPACT ASSESSMENT

The first step in processing of the data collected and synchronized from different IEDs is to ascertain the nature of the event causing waveform distortions. Accurate assessment of the event causing distortions can help determine the extent of disruption it can cause to normal grid operations. A planned event like load switching will usually produce few distortions at that instant, which would not sustain over time. However, weather effects, degrading equipment or an incipient failure would lead to sustained distortions over a period until they cascade into a full-fledged fault or blackout. The key to differentiate between the harmless and harmful event is to determine certain thresholds for distortions detected in one cycle or a certain time frame. Violation of these thresholds would help in classifying the event causing distortions. Hence, interpreting the distortions recorded against thresholds gives us a fair idea about the impact of the event. So, in order to assess fairly the impact of an event, two parameters are used:

2.1) TIME-FRAME

It is necessary to determine a proper time frame or a time period in which the distortions would be recorded in a dataset as explained in eqn. (2.21). The time frame is the minimum time interval in which the distortions recorded, would be summed and then compared against thresholds. The determination of a reasonable time frame is critical for anticipating failures. Incipient failure signatures are usually by nature intermittent and do not follow a pattern. A very small time frame would lead to deluge of data which could unreasonably burden the available computing resources. A very small time–frame can also lead to inaccurate detection as incomplete or insufficient information in those time frames may bias the decision-making process. In comparison, a large time frame can delay the decision-making process, which could prevent us from anticipating the failure. A large time frame can also average out the distortions detected leading to non-violation of thresholds and compromise distortion detection sensitivity. Hence, an accurate determination of a time frame is very important. Time-frame determination can be influenced by several factors like sampling rates, grid layout or specific DSO based requirements. In FADS, time-frame determination is flexible and user-dependent.

2.2) THRESHOLD VIOLATIONS

Threshold violations are the key determiner of the negative impact of an event affecting the grid. Hence, thresholds determination should be based on a meticulous and exhaustive approach. In order to achieve that, the time-tested method of Monte-Carlo trials is used in FADS. Since a same event or incipient failure will not always produce type or extent of distortions, comprehensive stochastic process like Monte-Carlo trials are used to

consider all random eventualities of waveform distortions for accurate determination of thresholds. Monte-Carlo trials have been already used in distribution system reliability evaluation studies [61-62].

3) COORDINATED MONITORING

Before discussing about using the Monte-Carlo Trials to determine the thresholds, it is very important to introduce the concept of coordinated monitoring. In order to understand the premise of coordinated monitoring, it is considered that an incipient failure in the grid causing waveform distortions. The waveform distortions would have a high probability to be non-uniform across the entire grid. Hence, the measurement points close to the location of incipient failure will pick up higher distortions compared to the measurement points far from the location. This mismatch could lead to erroneous results. In case, the incipient failure is affecting a certain section of the grid, there should be enough observability to only conduct operations in that section of the grid instead of affecting the entire grid. On the other hand, it is also important to know if the incipient failure cascading has begun to affect grid operations in other non-affected sections. This creates a small dilemma as to how to monitor the distortions. It can be resolved by coordinated monitoring by smart analysis of the distortion data from different measurement points.

Coordinated monitoring comprises of two different levels of monitoring. The lower level is the Local Measurement Device (LMD) level to gauge the *intensity of the event affecting the grid operations* at the place of measurement. The higher level is the Distribution System (DS) level (comprising analysis of distortion data from all the measurement devices present in the grid) to gauge the *impact of the event*. LMD level monitoring depends on the distortions recorded by the standalone measurement device at that point. However, for DS level monitoring, the concept of *Common Reporting's* is introduced. The time stamped synchronized dataset can be analyzed to observe how many measurement devices in the grid are recording distortions at the same time, also called Common Reporting's. Common Reporting's helps to estimate how evenly the incipient failure is affecting the entire grid operations across the overall network. This knowledge further helps us to plan the response strategies accordingly.

However, there is an obvious disadvantage attached to DS level monitoring. For large distribution grid like IEEE-34 node feeder, some measurement points at certain section might even report zero distortions. This will lead to an overall zero common reporting, which will mislead the DSO operator to assume that grid is not being affected. Hence, in order to refine further the DS level monitoring, the concept of *Grid Zoning* is introduced. Grid Zoning aims to divide the network into multiple zones of observation to provide better situational awareness of the grid. Grid Zoning monitoring will depend on common reporting's of distortions recorded by measurement points installed in that particular zone.

To summarize, coordinated monitoring entails:

- **LMD LEVEL MONITORING:** Distortion recorded at local device at particular measurement point.
- **DS LEVEL MONITORING:** The concept of Common Reporting's is introduced. Common Reporting's are the number of distortions recorded by each

measurement point in the grid at the same time instant. Further subdivided into grid zoning.

- **DS - GRID ZONING LEVEL MONITORING:** Common Reporting's of distortions recorded by all measurement points in the particular defined grid zone.

4) MONTE-CARLO TRIALS - THRESHOLD DETERMINATION

In the bid to determine thresholds, two most common distribution grid events are considered, which do not pose any specific threat to grid operations. The events are load switching and capacitor switching. Load switching is a common occurrence in distribution grids to match the demand-supply curves. Capacitor switching is also common and important as they are often used to correct the power factor. Capacitor switching has a tendency to produce harmonics, which can cause distortions and mislead FADS classification. The load and capacitor switching are simulated at different parts of the distribution grid several times and the distortions are recorded at different measurement points.

4.1) SETUP

The distribution grids used for the Monte-Carlo trials as explained in previous section of this chapter are IEEE-13 and IEEE-34 node feeders. The grids with measurement points are shown in Figure 2.6 and Figure 2.7 respectively. The time frame for the dataset recording the waveform distortions is kept at 0.1s. It implies that after every 0.1s, the existing dataset would move to stage B and a new dataset would be simultaneously created in stage A to record waveform distortions and the process will continue. In order to maintain the consistency of the simulations and the associated results, the measurement points to record distortions and the time frame of the datasets are kept the same when implementing FADS in different simulation scenarios in subsequent chapters. In the FADS application results discussed in the subsequent chapters in this thesis, the time frame of 0.1s is also referred as reporting interval.

The measurement device placement nodes for IEEE-13 node feeder are at nodes 633, 645, 684 and 692. The measurement device placement nodes for IEEE-34 node feeder are at nodes 812, 818, 830, 846, 858 and 862. The choice of measurement point placements is such that balanced data collection can take place throughout the entire grid with reasonable number of measurement devices. Such an approach has been taken to strike a fine balance between accuracy and cost-effectiveness in real-field deployment of FADS. Optimal determination of measurement points and number of measurement devices to collect relevant incipient failure signatures according to grid topology would require elaborate optimization techniques. Development of such a technique would require exhaustive investigative studies in collaboration with different DSOs. Since such a study was outside the scope of this thesis work, the thesis does not claim to provide guidelines on optimal placement of measurement points. However, such optimization studies can be conducted in future to further improve FADS implementation.

Both the distribution systems have been divided in two grid zones. The approach to zoning has been to divide the distribution system equally in two parts. Zoning is done

such that both the zones have equal number of measurement devices. As explained for the choice of measurement point placement, optimal grid zoning would also require further studies and tests, which is outside the scope of this thesis. The aim of the thesis is to introduce the new concept of grid zoning in context of FADS and reasonably implement the approach in various simulation scenarios to highlight its benefits in enhancing situational awareness. In practice, the division of distribution network into zones should be based upon multiple factors like line length, load distribution, availability of maintenance teams etc. The ultimate decision of zoning will depend on a particular DSO and the grid network in question.

The grid zones defined here would be consistent throughout the implementation of FADS in this thesis. For IEEE-13 node feeder:

- **ZONE 1**: Grid zone with measurement devices at nodes 633 and 645.
- **ZONE 2**: Grid zone with measurement devices at nodes 684 and 692.

For IEEE-34 node feeder:

- **ZONE 1**: Grid zone with measurement devices at nodes 812, 818 and 830.
- **ZONE 2**: Grid zone with measurement devices at nodes 846, 858 and 862.

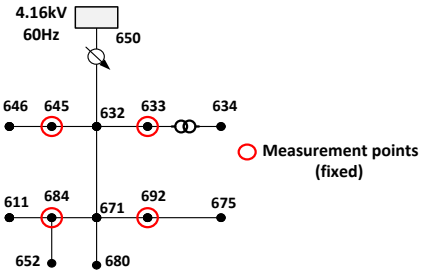

Figure 2.6: IEEE-13 Node Feeder with measurement points

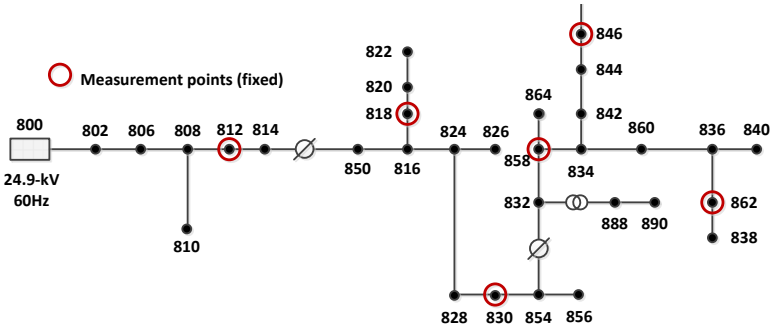

Figure 2.7: IEEE-34 Node Feeder with measurement points

4.2) MONTE-CARLO TRIALS - PLANNING

As discussed before, the Monte-Carlo trials are being conducted for load switching and capacitor switching events. In order to keep FADS comprehensive, both three-phase and two-phase load switching are simulated. Two-phase loads can cause unbalance in a three-phase system, hence it is necessary to consider waveform distortions from all eventualities. Similarly, capacitor switching scenarios are simulated by considering all three types of three-phase capacitor bank connections namely, star (Y) connected, delta (Δ) connected and star-ground (Y-G) connected. The loads and capacitors are separately positioned at different parts of the grid and the switching action takes place for a certain number of times. Some sections of the grid are strong and resilient to outside disturbances, while some are weak. Hence, same event at different sections of the grid can lead to different number of distortions. In order to factor in these occurrences, the positioning of events is moved such that it covers all different sections of the grid. An overview of the Monte-Carlo trials is presented in Table 2.1.

The incoming grid data recorded and analyzed are voltage waveforms. Compared to current waveforms, voltage waveforms are more resilient to distortions. Hence, distortion detection in voltage waveforms would be an enhanced test of FADS performance. Since voltage waveforms are more resilient, only events genuinely threatening grid operations usually produce noticeable distortions. Hence applying FADS in voltage waveforms should lead to comparatively more accurate event classification. There might be cases where current waveforms are better indicator of incipient failures. In such specific cases, the current measurement can be used by FADS or it can be implemented in parallel with other failure incipient technologies leveraging current measurements. The voltage waveforms are sampled at a rate of 128 samples per cycle, which is reasonable compromise between high-resolution and computing power requirements. Modern commercial digital fault recorder devices can record at sampling rates as high as 512 samples per cycle [63]. The analysis of voltage waveforms at 128 samples per cycle is kept consistent throughout the FADS implementation in this thesis.

The distortions recorded from switching events are recorded at the different measurement points. All the datasets reporting distortions are considered. It was found that generally the events of load and capacitor switching in the studies did not produce distortions after 0.3s of event commencement. Distortions recorded are summed and are represented as percentage of samples distorted to the total number of samples in each dataset containing distortion instances information for the time frame window of 0.1s (*also called reporting interval*). For example, in a 60Hz system with 128 samples/cycle sampling rate, there would be 768 samples in 0.1s. If 31 samples are reported to be distorted, then the percentage of distortion would be 4% approximately. As discussed in coordinated monitoring, the threshold determination is also done at two levels. The calculation of threshold at both levels is done for each Monte-Carlo trial for every switching event. The different levels of threshold determination are explained below.

TABLE 2.1
MONTE-CARLO TRIALS OVERVIEW

Load Switching

IEEE-13 Node Test Feeder

Types	Positions	No. of trials	Total trials
Two Phase (2-ϕ)	4	60	240
Three-Phase (3-ϕ)	4	60	240

IEEE-34 Node Test Feeder

Types	Positions	No. of trials	Total trials
Two Phase (2-ϕ)	9	60	540
Three-Phase (3-ϕ)	9	60	540

Capacitor Switching

IEEE-13 Node Test Feeder

Connection Type	Positions	No. of trials	Total trials
STAR	4	60	240
DELTA	4	60	240
STAR-GROUND	4	60	240

IEEE-34 Node Test Feeder

Connection Type	Positions	No. of trials	Total trials
STAR	9	60	540
DELTA	9	60	540
STAR-GROUND	9	60	540

TOTAL TRIALS = 3900

4.2.1) LMD LEVEL THRESHOLD

The LMD level threshold concerns with threshold determination at the local measurement device level. In this scenario, measurements from any one measurement point cannot be taken as reference as it will bias the calculation of the threshold. For each trial of the particular switching event, the measurement point recording highest percentage of distortions is considered. This distortion value consideration takes into view the highest recorded value so that the LMD thresholds are determined by taking into account the maximum negative effect the events can have on grid operations. Such an approach reduces false flag errors. An average percentage of distortions are then calculated for that particular event occurrence utilizing the total percentage value of highest recorded distortions and number of Monte-Carlo trials conducted to determine the LMD level thresholds.

4.2.2) DS LEVEL-GRID ZONE THRESHOLD

The DS level-Grid Zone threshold concerns with threshold determination of the different grid zones. In this scenario, at first the common reporting's of distortions recorded across all the measurement devices for each Monte-Carlo Trial of every switching event of both the zones are noted separately. This number is then converted into percentage value and then a final average percentage value for threshold of each grid zone of DS level is determined.

4.3) MONTE-CARLO TRIALS - EXECUTION

The large numbers of Monte-Carlo trials were simulated smoothly by creating a command script and executing it in the real-time environment of RTDS. A simple flowchart explaining the process for the estimation of the thresholds for capacitor switching based on the Monte Carlo trials has been shown in Figure 2.8. The same procedure will apply for load switching. As seen from Figure 2.9, the LMD level average percentage distortion values for IEEE-13 node feeder for load and capacitor switching are 2.1% and 4.8% respectively. Similarly, for IEEE-34 node feeder, the LMD threshold values for load and capacitor switching are 2.7% and 6.5% respectively. The DS-Grid Zone level threshold values for IEEE-13 node feeder, seen in Figure 2.10, for load switching are 0.8% for zone 1 and 1% for zone 2 respectively. The values for capacitor switching are 3.5% for zone 1 and 3.2% for zone 2 respectively. Similarly, in Figure 2.11, one can observe the DS-grid zone level threshold values for IEEE-34 node feeder. The values for load switching are 1.5% for zone 1 and 1.6% for zone 2. The values for capacitor switching are 4.1% for zone 1 and 4.6% for zone 2 respectively. The high voltage level of IEEE-34 node feeder might be one of the reasons for slightly high percentage of distortions compared to that of IEEE-13 node feeder. Other factors include capacitor rating, length of the grid etc. Hence, the bigger takeaway from this observation is that the threshold values are not universal in nature and should be recalibrated/optimized according to the system in question. Also, as expected, the average percentage of distortions is lower for Grid Zone level than LMD level. The obvious answer to such an occurrence is that the common reporting's across all devices in that particular zone for Grid Zone level threshold determination are considered, in comparison

to taking into account the highest number of distortions reported for LMD level threshold determination.

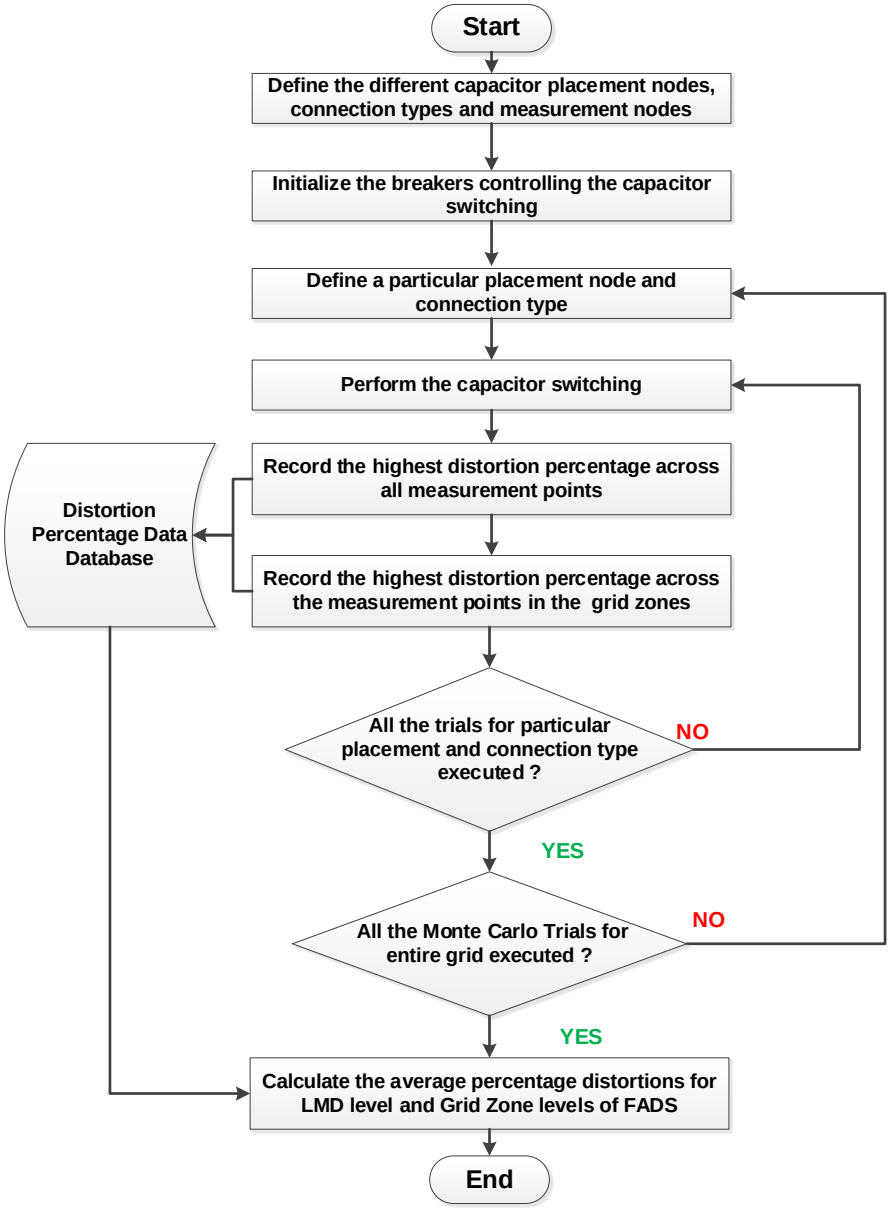

Figure 2.8: Monte Carlo Trial Flowchart for Capacitor Switching

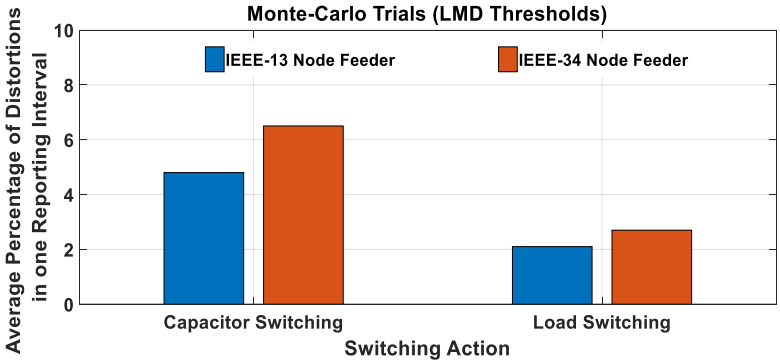

Figure 2.9: Monte-Carlo Trials LMD Threshold Determination

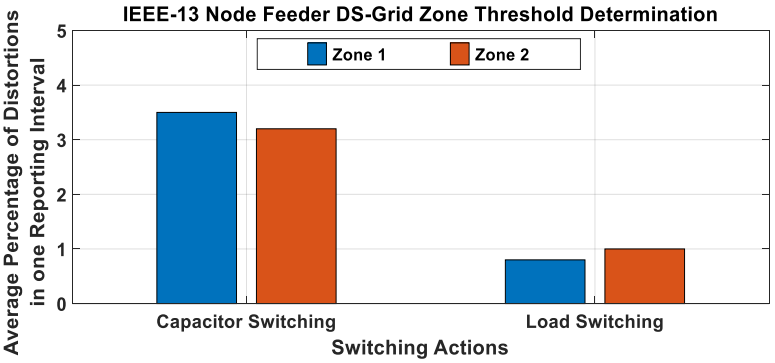

Figure 2.10: IEEE-13 Node Feeder DS-Grid Zone Threshold Determination

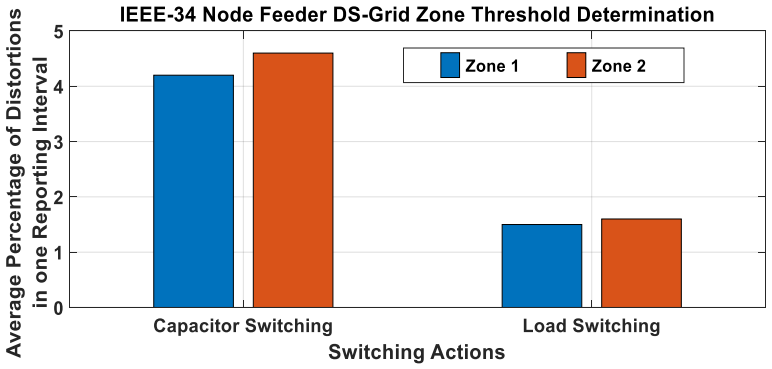

Figure 2.11: IEEE-34 Node Feeder DS-Grid Zone Threshold Determination

TABLE 2.2
FADS THRESHOLDS
(BOTH LMD AND DS-GRID ZONE LEVEL)

Test Feeder	Threshold Level	Threshold Value *(in percentage terms of total samples distorted in one dataset)*
IEEE-13 Node Feeder	**LMD**	**4.8%**
IEEE-13 Node Feeder	**DS Level - Grid Zone**	**3.5%**
IEEE-34 Node Feeder	**LMD**	**4.6%**
IEEE-34 Node Feeder	**DS Level - Grid Zone**	**6.5%**

In order to determine the threshold values for FADS implementation for the different test feeders, the highest average percentage of distortions value is considered. The same approach is considered for the different zones of the different test feeders and a same threshold value is set for all zones. Such a consideration reduces the chance of a false positive detection to a minimum. Table 2.3 summarizes the different threshold values for both LMD and DS-Grid Zone levels.

In summary, stage B forms an important functional block of FADS, where the incoming pre-processed data from stage A goes through synchronization and compared against thresholds at different levels so that more information can be gained about the event causing waveform distortions. The thresholds determined by Monte-Carlo studies give us an important and reliable parameter for distortion comparison, so that the classification between the harmful and non-harmful events can be reached. At the end of stage B, enough information has been extracted but there is a lack of refined interpretation to gain knowledge out of it. Stage C of FADS is responsible for that aspect.

C. STAGE C

Stage C is responsible for providing metrics so that we can interpret the incoming data from stage B to gain more knowledge on the severity of the event causing distortions and the possible location of the event in the grid. These two important knowledge parameters will help the DSO operators to plan a specific and precise response action.

1) SEVERITY RATING

It is not always enough to differentiate between events as harmful and non-harmful. A harmful event could be anything ranging from localized disturbance to a large-scale blackout affecting entire grid operations. A very harmful and severe event will cause numerous and sustained waveform distortions that would start reflecting in the measurement points in the entire grid with time but a relatively less severe event will cause fewer and localized waveform distortions. It is never a good idea to interrupt supply to the entire grid to fix comparatively less harmful localized grid events. The planning of the response actions also depends on how severe the event is. Faster mitigation response

in certain sections of the grid containing expensive components or having critical loads like hospital, train stations needs to be prioritized and the decision-making could be efficient if the severity of the event is known. Hence, there is a need of a severity rating to quantify the impact of the event at different sections of the grid. In order to achieve this quantification, the thresholds calculated in stage B are utilized. The severity rating as with the thresholds is also provided for two levels, LMD level and DS-Grid Zone level. In Table 2.3, the severity rating for both the levels can be seen. The interpretation and possible response action for the different severity levels is listed in Table 2.4.

In this subsection, the choice of severity rating scale and its interpretation leading to possible response action would be discussed in detail. Through the Monte-Carlo studies comprising of 3900 trials, the percentage of distorted samples for normal and common grid events was estimated. Using that as a baseline the severity rating scale was formulated. The planned load events are generally one-off events with negligible impact on grid operations. Hence, possible distortions due to load switching are kept as normal operation with a zero severity rating. A zero severity rating indicates the normal grid operation with no intervention needed as such. Capacitor switching, though relatively a harmless event, causes more distortions due to harmonics produced. Usually, it will not lead to any cascading effect but in order to be extra-cautious and have sufficient time in hand to prepare for a cascading effect, the percentage distortions of the capacitor rating have been rated 1 in severity rating scale. A severity rating of 1 would indicate normal grid operations but at the same time would also indicate to exercise caution by being on alert. Such a cautionary approach will help to keep a check for shift to higher severity ratings. The difference of percentage samples distorted in each reporting interval between load switching and capacitor switching events is around 3%-4% in our Monte-Carlo trials. Hence, a 4% buffer was used to differentiate between the different LMD severity rating levels. The overall percentage of distortions for Grid Zone level is less than LMD levels. Hence, for Grid Zone severity ratings, a slightly reduced buffer of 3% is used between the levels. The buffers are used throughout to define further levels and actions associated. In the empirical studies conducted, it was found that generally a single–phase to ground fault until 0.3s from the commencement of the fault had average percentage distortions in LMD levels ranging from 15% to around 35%. Hence, in the presented severity rating scale, keeping a margin of safety, anything beyond 11% in LMD levels is considered a full-scale fault and severity rating levels are not defined further than level 4.

The formulations discussed above are based on Monte-Carlo trials of the selected distribution systems. In real field implementation, such studies need to be conducted for any new grid topology to recalibrate FADS thresholds. In addition, in real power grids with high number of nodes, more than two levels of monitoring might be needed to achieve the desired observability and situational awareness. Hence, for coordinated monitoring the number of levels of monitoring is more dependent on the grid in question. The aim of the studies conducted in this thesis is to provide proof of concept of the contribution of different monitoring levels on the situational awareness of grid operations.

TABLE 2.3
SEVERITY RATING SCALE

LMD Level Rating	
IEEE-13 Node Test Feeder	
Percentage of distorted samples in each reporting interval	**Severity Rating**
< 3% distorted samples	**0**
(3-7)% distorted samples	**1**
(7-11)% distorted samples	**2**
> 11% distorted samples	**3**
IEEE-34 Node Test Feeder	
Percentage of distorted samples in each reporting interval	**Severity Rating**
< 4% distorted samples	**0**
(4-8)% distorted samples	**1**
(8-12)% distorted samples	**2**
> 12% distorted samples	**3**
DS-Grid Zone Level Rating	
IEEE-13 Node Test Feeder	
Percentage of distorted samples in each reporting interval	**Severity Rating**
< 2% distorted samples	**0**
(2-4)% distorted samples	**1**
(4-6)% distorted samples	**2**
> 6% distorted samples	**3**
IEEE-34 Node Test Feeder	
Percentage of distorted samples in each reporting interval	**Severity Rating**
< 3% distorted samples	**0**
(3-5)% distorted samples	**1**
(5-7)% distorted samples	**2**
> 7% distorted samples	**3**

TABLE 2.4
SEVERITY RATING INTERPRETATION
(BOTH LMD AND DS-GRID ZONE LEVEL)

Severity Rating Level	Interpretation	Possible Response
0	**Normal Operation *(Green Flag)***	**No intervention needed**
1	**Minimal Risk, some usual grid operations *(Yellow Flag)***	**On alert, to keep checking for change in severity rating**
2	**Definite risk, unusual happenings *(Orange Flag)***	**Plan adequate response and implement it**
3	**Major risk, fault occurrence imminent *(Red Flag)***	**Implement quickest response possible**

The average percentage of distortions for different zones for each IEEE-13 and IEEE-34 node feeders do not differ much. Hence, a uniform single Grid Zone severity rating levels has been formulated for simplified FADS implementation for both the benchmark test systems. The severity rating scale presented in this thesis is rudimentary in nature and not the ideal one. It is given as a proof of concept that in failure anticipation technologies, such a scale is needed to quantify properly the danger emanating from a particular incipient failure. As with other FADS parameters and thresholds, severity rating scale is also flexible and can be modified as per grid layout or DSO requirements. Additional alert levels and response actions linked to waveform magnitude levels can be added to it to make it more comprehensive. Similarly, the division of severity rating scales in accordance with the possible violation of thresholds was largely influenced from the Monte-Carlo studies conducted in this thesis. The severity ratings and the choice of buffer are flexible and may vary according to the grid but the concept is fundamental and would remain the same.

2) LOCATION

One of the most important factors for mitigating an incipient failure is to locate it. In absence of any inkling of the location of the event causing distortions, the response or the maintenance teams would have to scan the entire grid area. Such an exercise would be extremely time and resource consuming. As a result, the chances of incipient failure cascading to a full-fledged fault will increase manifold and the grid stability would be threatened. One of the additional benefits of the severity ratings scale is that the ratings can also help to locate the event. The grid zone level rating will help us identify the zone where the number of distortions reported is higher compared to other zones. Based on those observations, the search area would be reduced considerably. Hence, the response team can focus on locating the exact event location in a span of relatively smaller area in comparison to the entire geographical spread of the grid. Such an approach would also lead to better utilization of time and resources.

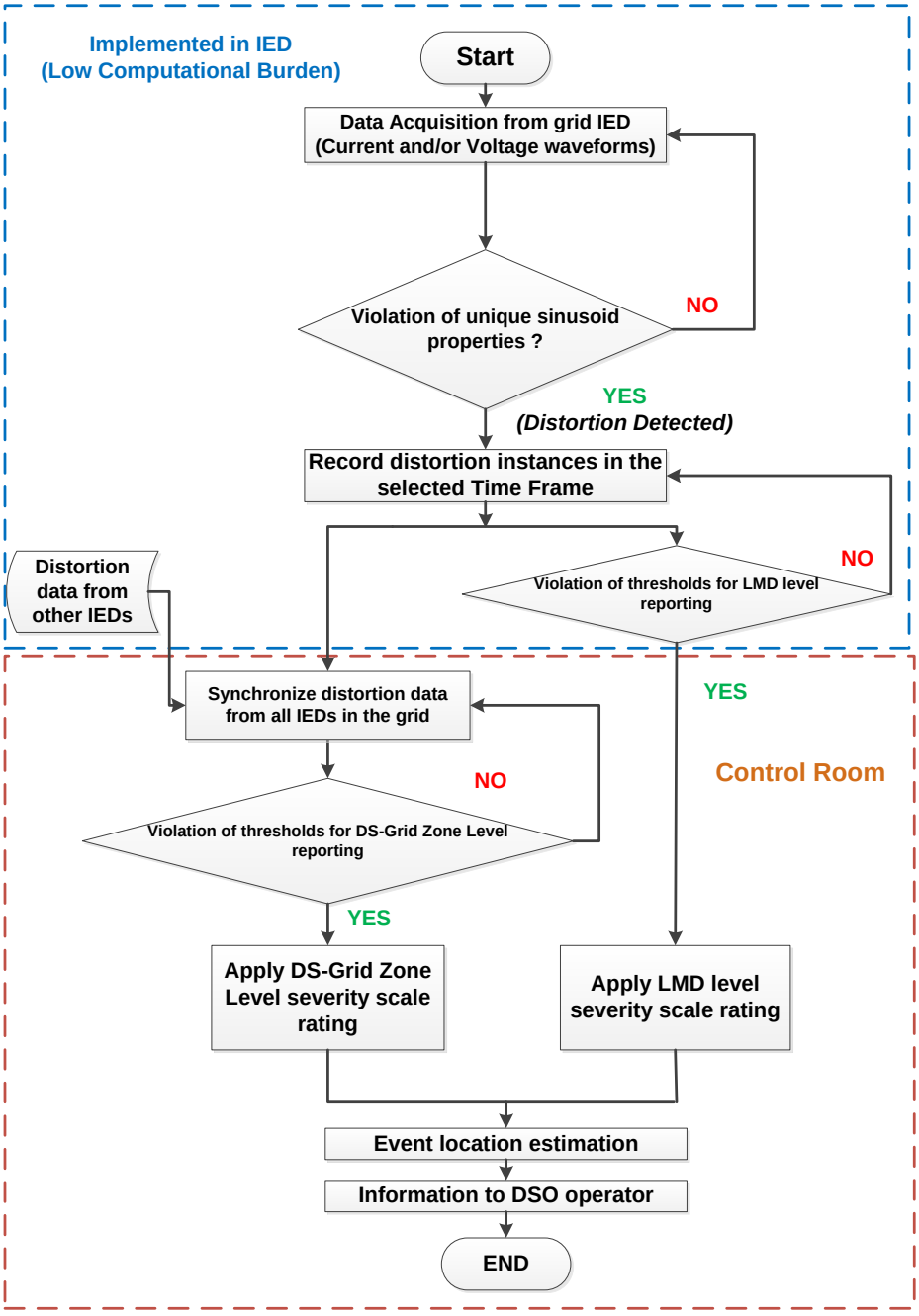

Figure 2.12: FADS Implementation Flowchart

The two-tier severity rating scales of LMD and Grid Zone level also complement each other. Let us consider a hypothetical situation where in the IEEE-34 node feeder system, an incipient failure is located between nodes 830 and 858. Such an event, located between two zones might be a challenging for the grid zoning proposed in this thesis as the measurement points ideally reporting highest number of distortions would be in two separate zones and the absence of common reporting's from other measurement points in the respective zones might lead to error in judgement. However, the high LMD level severity ratings at the measurement points would clearly indicate that the event is possibly located between the nodes 830 and 858. Hence, the area between nodes 830 and 858 is not a blind spot and LMD reporting can be used to locate possibly an incipient failure where the current grid zoning is apparently insufficient.

In summary, stage C mainly takes the processed data from stage B and extracts actionable knowledge from it. Stage C marks the last part of FADS implementation and the knowledge from stage C is to be transmitted to the grid operator at DSO level in real time. The input from stage C will help DSO anticipate failure, gauge the severity of the event and locate the area-span of the event in a time-efficient manner so that DSO's can plan adequate mitigation strategies. A simplified FADS implementation flowchart is present in Figure 2.12 to understand better the working process of FADS implementation.

2.5 REAL WORLD VS. LABORATORY IMPLEMENTATION

FADS is to be implemented ideally in real-time in field conditions. Stage A is itself implemented in the IEDs. The output of stage A is datasets with binary data of distortion detection i.e. zero if no distortion and 1, if there is a distortion. This output from all IEDs needs to be communicated to substations in order to be synchronized for stage B implementation of FADS. The IEC-61850 is the global standard for communication in substations and allows the integration of all protection, measurement and control actions [64]. The standard is meant to be interoperable implying that its implementation is universal and not restricted to any particular DSO. FADS intends to utilize this communication protocol and not burden substations with additional communication requirements. Since the communication would be of binary datasets, FADS intends to utilize the fast Generic Object Oriented Substation Event (GOOSE) protocol. Modern commercial IEDs are already implemented with these communication standards and protocols [65]. This eliminates extra costs of rewiring or reconfiguration of IEDs. The data processing in stage B and subsequent data interpretation of stage C is designed to be implemented in the control room of the substation. The final output of stage C is relayed to grid operator so that corrective actions can be planned.

However, in absence of any collaboration to implement FADS in real field conditions, FADS development and implementation across realistic test cases was conducted in real-time environment in laboratory conditions. Initial FADS implementation was conducted with simulating the cases in *RTDS* and then transferring the data from the waveforms to *MATLAB* [66], for distortion detection and data processing. The interfacing was done using a socket connection, which mimicked the suggested GOOSE protocol implementation in real field conditions. The medium of file exchange used for FADS implementation was the IEEE PSRC standardized, C37.111-1999 - IEEE Standard

Common Format for Transient Data Exchange (COMTRADE) [67], for data related to transient power system disturbances. In the latter stages of FADS development, the *C Builder* functionality of *RSCAD* software of *RTDS* system was used for modelling a custom power system component. This custom component was created and embedded with distortion detection and other data processing capabilities. The advantage of this approach was that interfacing across different systems were eliminated and the computational abilities of *RTDS* were utilized which made the FADS implementation faster in real time environment.

2.6 CONCLUSIONS

The FADS was introduced and its various stages of implementation were presented in this chapter. The mathematical formulation, identification of parameters, determination of thresholds, and assessment of event impacts associated with different stages of FADS implementation were presented and discussed in detail.

In the initial sections of this chapter, a comprehensive literature review of the existing failure anticipation technologies was presented. Despite recent developments, the lack of a holistic failure anticipation tool was highlighted. The main contribution of this chapter was to develop and introduce FADS as that tool and fill the research gap. FADS implementation is executed in three stages including both device level and system level deployment. The critical aspect of defining a waveform distortion in context of FADS and the mathematical formulations to support the theory of waveform distortion detection was provided in stage A. Stage B of FADS implementation involved using a system of pre-defined indicators, parameters and violation of certain thresholds to gauge the negative impact of event causing waveform distortions. Comprehensive stochastic tools like Monte-Carlo Trials were used to determine thresholds. Stage C provided metrics to accurately interpret the event damage potential and locate its area of occurrence. The working of these three stages in synchronization with each other helps to create comprehensive failure anticipation tool i.e. FADS and increases the overall situational awareness of the grid operations.

The low computational burden of FADS was highlighted by how FADS leverages fundamental mathematical properties of electrical waveforms to detect distortions instead of using complex mathematical approaches. The frugality of FADS is reflected from the fact that a part of FADS implementation involving data pre-processing can take place at the device level on the already existing IEDs while the rest of data processing can take place at substation level with limited resource consumption. There is no need as such of deploying additional FADS implementation specific devices on the grid. FADS integration on conventional protection devices can lead to the creation of a multi-purpose IED to tackle all protection issues in distribution grids. All these features of FADS further display the ease of implementation as claimed in the *Introduction* section of this chapter. The low computational burden and ease of implementation feature of FADS can serve as a major advantage when combining it with other expert systems or approaches in order to predict failures in power grid. Hence, FADS can be an easy and efficient fit in any larger failure prediction system consisting of a combination of multiple approaches.

To summarize, the structure and working of FADS is designed such that it can be implemented as a cost-effective, efficient comprehensive failure anticipation technology and detect faults where conventional systems fail. However, FADS performance is reliant to a considerable extent on correct determination of thresholds and severity levels as any misalignment could potentially lead to incorrect classification and wrong results. That being said, FADS is very flexible since most of the parameters are user-dependent which can be customized according to grid requirements and can be systematically improved over time. However, future studies should consider how thresholds and other parameters change with change in grid layout and voltage levels. In the subsequent chapters, FADS will be implemented across various scenarios mimicking real-life situations and its performance would be evaluated.

REFERENCES

[1] S. Kulkarni, D. Lee, A. J. Allen, S. Santoso, T. A. Short, "Waveform characterization of animal contact tree contact and lightning induced faults", *Proc. IEEE Power Energy Soc. Gen. Meeting*, Jul. 2010.

[2] T. S. Sidhu, Z. Xu, "Detection of incipient faults in distribution underground cables", *IEEE Transactions Power Del.*, vol. 25, no. 3, pp. 1363-1371, Jul. 2010

[3] C. Zhou, N. Zhou, S. Pan, Q. Wang, T. Li and J. Zhang, "Method of cable incipient faults detection and identification based on wavelet transform and gray correlation analysis," *2015 IEEE Innovative Smart Grid Technologies - Asia (ISGT ASIA)*, Bangkok, 2015, pp. 1-5.

[4] M. J. Mousavi and K. L. Butler-Purry, "Detecting Incipient Faults via Numerical Modeling and Statistical Change Detection," in *IEEE Transactions on Power Delivery*, vol. 25, no. 3, pp. 1275-1283, July 2010.

[5] X. Wang, Y. Song, "Sheath fault detection and classification based on wavelet analysis", *Eur.Trans. Elect. Power*, vol. 16, pp. 327-344, 2006.

[6] A. Lazkano, J. Ruiz, E. Aramendi, L. A. Leturiondo, "Evaluation of a new proposal for arcing fault detection method based on wavelet packet analysis", *Proc. IEEE Power Eng. Soc. Summer Meeting*, vol. 3, pp. 1328-1333, 2001-Jul.-1519.

[7] J. Seshadrinath, B. Singh and B. K. Panigrahi, "Incipient Interturn Fault Diagnosis in Induction Machines Using an Analytic Wavelet-Based Optimized Bayesian Inference," in *IEEE Transactions on Neural Networks and Learning Systems*, vol. 25, no. 5, pp. 990-1001, May 2014.

[8] J. Seshadrinath, B. Singh and B. K. Panigrahi, "Incipient Turn Fault Detection and Condition Monitoring of Induction Machine Using Analytical Wavelet Transform," in *IEEE Transactions on Industry Applications*, vol. 50, no. 3, pp. 2235-2242, May-June 2014.

[9] M. A. Hmida and A. Braham, "An On-Line Condition Monitoring System for Incipient Fault Detection in Double-Cage Induction Motor," in *IEEE Transactions on Instrumentation and Measurement*, vol. 67, no. 8, pp. 1850-1858, Aug. 2018.

[10] M. S. Naderi, G. B. Gharehpetian, M. Abedi and T. R. Blackburn, "Modeling and detection of transformer internal incipient fault during impulse test," in *IEEE Transactions on Dielectrics and Electrical Insulation*, vol. 15, no. 1, pp. 284-291, February 2008.

[11] B. Kasztenny, I. Voloh, C. G. Jones, G. Baroudi, "Detection of incipient faults in underground medium voltage cables", *Proc. 61st Annu. Conf. Protect. Relay Eng.*, pp. 349-366, Apr. 2008.

[12] W. Zhang, X. Xiao, K. Zhou, W. Xu, Y. Jing, "Multicycle incipient fault detection and location for medium voltage underground cable", *IEEE Transactions Power Del.*, vol. 32, no. 3, pp. 1450-1459, Jun. 2017.

[13] M. J. Mousavi, J. J. McGowan, J. Stoupis, V. D. Donde, *Apparatus and method for adaptive fault detection in MV distribution circuits*, Mar. 2013.

[14] C. J. Kim, J. H. Shin, M. Yoo, G. W. Lee, "A study on the characterization of the incipient failure behavior of insulators in power distribution line", *IEEE Transactions Power Del.*, vol. 14, no. 2, pp. 519-524, Apr. 1999

[15] S. Bhowmick, S. Nandi, "Online detection of an interturn winding fault in single-phase distribution transformers using a terminal measurement-based modeling technique", *IEEE Tranactions. Power Del.*, vol. 30, no. 2, pp. 1007-1015, Apr. 2015

[16] A. Razi-Kazemi, M. Vakilian, K. Niayesh, M. Lehtonen, "Circuit-breaker automated failure tracking based on coil current signature", *IEEE Transactions Power Del.*, vol. 29, no. 1, pp. 283-290, Feb. 2014.

[17] W. Bassi, H. Tatizawa, "Early prediction of surge arrester failures by dielectric characterization", *IEEE Elect. Insul. Mag.*, vol. 32, no. 2, pp. 35-42, Mar./Apr. 2016.

[18] P. A. Venikar, M. S. Ballal, B. S. Umre and H. M. Suryawanshi, "Transformer incipient inter-turn fault detection based on no-load current harmonic analysis," *2015 IEEE Eindhoven PowerTech*, Eindhoven, 2015, pp. 1-5.

[19] C. Wang, X. Liu and Z. Chen, "Incipient Stator Insulation Fault Detection of Permanent Magnet Synchronous Wind Generators Based on Hilbert–Huang Transformation," in *IEEE Transactions on Magnetics*, vol. 50, no. 11, pp. 1-4, Nov. 2014, Art no. 8206504.

[20] M. Jannati, B. Vahidi and S. H. Hosseinian, "Incipient Faults Monitoring in Underground Medium Voltage Cables of Distribution Systems Based on a Two-Step Strategy," in *IEEE Transactions on Power Delivery*, vol. 34, no. 4, pp. 1647-1655, Aug. 2019.

[21] B. Gao, R. Torquato, W. Xu and W. Freitas, "Waveform-Based Method for Fast and Accurate Identification of Subsynchronous Resonance Events," in *IEEE Transactions on Power Systems*, vol. 34, no. 5, pp. 3626-3636, Sept. 2019.

[22] A. S. Bretas, A. R. Herrera-Orozco, C. A. Orozco-Henano, L. U. Iurinic, J. Mora-Florez, "Incipient fault location method for distribution networks with underground shielded cables: A system identification approach", *Int. Trans. Elect. Energy Syst.*, vol. 27, no. 12, pp. 1-19, Dec. 2017.

[23] S. Kulkarni, S. Santoso and T. A. Short, "Incipient Fault Location Algorithm for Underground Cables," in *IEEE Transactions on Smart Grid*, vol. 5, no. 3, pp. 1165-1174, May 2014.

[24] D. R. Morais, J. G. Rolim, "A hybrid tool for detection of incipient faults in transformers based on the dissolved gas analysis of insulating oil", *IEEE Transactions Power Del.*, vol. 21, no. 2, pp. 673-680, Apr. 2006.

[25] J. Jiang, R. Chen, M. Chen, W. Wang, C. Zhang, "Dynamic fault prediction of power transformers based on hidden Markov model of dissolved gases analysis", *IEEE Transactions Power Del.*, vol. 34, no. 4, pp. 1393-1400, Aug. 2019.

[26] Experiences in the interpretation of incipient faults in power transformers by dissolved gas-in-oil chromatography analysis (A Progress Report)", Proc. Minutes Forty-Second Int. Conf. Double Clients, 1975.

[27] S. A. Wani, D. Gupta, M. U. Farooque and S. A. Khan, "Multiple incipient fault classification approach for enhancing the accuracy of dissolved gas analysis (DGA)," in *IET Science, Measurement & Technology*, vol. 13, no. 7, pp. 959-967, 9 2019.

[28] T. Ghanbari, "Kalman filter based incipient fault detection method for underground cables," in IET Generation, Transmission & Distribution, vol. 9, no. 14, pp. 1988-1997, Oct. 2015.

[29] M.F. Faisal, A. Mohamed, H. Shareef, "Prediction of incipient faults in underground power cables utilizing S-transform and support vector regression", *Int. J. Electr. Eng. Inf.*, vol. 4, no. 2, pp. 186-201, 2012.

[30] K. L. Butler-Purry, J. Cardoso, "Characterization of underground cable incipient behavior using time-frequency multi-resolution analysis and artificial neural networks", *Proc. IEEE Power Energy Soc. General Meeting Convers. Del. Elect. Energy 21st Century*, pp. 1-11, 2008.

[31] S. Ebron, D. L. Lubkeman and M. White, "A neural network approach to the detection of incipient faults on power distribution feeders," in *IEEE Transactions on Power Delivery*, vol. 5, no. 2, pp. 905-914, April 1990.

[32] A. Kumar, "A neural network approach to the detection of incipient faults on power distribution feeders", *Middle-East J. Sci. Res.*, vol. 20, no. 7, pp. 799-803, 2014.

[33] Y. Wang, H. Lu, X. Xiao, X. Yang and W. Zhang, "Cable incipient fault identification using restricted Boltzmann machine and stacked autoencoder," in *IET Generation, Transmission & Distribution*, vol. 14, no. 7, pp. 1242-1250, 14 4 2020.

[34] IEEE *Recommended Practice for Monitoring Electric Power Quality*, IEEE Standard 1159-2009, 2009.

[35] B. Li, Y. Jing and W. Xu, "A Generic Waveform Abnormality Detection Method for Utility Equipment Condition Monitoring," in *IEEE Transactions on Power Delivery*, vol. 32, no. 1, pp. 162-171, Feb. 2017.

[36] A. F. Bastos and S. Santoso, "Condition Monitoring of Circuit Switchers for Shunt Capacitor Banks Through Power Quality Data," in *IEEE Transactions on Power Delivery*, vol. 34, no. 4, pp. 1499-1507, Aug. 2019.

[37] T.E. Grebe, "Effective collection and management of power quality data for analysis and detection of incipient distribution system components faults and identification of their locations," CEATI Report No. T124700-5159, Sep. 2013.

[38] L. A. Irwin, "Real experience using power quality data to improve power distribution reliability," *Proceedings of 14th International Conference on Harmonics and Quality of Power - ICHQP 2010*, Bergamo, 2010, pp. 1-4.

[39] IEEE Working Group on Power Quality Data Analytics, Tech. Rep. 73: Electrical signatures of power equipment failures. Dec 2019. [online] Available: http://grouper.ieee.org/groups/td/pq/data/.

[40] G. W. Chang, Y. Hong and G. Li, "A Hybrid Intelligent Approach for Classification of Incipient Faults in Transmission Network," in *IEEE Transactions on Power Delivery*, vol. 34, no. 4, pp. 1785-1794, Aug. 2019.

[41] Hydro Quebec, MILE, [online], Available: http://www.hydroquebec.com/innovation/en/pdf/2010G080-26A-MILES.pdf

[42] Distribution Fault Anticipator Phase I: Proof of Concept Final Report, Palo Alto, CA, EPRI Publ. 1001879, pp. 120, Dec. 2001.

[43] Distribution Fault Anticipator Phase II: Algorithm Development and Second-Year Data Collection, Palo Alto, CA, EPRI Publ. 1010662, pp. 58, Nov. 2005.

[44] Distribution Fault Anticipator Phase III: System Integration, Technical Update, Palo Alto, CA, EPRI Publ. 1012435, pp. 48, Dec. 2006.

[45] J. A. Wischkaemper, C. L. Benner, B. D. Russell and K. Manivannan, "Application of Waveform Analytics for Improved Situational Awareness of Electric Distribution Feeders," in *IEEE Transactions on Smart Grid*, vol. 6, no. 4, pp. 2041-2049, July 2015.

[46] B. D. Russell and C. L. Benner, "Intelligent Systems for Improved Reliability and Failure Diagnosis in Distribution Systems," in *IEEE Transactions on Smart Grid*, vol. 1, no. 1, pp. 48-56, June 2010.

[47] B. D. Russell, C. L. Benner, R. M. Cheney, C. F. Wallis, T. L. Anthony and W. E. Muston, "Reliability improvement of distribution feeders through real-time, intelligent monitoring," *2009 IEEE Power & Energy Society General Meeting*, Calgary, AB, 2009, pp. 1-8.

[48] J. S. Bowers, A. Sundaram, C. L. Benner, B. Don Russell, "Outage avoidance through intelligent detection of incipient equipment failures on distribution feeders", *Power & Energy Soc. 2008 General Meeting*, July-20-24, 2008.

[49] K. Manivinnan, C. L. Benner, B. D. Russell and J. A. Wischkaemper, "Automatic identification, clustering and reporting of recurrent faults in electric distribution feeders," 2017 19th International Conference on Intelligent System Application to Power Systems (ISAP), San Antonio, TX, 2017, pp. 1-6.

[50] J. A. Wischkaemper, C. L. Benner, B. D. Russell and K. M. Manivannan, "Waveform analytics-based improvements in situational awareness, feeder visibility, and operational efficiency," *2014 IEEE PES T&D Conference and Exposition*, Chicago, IL, 2014, pp. 1-5.

[51] C. L. Benner, R. A. Peterson and B. D. Russell, "Application of DFA Technology for Improved Reliability and Operations," *2017 IEEE Rural Electric Power Conference (REPC)*, Columbus, OH, 2017, pp. 44-51.

[52] J. A. Wischkaemper, C. L. Benner and B. Don Russell, "A new monitoring architecture for distribution feeder health monitoring, asset management, and real-time situational awareness," *2012 IEEE PES Innovative Smart Grid Technologies (ISGT)*, Washington, DC, 2012, pp. 1-7.

[53] C. L. Benner and B. D. Russell, "Distribution incipient faults and abnormal events: case studies from recorded field data," *57th Annual Conference for Protective Relay Engineers, 2004*, College Station, TX, USA, 2004, pp. 86-90.

[54] K. P. Schneider *et al.*, "Analytic Considerations and Design Basis for the IEEE Distribution Test Feeders," in *IEEE Transactions on Power Systems*, vol. 33, no. 3, pp. 3181-3188, May 2018.

[55] B. M. Aucoin and B. D. Russell, "Distribution High Impedance Fault Detection Utilizing High Frequency Current Components," in *IEEE Power Engineering Review*, vol. PER-2, no. 6, pp. 46-47, June 1982.

[56] *Real Time Digital Simulator (RTDS)*, [online], Available: http://www.rtds.com/

[57] D. Sabolic, "On the distribution network narrowband noise statistics," in *IEEE Transactions on Power Delivery*, vol. 18, no. 1, pp. 66-68, Jan. 2003.

[58] L. Euler, "De summis serierum reciprocarum ex potestatibus numerorum naturalium ortarum dissertatio altera." *Miscellanea Berolinensia* **7**, pp. 172-192, 1743.

[59] L. Euler, *Introductio in Analysin Infinitorum, Vol. 1*. Bosquet, Lucerne, Switzerland: pp. 104, 1748.

[60] J. H. Conway, and R. K. Guy, "Euler's Wonderful Relation." *The Book of Numbers.* New York: Springer-Verlag, pp. 254-256, 1996.

[61] R. Billinton and Peng Wang, "Teaching distribution system reliability evaluation using Monte Carlo simulation," in *IEEE Transactions on Power Systems*, vol. 14, no. 2, pp. 397-403, May 1999.

[62] G. T. Heydt and T. J. Graf, "Distribution System Reliability Evaluation Using Enhanced Samples in a Monte Carlo Approach," in *IEEE Transactions on Power Systems*, vol. 25, no. 4, pp. 2006-2008, Nov. 2010.

[63] Reason DR60 Digital Fault Recorder, General Electric Grid Solutions, [online], Available: https://www.gegridsolutions.com/measurement_recording_timesync/catalog/dr60.htm

[64] IEEE Recommended Practice for Implementing an IEC 61850-Based Substation Communications, Protection, Monitoring, and Control System," in IEEE Std 2030.100-2017 , vol., no., pp.1-67, 19 June 2017.

[65] P. Palensky and D. Dietrich, "Demand Side Management: Demand Response, Intelligent Energy Systems, and Smart Loads," in *IEEE Transactions on Industrial Informatics*, vol. 7, no. 3, pp. 381-388, Aug. 2011.

[66] *MATLAB (R2017b)*, [online], Available: https://www.mathworks.com/

[67] IEEE Standard Common Format for Transient Data Exchange (COMTRADE) for Power Systems," in IEEE Std C37.111-1999 , vol., no., pp.1-55, 15 Oct. 1999.

[68] R. Bhandia, J. D. J. Chavez Muro, M. Cvetkovic and P. Palensky, "High Impedance Fault Detection using Advanced Distortion Detection Technique," in *IEEE Transactions on Power Delivery*, doi: 10.1109/TPWRD.2020.2973829.

[69] R. Bhandia, M. Cvetković and P. Palensky, "Improved Grid Reliability by Robust Distortion Detection and Classification Algorithm," *2018 IEEE PES Innovative Smart Grid Technologies Conference Europe (ISGT-Europe)*, Sarajevo, 2018, pp. 1-6.

[70] R. Bhandia, J. J. Chavez, M. Cvetkovic and P. Palensky, "High Impedance Fault Detection in Real-Time and Evaluation Using Hardware-In-Loop Testing," *IECON 2018 - 44th Annual Conference of the IEEE Industrial Electronics Society*, Washington, DC, 2018, pp. 182-18.

CHAPTER 3

HIGH IMPEDANCE FAULT DETECTION AND SENSITIVITY ANALYSIS

3.1 INTRODUCTION

HIFs mainly occur when an electrical conductor breaks and makes unwanted contact with high impedance objects like concrete, asphalt, grass etc. HIFs generally do not develop over time as an incipient failure before striking with full impact. A damaged wire or failing conductor will usually continue to fail over time and manifest as incipient failure before the fully damaged conductor leads to an HIF. Investigation of such incipient failures related to equipment damage by FADS can prevent such a situation but if somehow HIF still manages to occur in the grid, it is important to detect it fast and take corrective actions. An undetected HIF can be extremely hazardous as it might result in an electrified conductor exposed to public [1].

HIFs by nature are highly unpredictable and characterized by random and asymmetric behavior. The low fault current drawn by HIFs is not enough to trigger traditional overcurrent relays. In effectively grounded distribution systems, the HIF fault current values typically range between (0-75) A. Table 3.1 lists the different fault currents on various surfaces as documented in [2]. As a result, conventional protections schemes underperform in detecting HIFs. According to the report compiled by Power System Relaying Committee (PSRC), from the 200 HIF events staged over a period of time, only 35 were detected and cleared by conventional protection systems [2], which is a detection rate of 20%. In a study conducted on the Brazilian electrical distribution grid in 2013-14, it was found that HIFs are the third major cause of electrical accidents and there is an urgent need for reliable solutions to detect and locate HIFs [3]. The unstable nature of HIF implies that it does not follow any specific patterns, which make HIF detection more difficult. Despite several studies conducted over decades, there is a still a lack of a reliable, comprehensive and widely accepted HIF detection scheme, which can be implemented in real-time.

In context of FADS implementation also, HIF makes for an interesting and compelling study case. The unstable and nonlinear nature of HIF might or might not produce specific

Parts of this chapter have been published in IEEE Transactions on Power Delivery journal [71].

TABLE 3.1
TYPICAL HIF CURRENT FOR DIFFERENT SURFACES (12.5 KV FEEDER)

Surface	HIF current (A)
Dry Sand or Dry Asphalt	0
Wet Sand	15
Dry Sod	20
Dry Grass	25
Wet Sod	40
Wet Grass	50
Reinforced Concrete	75

patterns but it invariably leads to distortions in the electrical waveforms. Hence, HIF detection provides an opportunity for FADS to display its efficacy to complement the working of conventional protection schemes and highlight the dual functionality of FADS.

3.2 STATE-OF-THE-ART

The studies based on developing HIF detection techniques can be broadly grouped in three main categories, the first two categories are domain-based, namely: time-domain and frequency-domain algorithms. The third category consists of techniques based on combining algorithms/tools to obtain the desired effect. Traditional time-domain based techniques used for HIF detection include the use of processing tools based on mathematical morphology to detect HIF [1], comparison of negative and positive current peaks to calculate current flicker and determine asymmetry in fault current [4], extracting signatures from current waveforms by observing change in ratio between substation and line ground resistances during HIF [5], ratio ground relaying based techniques [6], analyzing chaotic properties of HIF by fractal geometry techniques [7], transient analysis of disturbances to observe change in crest factor [8] and superimposition of voltage signals of certain frequencies to detect HIF signatures [9]. In [10-12], estimated parameters of an assumed HIF are used to detect and locate real-life HIF. The nonlinear voltage-current characteristic prolife of HIF has been leveraged in [13] to detect HIF.

Traditional frequency-domain based techniques include monitoring of feeder current to find burst noise signal indicating HIF event [14], a range of different algorithms based on lower order harmonics are used to detect HIF in [15-20], harmonic energy and waveform distortion based technique in [21], inter-turn harmonics based technique in [22] and strong harmonic based detection and location based in [23]. High frequency components based HIF detection techniques have been used in [24-26]. Fourier analysis based technique has been used in [27]. HIF detection techniques involving combination of time and frequency domains include Hilbert-Huang transform based techniques [28], wavelet transform based techniques in [29-35] and time-frequency analysis method in [36].

In recent times, artificial intelligence and learning based methods have been extensively used for HIF detection. Pattern recognition based methods have been used

exclusively in [37-39] and expert system in [40] to identify and conduct analysis of possible HIF specific features. Several learning techniques involving algorithms based on decision-tree techniques [41], ANN based methods [42-44], neural networks [45-47] and fuzzy logic [48-50] have been used to detect HIF. Wavelet transformation along with pattern recognition has been used in [51-52] to extract HIF features in order to detect them. Hilbert-Huang transform along with ANN based technique has been used in [53]. KLD based technique has been used in [54]. The Kalman filtering based techniques have been used in [55-56] to overcome certain shortcomings of Fourier analysis. Several other HIF detection techniques found in [57-59] involve combination of multiple tools but they cannot be grouped under one common category of detection. An exhaustive study of the HIF detection techniques has been well documented in [60]. In practical terms, General Electric (GE) and Schweitzer Engineering Laboratories (SEL) have implemented the high impedance fault detection algorithms developed by research conducted in EPRI [61], in their digital relays.

The above-discussed HIF techniques have different success rates but a comprehensive HF detection technology is still missing. Some techniques target specific HIF properties that might not always produce reliable results due to the nonlinear nature of HIF. The mathematical complexity and resource requirements of some techniques affect their swiftness of operation and accuracy. Majority of techniques provide no concrete suggestion on how HIF can also be located based on detection results.

3.3 HIF MODEL

The most important thing for HIF detection studies is an accurate HIF model. An accurate HIF model will help to simulate HIFs as accurate and realistic as possible. Evaluating performance of algorithms against such model is always desired for accurate assessment. However, the random nature of HIF makes it difficult to develop accurate models. Some models like Mayr's [62] and Cassie's [63] models are adept in modeling the arcing

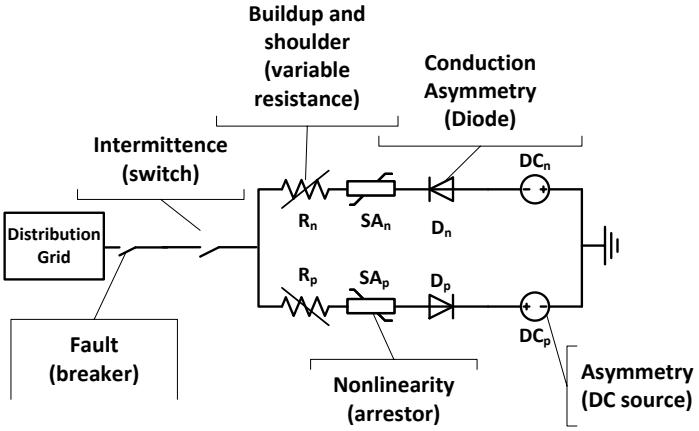

Figure 3.1: HIF Model

characteristics of HIF. Improvements of those models are the Schavemaker [64] and Schwarz [65] arc models. However, arc models mainly base their model on heat accumulation theory and may not be suitable for stable HIFs. In recent studies, nonlinear resistance based models have been used to emulate the nonlinear behavior of HIF. Such models have been improved with usage of power electronics, diodes and DC voltage sources to increase the randomness and asymmetry as observed in [1]. The model in [1] is adaptation of the HIF model used for staged real-field event in [4]. In this thesis, we adapt the model and remodel in RTDS environment. The HIF model can be seen in Figure 3.1. The different components of the model are explained in subsequent subsection.

The remodeling of HIF model in RTDS has been done such that typical HIF current characteristic as explained in [33] are preserved. The typical HIF current characteristics are:

- *Build-up*: The gradual increase of the current amplitude to its maximum.
- *Shoulder*: The period in which the build-up stops and current amplitude remains constant.
- *Asymmetry*: Fault current having different random peak values for positive and negative half-cycles.
- *Nonlinearity*: Current value changes randomly from cycle to cycle resulting in a nonlinear voltage-current characteristic curve.
- *Intermittence*: The time-period of arcing between two bursts.

The HIF model shown in Figure 3.1 consists of two DC sources (DC_N and DC_P) whose magnitudes are different from each other to produce the magnitude asymmetry between the positive and negative half-cycles. The DC sources are connected to a pair of diodes (D_N and D_P) that produce an asymmetric conductance due to voltage differences in their terminals. The diodes are connected to a pair of surge arrestors (SA_p and SA_n), which are responsible for producing the nonlinear characteristics. The surge arrestors are connected in turn to time variant resistances (R_p and R_n). The magnitude of such time-variant resistances is varied to create the buildup and shoulder characteristics similar to the transient analysis control (TACS) used in [32], [33] and [66]. Finally, the variable resistors are connected to the distribution grid via single switch that produces the intermittence. In Figure 3.2, the HIF current characteristics can be seen with intermittence around 0.1s and the build-up and shoulder characteristics starting around 0.3s.

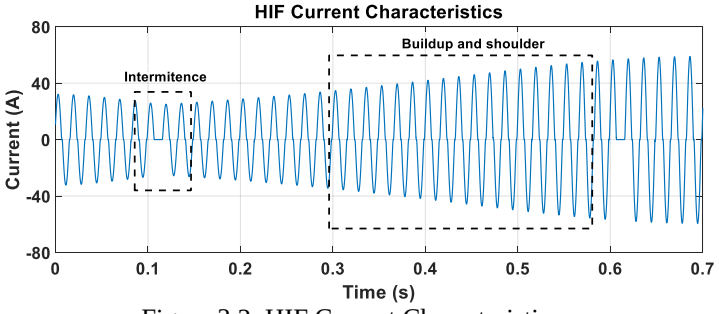

Figure 3.2: HIF Current Characteristics

The HIF model is implemented for both IEEE-13 and IEEE-34 node feeders. Since they have different voltage levels, the HIF model components are varied accordingly to achieve the desired HIF current characteristics. The resistances R_n and R_p have random variation from a minimum of 1Ω to maximum 56Ω. The ideal diodes, D_N and D_P have resistances of 0.01Ω and 0.001Ω respectively. DC_N and DC_P are the DC sources with voltage range of (0-5) V.

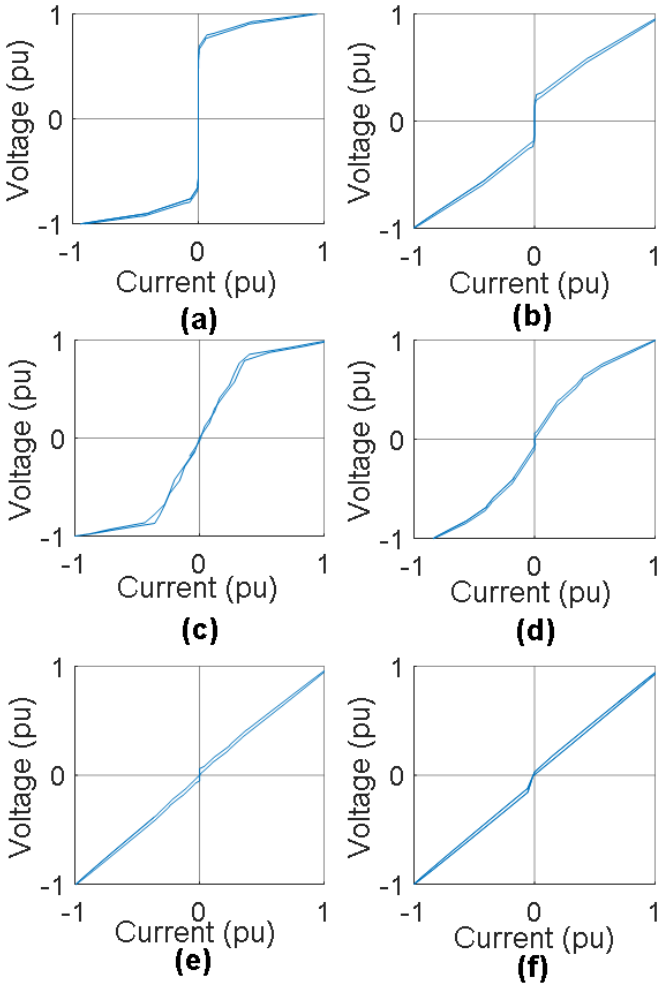

Figure 3.3: Different HIF V-I Characteristics obtained from the same HIF model resembling real-field data: (a) Concrete, (b) Wet grass, (c) Dry tiles, (d) Damp sand, (e) Dry rubber and (f) Damp tiles [4, 13].

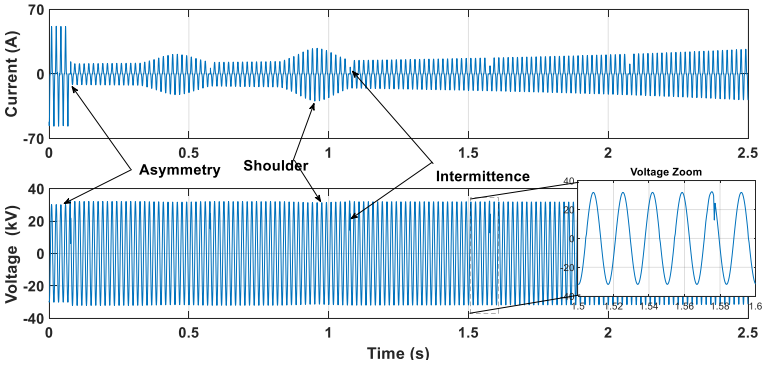

Figure 3.4: Current and Voltage waveforms for HIF for concrete surface.

As observed in Table 3.1, HIF currents can be different for different surfaces. The surfaces have different resistances and accordingly the HIF current value will change. The Voltage-Current (V-I) characteristics are a useful parameter to monitor those subtle changes. The non-linearity element in the HIF model is varied to get the different V-I characteristics for different surfaces. The different V-I characteristics can be seen in Figure 3.3. The characteristics obtained are similar to those obtained from real field tests in [4] and [13]. As can be seen from Figure 3.3, the HIF for surfaces with high fault currents have their V-I characteristics quite flat near zero implying low impedance and vice-versa. The HIF current and corresponding voltage waveforms for the concrete surface can be observed in Figure 3.4.

3.4 SIMULATION CASES

The nature and characteristics of HIF are such that the waveform distortions arising due to it can be wrongly attributed to other common grid events like load switching, capacitor switching, feeder energization etc. On the other hand, it is also important to be able to distinguish and detect HIF in case both the HIF and normal switching actions have taken place at the same time. Hence, in or simulation cases, the robustness of FADS is evaluated to both false positives and false negatives. In majority of the HIF detection methods discussed before, the standard test of algorithm robustness is to differentiate HIF from switching events. Recent articles have started to include simulation cases involving events like motor starting. In this thesis, most of such events have been considered and divided into short transient and long transient events. The different HIF currents from different

TABLE 3.2
SIMULATION CASE EVENT PLACEMENT NODES

Short Transient Events

IEEE-34 Node Test Feeder

Simulation Case	Scenario	HIF node	2-ϕ load node	3-ϕ Capacitor node
I. Robustness to false positives	A	-	816	836
	B	-	854	834
	C	-	-	-
II. Robustness to false negatives	A	854	836	816
	B	834	836	854

IEEE-13 Node Test Feeder

Simulation Case	Scenario	HIF node	2-ϕ load node	3-ϕ Capacitor node
III. Robustness to false positives	A	-	646	634
	B	-	680	671
IV. Robustness to false negatives	A	675	646	634
	B	675	680	671

Long Transient Events

IEEE-13 Node Test Feeder

Simulation Case	HIF node	Motor node	Feeder Energization Switch
V. Motor Starting	675	634	-
VI. Feeder Energization	675	-	Between node 632 and node 671

Sensitivity Test

IEEE-13 Node Test Feeder

Simulation Case	HIF Node
VII. Sensitivity Test	675

based on waveforms distortion detection, it is imperative to conduct a sensitivity analysis of FADS performance for HIF fault currents from different surfaces. Hence, a sensitivity test of FADS performance for HIF fault current from different surfaces has also been conducted. The different simulation cases along with event placement points for HIF detection can be seen in Table 3.2. The measurement points for the different test systems remain the same as explained in Chapter 2.

The short transient event is simulated for both IEEE-13 and IEEE-34 node feeders. However, the long transient event and sensitivity test are conducted only for IEEE-13 node feeder. Such an approach is followed because based on the IEEE PSRC report cited in [2], HIF has a much higher probability of occurring in systems of voltage rating of 15 kV and below. Hence, the IEEE-13 node feeder was deemed more relevant for performing additional robustness tests of FADS.

A. SHORT TRANSIENT EVENTS

Short transient events can be defined as grid events which occur over a small time - period and the effects can be felt only for few cycles. Usually, the events are switching events and the effect on grid operations, if any, do not sustain over time. Such events are generally planned and harmless to the stable operations of the grid. In this thesis, the load and capacitor switching are considered as short transient events.

1) ROBUSTNESS TO FALSE POSITIVES

Load switching is a temporary event, which might produce distortions in few samples of the waveform at the instant of switching but the distortions will not sustain over time and severity rating thresholds will not be violated. Capacitor switching also leads to temporary high frequency oscillatory transients causing momentary waveform distortions but the effect does not last long after the switching event is over. HIF event, if not cleared will lead to continuous generation of low fault current with usually all the characteristics as seen in Figure 3.3. Such an occurrence will lead to rather sustained but varying distortions of the waveforms. However, as the differences are generally small to achieve clear distinction between the events, load or capacitor switching has the potential to mislead FADS into identifying them as events harmful to grid. Hence, FADS implementation should be robust against such false positives and not identify them as potentially harmful events.

In order to increase the complexity for FADS implementation to get a more enhanced and stringent test of FADS robustness, the test for robustness is created by simulating both load and capacitor switching at the same time in order to increase the chance of false detection. The complications are notched up a grade further when the events are simulated for two scenarios (A and B); these scenarios differ by event placement points as shown in Table II. In scenario B, the events happen at close proximity to each other, while in scenario A the events are geographically distant from each other. In Scenario B, the closer geographical proximity of event occurrences would have a combined effect and invariably lead to higher number of distorted samples at the near-by measurement devices. As a result, there is a high possibility of measurement points going up on the severity scale. This increase in severity scale can mislead FADS in deducing normal switching

events as possibly harmful event. Hence, scenario B has a significantly greater chance of leading FADS to a false positive detection and serves as the ultimate test of FADS robustness.

The complicated simulation cases with even more stringent scenarios to evaluate the robustness of any technique designed for HIF detection is novel and has not been yet used in evaluation of any other HIF detection technique to the best knowledge of the author. The scenarios discussed are also implemented for the rest of the simulation cases involving FADS implementation for HIF detection.

Harmonics resulting from events other than incipient failures or HIF also have the potential to distort the waveforms. However, occurrence of such harmonics would be generally rare and not enough to trigger FADS thresholds. For voltage waveforms in a system below 69kV, the IEEE standards recommend 3% distortion limit of individual harmonics and a 5% Total Harmonic Distortion (THD) limit [67]. Hence, FADS should be insensitive to false positives from harmonic distortions within the prescribed limits. The test of robustness of FADS to harmonics distortion forms Scenario C for the simulation case I.

2) ROBUSTNESS TO FALSE NEGATIVES

As important as it is to be robust against false positives, it is also important to be robust against false negatives and detect HIF accurately. In this simulation case, the robustness of FADS to false negatives is investigated, i.e. the ability to FADS to distinguish and detect HIF even when normal grid events like load and capacitor switching are simulated at the same time as HIF. This simulation case is also performed for two scenarios with events happening at close proximity to each other in scenario B. As for false positives, Scenario B also acts as the ultimate test for FADS for false negatives also. In this case, the main challenge is to locate accurately the HIF, especially in Scenario B.

B. LONG TRANSIENT EVENTS

Normal grid events, whose effects can be felt for a considerably longer period after its commencement can be termed as long transient event. The events generally lead to longer and continuous distortions. The extent of distortions produced by such events might vary but the time period through which the distortions extend has the potential to mislead FADS detection of HIF. In this thesis, motor start and feeder energization are considered as long transient events.

1) ROBUSTNESS TO MOTOR STARTING

Motor starting is a common occurrence in distribution grids and takes longer to reach steady state than events like load or capacitor switching. Hence, in this simulation case the robustness of FADS is evaluated to motor starting. Since, majority of the dynamic loads in power systems are induction machines [68], an induction machine with parameters from [69] has been used in our simulation studies. The motor is connected at node 634 while HIF is simulated at node 675 for IEEE-13 node feeder as seen in Table 3.2. The HIF and motor starting is simulated at the same time to increase the complexity of detection for FADS.

2) ROBUSTNESS TO FEEDER ENERGIZATION

Feeder energization leads to transients that can be mistaken for HIF signature. Hence, in this simulation case, a switch between the nodes 632 and 671 is used. The lower half of IEEE-13 Feeder remains un-energized initially. The HIF and the switching leading to feeder energization are simulated at the same time.

C. SENSITIVITY TEST

FADS performance is influenced by the waveform distortions. As summarized in [70], HIF currents and their characteristics can vary according to the fault surface. The number of distortions and the frequency of their occurrence in the monitored sinusoidal waveforms will depend on the HIF V-I characteristics. Hence, it is important and prudent to evaluate ADDT's sensitivity to different HIF V-I characteristics arising from different fault surfaces. The sensitivity test utilizes the different characteristics obtained in Fig. 6 since they resemble the data obtained from field tests. The sensitivity test is conducted for the IEEE-13 node feeder.

In simulation cases of IEEE-34 node feeder, HIF is always simulated at phase A to ground. The 2-phase load switching is an unbalanced load switching between phases A-B. The sampling rate of the voltage waveforms and time frame for the dataset recording distortions is same as explained in Chapter 2. The capacitor bank is star grounded with capacitance of 1.2835μF. Load and capacitor bank are switched OFF after three cycles. In simulation cases of IEEE-13 node feeder, HIF is always simulated at phase C to ground. In all the simulation cases, the load switching, capacitor bank switching, motor starting, feeder energization and HIF (cases where applicable) all are triggered at $t = 0.105s$. In case of motor starting HIF is cleared after 3s of initiation while in case of feeder energization HIF is cleared at 1s.

3.5 SIMULATION RESULTS

In this subsection, the implementation results are discussed. FADS implementation involves considerable amount of data processing per simulation case. In order to avoid overloading the reader with too much information, the observations are summarized such that a reasonable conclusion can be drawn. However, in order to give an idea of the actual FADS operation in real time, the interesting and complex simulation case II, scenario B has been discussed at first and in complete detail.

A. SHORT TRANSIENT EVENTS

1) IEEE-34 NODE TEST FEEDER

1.1) SIMULATION CASE II, SCENARIO B

The complexity of this simulation case lies in the fact that the events of HIF, load and capacitor switching are simulated at close proximity to each other and at the same time in order to mislead the FADS into mistaking HIF for a normal grid event. The voltage waveforms from different measurement points can be seen in Figure 3.5. The FADS implementation result of distortions recorded and the associated LMD severity rating for

the different nodes have been divided and presented in Table 3.3 and Table 3.4 to fit the contents clearly within the thesis page layout regulations. The distortions recorded for the first 0.4s after event commencement is shown since after that a decision can be taken.

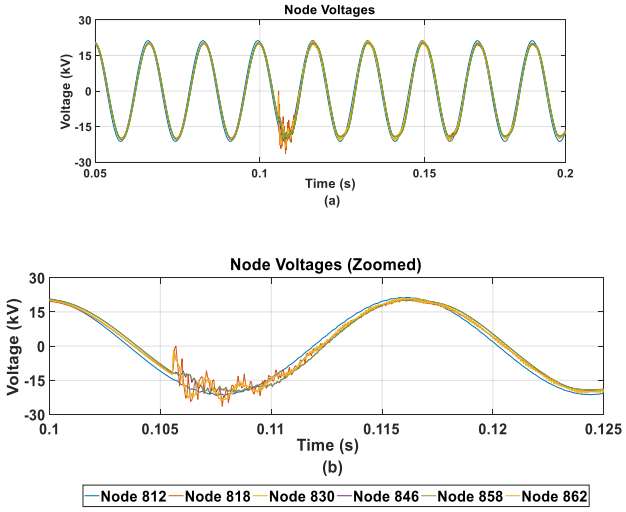

Figure 3.5: Measured voltages at different measurement points for Simulation Case II, Scenario B. HIF event and capacitor and load switching occur at t=0.105s.(a) Node Voltages, (b) Node Voltages (Zoomed)

TABLE 3.3
SIMULATION CASE II, SCENARIO B, FADS IMPLEMENTATION RESULTS -1 (PHASE A)

Reporting Interval	Node 812		Node 818		Node 830	
	Distortions Recorded	LMD Severity Rating	Distortions Recorded	LMD Severity Rating	Distortions Recorded	LMD Severity Rating
T1=(0.0-0.1)s	0	0	0	0	0	0
T2=(0.1-0.2)s	57	1	62	1	87	2
T3=(0.2-0.3)s	32	0	34	0	79	2
T4=(0.3-0.4)s	19	0	23	0	64	1

TABLE 3.4
SIMULATION CASE II, SCENARIO B, FADS IMPLEMENTATION RESULTS -2 (PHASE A)

Reporting Interval	Node 846		Node 858		Node 862	
	Distortions Recorded	LMD Severity Rating	Distortions Recorded	LMD Severity Rating	Distortions Recorded	LMD Severity Rating
T1=(0.0-0.1)s	0	0	0	0	0	0
T2=(0.1-0.2)s	95	2	99	2	97	2
T3=(0.2-0.3)s	88	2	96	2	93	2
T4=(0.3-0.4)s	92	2	93	2	85	2

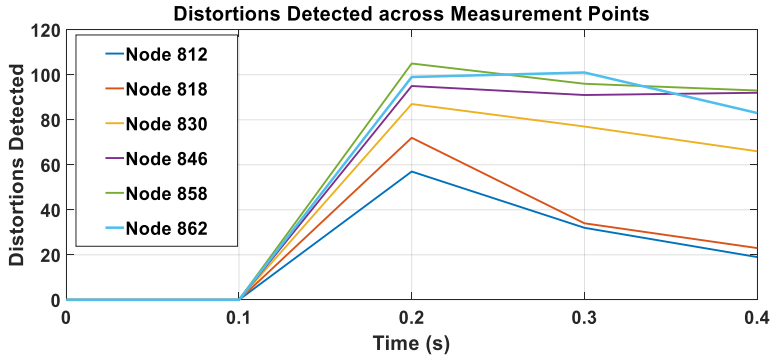

Figure 3.6: Distortions detected different measurement points for Simulation Case II, Scenario B

It can be observed that as the events are simulated, FADS reports increased waveform distortions from all the measurement points. Accordingly, the severity rating of the measurement points also change. The measurement points near the event of HIF show higher amount of distorted samples in comparison to other measurement points. The device at node 858 indicates a severity rating of level 2 and sustains it over next three reporting intervals. The measurement devices at node 862 and 846 also show sustained high severity rating for the same reporting intervals. Node 830 is comparatively far from HIF event but still sustains severity rating of 2 for two time intervals possibly due to combined effect of HIF and capacitor switching. However as the effect of capacitor switching FADSes away, the severity rating goes a level down. Nodes 812 and 818,

TABLE 3.5
SIMULATION CASE II, SCENARIO B (FADS RESULTS WITH GRID ZONING IMPLEMENTED)

Reporting Interval	No Grid Zoning (Overall Network)		Zone 1 (Nodes 812, 818, 830)		Zone 2 (Nodes 846, 858, 862)	
	Common Reporting's	Severity Rating	Common Reporting's	Grid Zone Severity Rating	Common Reporting's	Grid Zone Severity Rating
T1	0	0	0	0	0	0
T2	29	1	42	1	56	2
T3	20	0	18	0	53	2
T4	9	0	14	0	49	2

similarly sustain severity rating level 1 for first reporting interval but as the load switching effect FADSes away, the severity rating for the nodes goes to level 0. Based on these observations, the event can be classified as a potentially harmful event that is occurring somewhere between nodes 830, 846, 858 and 862. The variation of distortions detected over time for different measurement points are shown graphically in Figure 3.6.

The next step would be to narrow down the location of the HIF event accurately so that quicker corrective actions can be taken by the DSO maintenance teams. In order to locate HIF, the concept of common reporting's and grid zoning of FADS is utilized. The results of the grid zoning of the recorded distortions can be observed in Table 3.5. Based on observations from Table 3.5; the common reporting's of the undivided network shows severity rating of level 1 only for one reporting period, as the measurement points far from HIF (nodes 812, 818) report too few distortions. However, this is an incorrect representation of grid condition. When observing zone based data, it can be seen that Zone 1 also has severity rating level 1 for one reporting interval. It indicates that while

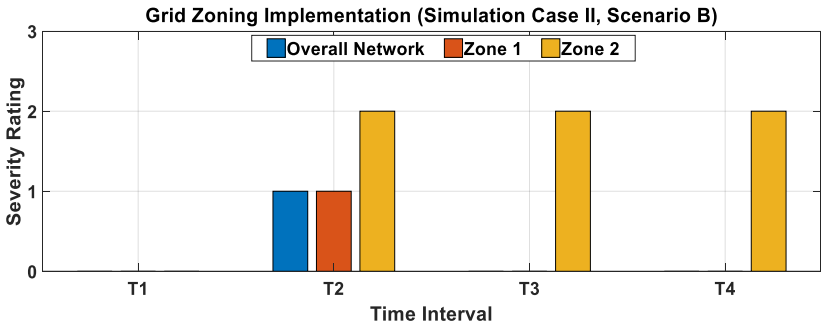

Figure 3.7: Variation of severity ratings for different zones with grid zoning implementation for FADS for Simulation Case II, Scenario B.

Zone 1 is initially affected, the impact fades away quickly and severity rating goes to level 0 from level 1. However, Zone 2 remains affected throughout indicating potentially harmful event taking place in the area covered by the zone. This information will be relayed to the DSO operator and based on the knowledge gained from the interpretation by severity ratings, the area of operation for maintenance teams will reduce considerably as the location of the harmful event can be narrowed down to area between nodes 858, 846 and 862. This will ensure efficient dispatch of resources and quicker mitigation of the event. Figure 3.7 shows the variation of severity ratings for different zones. Hence, FADS implementation combined with grid zoning is effective in detecting a potentially harmful event (in this case HIF). The use of grid zoning gives fair idea of the location of the harmful event.

1.2) SIMULATION CASE I, SCENARIO A

Simulation Case I is test of FADS robustness to false positives. In the scenario A of simulation case I, the load and capacitor switching events are distanced from each other. Based on FADS analysis, the severity ratings of all measurement points at different nodes and the overall network based on common reporting's don't violate the thresholds and severity ratings remain at level 0 indicating normal grid operations.

1.3) SIMULATION CASE I, SCENARIO B

This case-scenario provides a tough test of ADDT's robustness to false positives. The load and capacitor switching events are close to each other. Based on ADDT analysis, the severity ratings of all measurement devices at different nodes and the severity rating of the different nodes and grid zoning, based on common reporting's are shown in Figure 3.8. The measurement point at node 858 goes to level 1 of severity rating indicating minimal risk but the other measurement points and the zones indicate a severity rating of 0. This is possibly because of capacitor switching at node 834 but as the effect of switching fades away, severity rating of level 1 at node 858 is not sustained and it scales down and remains at level 0 indicating normal grid operations.

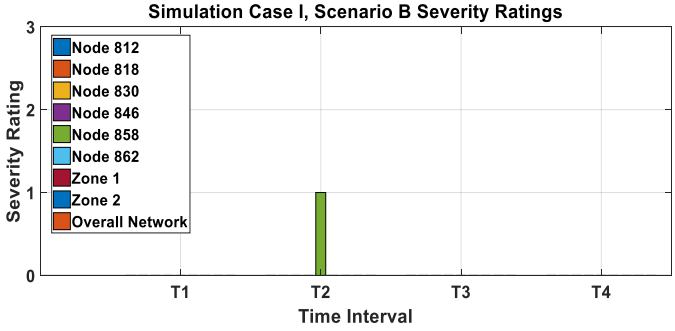

Figure 3.8: Node and grid zone severity ratings for Simulation Case I, Scenario B

1.4) SIMULATION CASE I, SCENARIO C

In this scenario, the 3rd, 5th and 11th order harmonics are injected at 3%, 1% and 1% of the fundamental frequency voltage at the power frequency of 60Hz respectively. The total

harmonic distortion (THD) stands at around 4.54%. All the harmonic values are within IEEE recommended limits. In Figure 3.9, the FFT analysis of the harmonic injected voltage waveform can be seen. Based on observations from FADS analysis, no violation of thresholds is observed and hence the severity rating for all the measurement points and overall network remains at level 0.

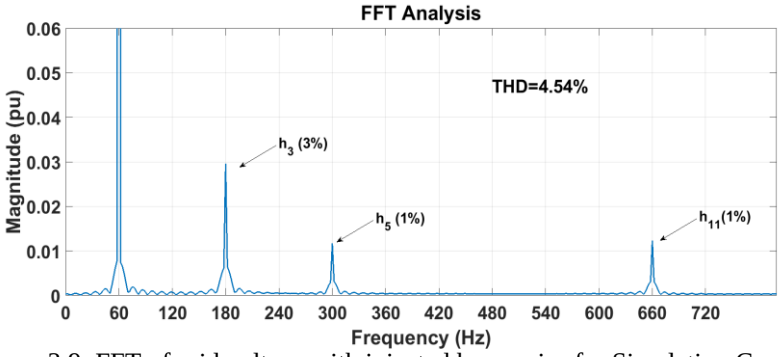

Figure 3.9: FFT of grid voltage with injected harmonics for Simulation Case I, Scenario C

1.5) SIMULATION CASE II, SCENARIO A

This simulation case and scenario is a test of ADDT's robustness to false negatives. The HIF, load and capacitor switching events are spaced out from each other. Based on FADS implementation, severity ratings of all measurement devices and grid zoning are shown in Figure 3.10. The measurement points at nodes 818, 830, 846, 858 and 862 indicate increase in severity levels. However, with time, the severity rating of nodes 846 and node 858 sustains at level 1 while that of node 830 escalate and sustain at level two. Prima facie, the location could be zeroed down to areas between nodes 830, 846 and 858. The severity rating for zones however does not change as nodes 812, 818, and 862 hardly detect any distortions. As the area between the nodes identified do not exactly fit into a grid zone, the shortcoming of grid zoning concept can be observed. However, the LMD level severity ratings at different zones can help in narrowing down the area to be surveyed by maintenance teams to locate the HIF between the nodes 830, 858 and 846.

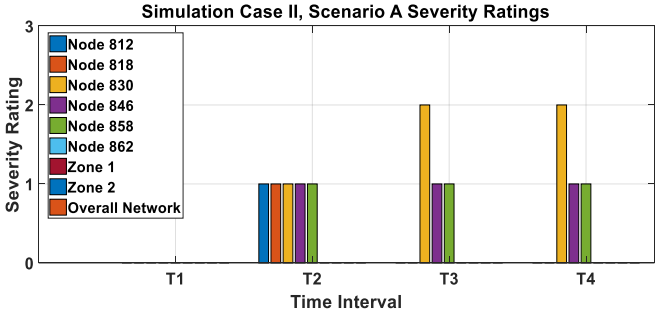

Figure 3.10: Node and grid zone severity ratings for Simulation Case II, Scenario A

2) IEEE-13 NODE TEST FEEDER

2.1) SIMULATION CASE III, SCENARIO A

This simulation case and scenario is similar to *Simulation Case I, Scenario A*. The events of load and capacitor switching are far from each other and occur simultaneously at nodes 646 and 634 respectively. As seen in Figure 3.11, the measurement point at node 633 shows severity rating 1 for two reporting periods but other devices stay at level 0. The results from grid zoning also show no change in severity levels indicating no harm to grid operations.

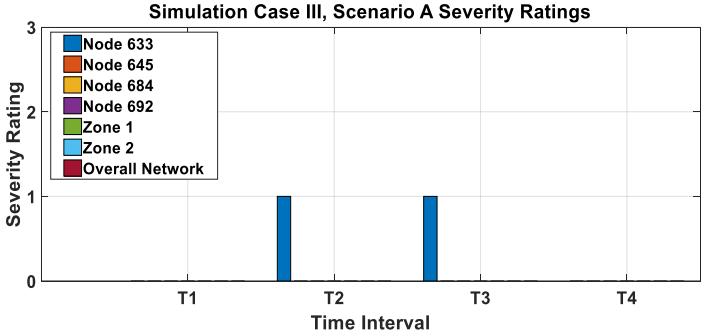

Figure 3.11: Node and grid zone severity ratings for Simulation Case III, Scenario A

2.2) SIMULATION CASE III, SCENARIO B

This simulation case and scenario is similar to *Simulation Case I, Scenario B*. The events of load and capacitor switching are closer to each other leading to measurement points at node 684 and node 692 to indicate severity level 1 for just one reporting period but the ratings of other devices and the grid zoning stay at level 0 indicating normal grid operations. The severity ratings can be seen in Figure 3.12.

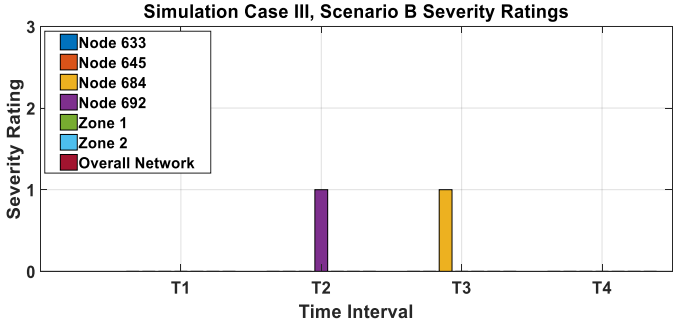

Figure 3.12: Node and grid zone severity ratings for Simulation Case III, Scenario B

2.3) SIMULATION CASE IV, SCENARIO A

This simulation case and scenario is similar to *Simulation Case II, Scenario A*. All the three events of HIF, load and capacitor switching happen at same time respectively but the placements of events are spaced out from each other. As seen in Figure 3.13, measurement devices at nodes 633, 684 and 692 indicate severity rating level 1 at the first reporting periods. The node at 684 sustains level 1 and in the fourth reporting period moves to level 2. The severity rating of nodes 692 increases and sustains level 2. The grid zoning results also move from level 1 severity rating at third reporting interval to level 2 at the fourth reporting interval. These observations indicate that a potentially harmful event has occurred in Zone 2.

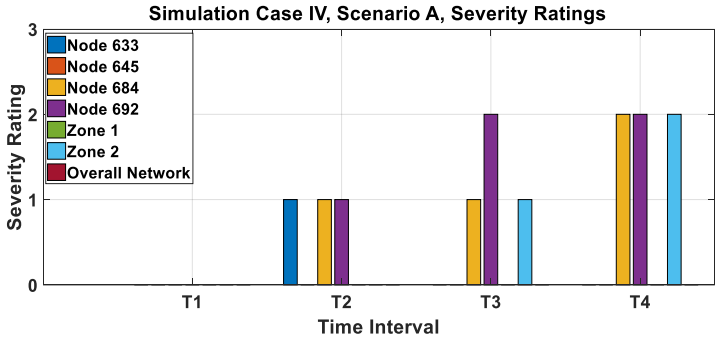

Figure 3.13: Node and grid zone severity ratings for Simulation Case IV, Scenario A

2.4) SIMULATION CASE IV, SCENARIO B

This simulation case and scenario is similar to *Simulation Case II, Scenario B*. The simulation of all the events at close proximity to each other causes severity level 1 rating across all measurement devices except at node 692. The measurement device at node 692 maintains severity level 2 throughout. As seen in Figure 3.14, the grid zoning results indicate severity rating level 1 initially for the all the measurement devices, different Zones and overall network. However, in the following reporting periods, the severity rating of device at node 684 increases to severity level 2. The severity level 2 of devices

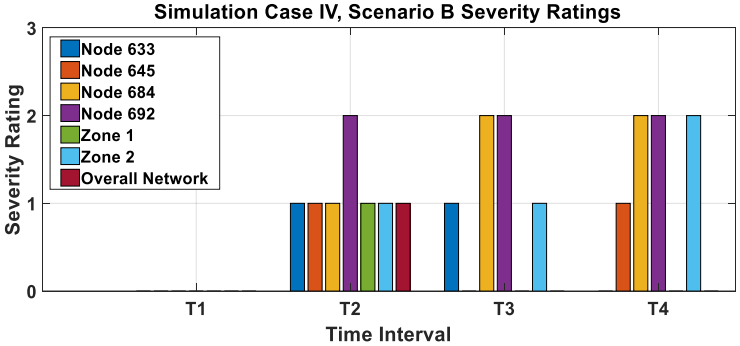

Figure 3.14: Node and grid zone severity ratings for Simulation Case IV, Scenario B

at node 684 and 692 sustains leading to eventual increase of severity rating of Zone 2 to level 2 indicating a potentially harmful event occurrence in that area.

B. LONG TRANSIENT EVENTS

The long transient events pertaining to motor starting and feeder energization is conducted for IEEE-13 node test feeder.

1) SIMULATION CASE V, MOTOR STARTING

Motor starting is a phenomenon with a long transient and lasts until the motor accelerates to the full rated speed. During this time, high current is drawn and there is considerable voltage drop until slowly motor reaches a steady state of operation. FADS robustness against motor starting transients is evaluated in this simulation case. The motor at node 634 and HIF at node 675 are initiated at $t = 0.105\ s$. The voltage at node 634 during the motor start process can be seen in Figure 3.15, which lasts until almost 6s.The reporting period is 0.1 s. Hence, there would be 60 reporting intervals for 6s. Due to the enormity of data generated a concise summary of FADS implementation results are presented via means of a scatter graphical representation in Figure 3.16 and Figure 3.17.

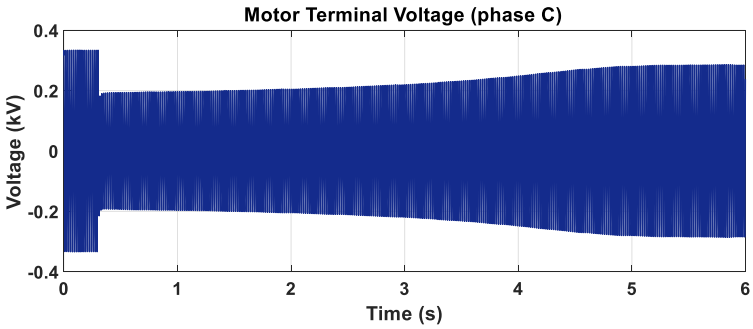

Figure 3.15: Voltage at Node 634(phase C) during motor starting event

In Figure 3.16, it can be observed that the node 692 mostly indicates level 2 rating until almost 3s and after that it scales down to level 0. Similarly, node 684 indicates rating of level 1 and level 2 intermittently until 3s. Node 645 measurements indicate level 1 for few instants and single indication of level 2 rating in the first 3s and show one instance of level 1 around 4s. Node 633 measurements largely remain at level 0 barring few instances of level 1 rating. The conclusion that can be drawn from these observations is that motor starting does not lead to many distortions that will violate FADS thresholds. The amplitude of the voltage waveforms do vary as the motors attains steady state but the sinusoidal nature of the waveforms is also retained. Since, the fundamental properties of sinusoids are hardly violated during the motor start transient; it leads to very few distortions as observed in severity ratings of the closest measurement point at node 633.

In Figure 3.17, the grid zoning severity ratings for simulation case V can be observed. It can be seen that overall network severity rating remains at level 0 almost throughout

the 6s, which is misleading since a HIF event does occur. Zone 1 shows few level 1 indications during first 3s and one level 1 rating around 3.75s but otherwise remains at level 0. This indicates little effect from motor starting occurring in the area observed in Zone 1. The considerable distance from HIF event is also one of the factors for such severity ratings of Zone 1. Zone 2 indicates level 2 rating for several instances during the first 3s. The sustained high severity rating of Zone 2 indicates a possible occurrence of a potentially harmful event (in this case HIF) in the area observed.

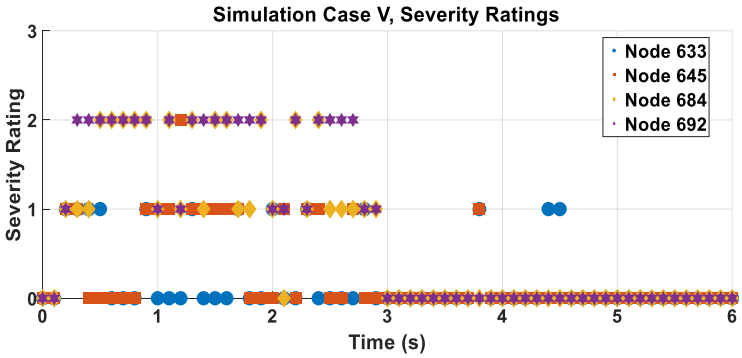

Figure 3.16: Node severity ratings for Simulation Case V

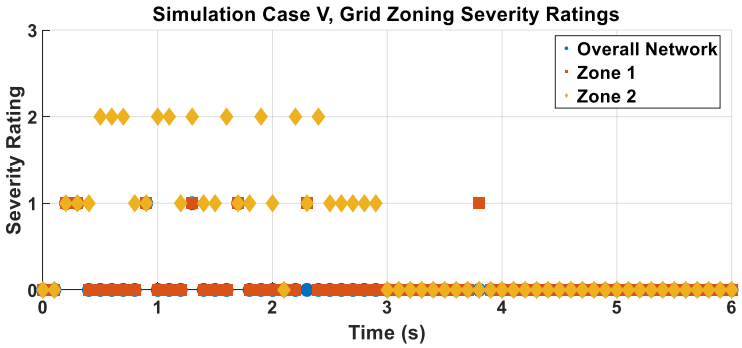

Figure 3.17: Grid Zoning based severity ratings for Simulation Case V

2) SIMULATION CASE VI, FEEDER ENERGIZATION

Feeder energization is another common occurrence in active distribution grids. As detailed in Table 3.2, the switches between nodes 632 and 671 are switched on simultaneously with the HIF event in node 675 at $t = 0.105\ s$. The voltage pattern recorded from the measurement device at node 692 can be observed in Figure 3.18.

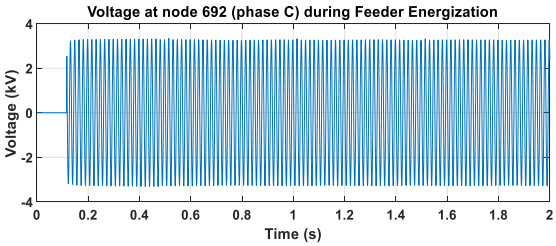

Figure 3.18: Voltage at Node 692 during Feeder Energization Event

The severity levels for the different measurement points at different nodes can be seen in Figure 3.19. Nodes 633 and 645 indicate few instances of level 1 rating mostly until 1s and then scale down to level 0. The fact that this zone of feeder is already energized and there is considerable distance from the HIF event leads to few distortions. Severity rating at node 684 mostly remains at level 1 with few instances of level 2 rating during the first 1s. However, it scales to level 1 on three different instances after 1s probably on account of distortions produced due to feeder energization. Node 692 gradually scales up and subsequently maintains level 2 for major portion of the first 1s. Afterwards it scales down to level 0 barring two instances. The feeder energization event produces few and far between distortions which does not lead to consistent violation of ADDT thresholds for high severity levels which becomes more evident as HIF event is cleared at 1s.

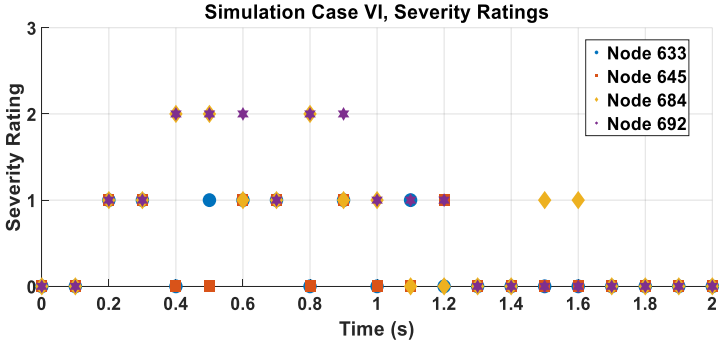

Figure 3.19: Node severity ratings for Simulation Case VI

The grid zoning results for the feeder energization event can be observed in Figure 3.20. It can be observed that Zone 2 intermittently maintains level 2 and level 1 rating during the first 1s in comparison to Zone 1 or overall network severity ratings. Hence, one can easily deduce the possibility of a potentially harmful event occurring in Zone 2 and investigate further in that area.

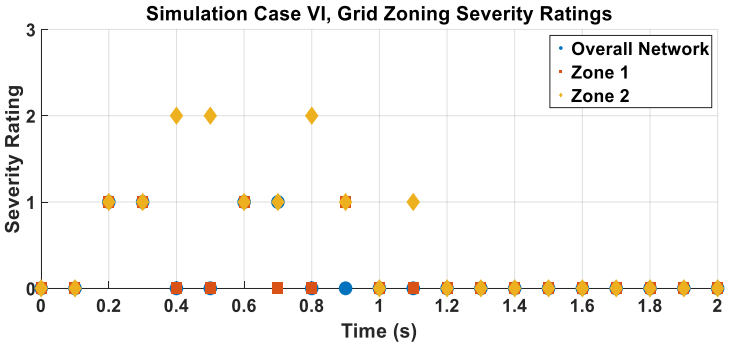

Figure 3.20: Grid Zoning based severity ratings for Simulation Case VI

C. Simulation Case VII, Sensitivity Test

HIF currents from different surfaces are used to conduct the sensitivity test. The distortions detected over a period of 0.5s for measurement devices at different nodes compared against different HIF event currents simulated on node 675 at 0.105s are shown in Figure 3.21.

As observed from Figure 3.21, the measurement point at node 692 records higher number of distortions for almost all HIF fault surfaces in comparison to other nodes mainly because it is closest to the event location at node 675. The distortions recorded across all nodes show maximum value for HIF fault surface of concrete. This could be attributed to the fact that V-I characteristic for concrete in Figure 3.3 is quite flat near zero implying low impedance and subsequently high fault current. The distortions recorded for surfaces of wet grass, dry rubber and damp sand are similar for all the nodes except node 645 where distortions for wet grass are higher. The distortions recorded for damp and dry tiles show least amount of distortions. The difference can be more clearly observed in node 692 and node 645 recordings. The low amount of distortions correlates to weak fault current which can also be ascertained from the fact that the V-I characteristics for both damp and dry tiles are rather steep and not very flat near zero. Such weak fault current will lead to very few common reporting's in grid zone level severity rating which might cause FADS not to classify the event as harmful. LMD level severity ratings of nodes 684 and 692 can help overcome such an eventuality but nodes 684 and 692 almost report same number of distortions. Such a situation will increase the area to be surveyed by maintenance team. Hence, a weak HIF might lead to comparatively higher resource and time consumption to locate the event even if the HIF is successfully detected with FADS implementation.

However, more such case studies with real field data would be required to conduct an exhaustive evaluation of FADS robustness to weak HIFs. The severity level ratings structure is currently quite simple. A more robust approach would be to broaden the severity level ratings table to create subsections within each level to better classify the distortions and better accommodate weak HIFs. In order to guarantee success, such an exercise would need to be performed in close collaboration with DSO operators using the network specific data and measurements of extensive field-staged HIFs

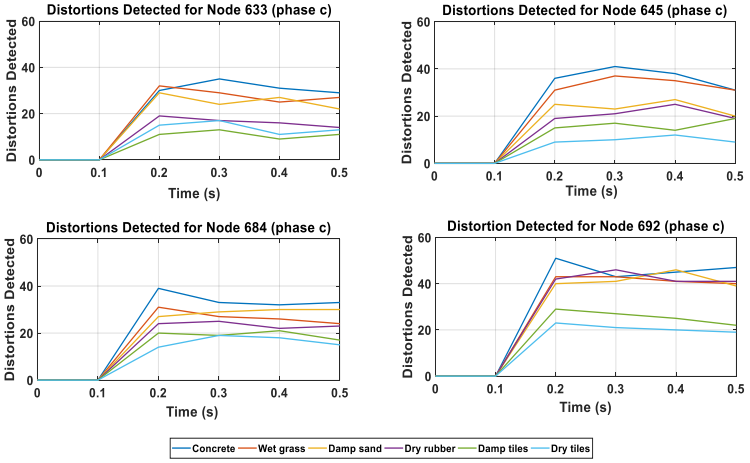

Figure 3.21: Simulation Case VII, Sensitivity Test. Distortions detected across different nodes for different HIF V-I characteristics for different fault surfaces

3.6 DISCUSSIONS

The HIF detection results have been obtained for FADS implementation in a multitude of simulation cases and scenarios. It would be therefore be prudent to compare the FADS performance with some of the existing HIF detection techniques. Majority of the simulation cases discussed in section 3.2 either detect independent HIF or differentiate HIF from normal switching activities with exception of [33] and [53]. The comprehensiveness of FADS is reflected from it performance in detecting HIF for both short and long transient events. As mentioned before, the creation of two scenarios and simultaneous occurrence of HIF with switching events are a novelty and act as an ultimate test of FADS performance. Considering the first reporting of severity rating level 2 as an early indicator of a harmful event, FADS performance is faster than techniques in [7], [57] and comparable to techniques in [1], [27]. Except for techniques [10], [33] and [48], other HIF techniques do not provide any reasonable estimate for location estimation of HIF. FADS conducts sensitivity test for HIF from different surfaces so that its performance can be evaluated for both weak and strong HIF occurrences. Such comparison is missing in other techniques except in [13], [21]. Comparison with some

other techniques is made difficult by the fact that not all techniques clearly state their performance across all parameters like test-case design, resource consumption, time taken etc.

3.7 CONCLUSIONS

In this chapter, FADS was validated in a number of scenarios for detecting HIF. A separate sensitivity analysis was also done for FADS. The study was conducted to distinguish and detect HIF in a variety of simulation cases. A reliable HIF model that can generate all the major characteristics of HIF fault current was used to generate the fault currents for different surfaces. FADS implementation results highlighted how the HIF in different cases were detected and the area of occurrence located successfully. FADS leveraging the waveform distortions was able to distinguish HIF from normal grid switching actions event when they were simulated simultaneously at close geographical proximity. In IEEE-13 node feeder, additional long transient events were also simulated to have a comprehensive evaluation of FADS performance. The grid zoning concept of FADS helps to narrow down the search area considerably. The benefits of grid zoning in locating HIF event was highlighted by comparing it to the results obtained with no grid zoning. However, it was also observed that in some situations the rudimentary grid zoning might mislead the grid operator but in those cases, the LMD level severity rating complements the perceived shortcoming of grid zoning. This also highlights the advantage of two-tier FADS severity rating concept.

The sensitivity test helped to understand the extent of waveform distortions done by weak HIFs and evaluate the FADS performance for the same. FADS may underperform for very weak HIFs but it would still detect them. The swiftness of FADS detection and other important parameters were compared with other existing HIF techniques and the advantages of FADS were highlighted. Further studies would be required in order to improve systematically FADS, so that it can be more robust for HIF detection. Evaluation of FADS for field-staged HIF conditions caused by tree contact where the overhead line remains unbroken and the operation of nonlinear loads along with HIF would be an interesting case study for future.

Finally, this chapter shows the overall successful performance of FADS in HIF detection. FADS imbedded in commercial digital relays can provide a comprehensive solution for detecting HIFs in real field implementation. Detection of HIF is just one application specialty of FADS and further discussion on FADS application cases in presented in subsequent chapters.

REFERENCES

[1] S. Gautam and S. M. Brahma, "Detection of High Impedance Fault in Power Distribution Systems Using Mathematical Morphology," in *IEEE Transactions on Power Systems*, vol. 28, no. 2, pp. 1226-1234, May 2013.

[2] High Impedance Fault Detection Technology Mar. 1996 [online]. Report of PSRC Working Group D15. Available: http://www.pes-psrc.org/kb/published/reports/High_Impedance_Fault_Detection_Technology.pdf

[3] W. C. Santos, F. V. Lopes, N. S. D. Brito and B. A. Souza, "High-Impedance Fault Identification on Distribution Networks," in *IEEE Transactions on Power Delivery*, vol. 32, no. 1, pp. 23-32, Feb. 2017.

[4] A. F. Sultan, G. W. Swift and D. J. Fedirchuk, "Detecting arcing downed-wires using fault current flicker and half-cycle asymmetry," in *IEEE Transactions on Power Delivery*, vol. 9, no. 1, pp. 461-470, Jan. 1994.

[5] J. Carr, "Detection of High Impedance Faults on Multi-Grounded Primary Distribution Systems," in *IEEE Transactions on Power Apparatus and Systems*, vol. PAS-100, no. 4, pp. 2008-2016, April 1981.

[6] R. E. Lee and M. T. Bishop, "Performance Testing of the Ratio Ground Relay on a Four-Wire Distribution Feeder," in *IEEE Transactions on Power Apparatus and Systems*, vol. PAS-102, no. 9, pp. 2943-2949, Sept. 1983.

[7] A. V. Mamishev, B. D. Russell and C. L. Benner, "Analysis of high impedance faults using fractal techniques," in *IEEE Transactions on Power Systems*, vol. 11, no. 1, pp. 435-440, Feb. 1996.

[8] C. J. Kim and B. D. Russell "Analysis of distribution disturbances and Arcing faults using the crest factor" *Elect. Power Syst. Res.*, vol. 35 pp. 141-148 1995.

[9] I. Zamora, A. J. Mazon, K. J. Sagastabeitia and J. J. Zamora, "New Method for Detecting Low Current Faults in Electrical Distribution Systems," in *IEEE Transactions on Power Delivery*, vol. 22, no. 4, pp. 2072-2079, Oct. 2007.

[10] S. H. Mortazavi, Z. Moravej and S. M. Shahrtash, "A Searching Based Method for Locating High Impedance Arcing Fault in Distribution Networks," in *IEEE Transactions on Power Delivery*, vol. 34, no. 2, pp. 438-447, April 2019.

[11] A. R. Herrera-Orozco et al., "Incipient fault location formulation: A time-domain system model and parameter estimation approach", *Elect. Power Energy Syst.*, vol. 90, pp. 112-123, Sep. 2017.

[12] W. Zhang, Y. Jing and X. Xiao, "Model-Based General Arcing Fault Detection in Medium-Voltage Distribution Lines," in *IEEE Transactions on Power Delivery*, vol. 31, no. 5, pp. 2231-2241, Oct. 2016.

[13] B. Wang, J. Geng and X. Dong, "High-Impedance Fault Detection Based on Nonlinear Voltage–Current Characteristic Profile Identification," in *IEEE Transactions on Smart Grid*, vol. 9, no. 4, pp. 3783-3791, July 2018.

[14] M. Aucoin and B. D. Russell, "Detection of Distribution High Impedance Faults Using Burst Noise Signals near 60 HZ," in *IEEE Transactions on Power Delivery*, vol. 2, no. 2, pp. 342-348, April 1987.

[15] D. I. Jeerings and J. R. Linders, "Unique aspects of distribution system harmonics due to high impedance ground faults," in *IEEE Transactions on Power Delivery*, vol. 5, no. 2, pp. 1086-1094, April 1990.

[16] Keng-Yu Lien, Shi-Lin Chen, Ching-Jung Liao, Tzong-Yih Guo, Tsair-Ming Lin and Jer-Sheng Shen, "Energy variance criterion and threshold tuning scheme for high impedance fault detection," in *IEEE Transactions on Power Delivery*, vol. 14, no. 3, pp. 810-817, July 1999.

[17] S. M. Shahrtash and M. Sarlak, "High Impedance Fault Detection Using Harmonics Energy Decision Tree Algorithm," *2006 International Conference on Power System Technology*, Chongqing, 2006, pp. 1-5.

[18] A. E. Emanuel, D. Cyganski, J. A. Orr, S. Shiller and E. M. Gulachenski, "High impedance fault arcing on sandy soil in 15 kV distribution feeders: contributions to the evaluation of the low frequency spectrum," in *IEEE Transactions on Power Delivery*, vol. 5, no. 2, pp. 676-686, April 1990.

[19] D. I. Jeerings and J. R. Linders, "A practical protective relay for down-conductor faults," in *IEEE Transactions on Power Delivery*, vol. 6, no. 2, pp. 565-574, April 1991.

[20] "High impedance fault detection using third harmonic current," Hughes Aircraft Company, Westchester, CA, USA, EPRI Tech. Rep. EL-2430, Jun. 1982.

[21] M. Wei *et al*., "High Impedance Arc Fault Detection Based on the Harmonic Randomness and Waveform Distortion in the Distribution System," in *IEEE Transactions on Power Delivery*, vol. 35, no. 2, pp. 837-850, April 2020.

[22] J. R. Macedo, J. W. Resende, C. A. Bissochi, D. Carvalho and F. C. Castro, "Proposition of an interharmonic-based methodology for high-impedance fault detection in distribution systems," in *IET Generation, Transmission & Distribution*, vol. 9, no. 16, pp. 2593-2601, 3 12 2015.

[23] J. Zhou, B. Ayhan, C. Kwan, S. Liang and W. Lee, "High-Performance Arcing-Fault Location in Distribution Networks," in *IEEE Transactions on Industry Applications*, vol. 48, no. 3, pp. 1107-1114.

[24] B. M. Aucoin and B. D. Russell, "Distribution High Impedance Fault Detection Utilizing High Frequency Current Components," in *IEEE Power Engineering Review*, vol. PER-2, no. 6, pp. 46-47, June 1982.

[25] A. N. Milioudis, G. T. Andreou and D. P. Labridis, "Detection and Location of High Impedance Faults in Multiconductor Overhead Distribution Lines Using Power Line Communication Devices," in *IEEE Transactions on Smart Grid*, vol. 6, no. 2, pp. 894-902, March 2015.

[26] D. P. S. Gomes, C. Ozansoy and A. Ulhaq, "High-Sensitivity Vegetation High-Impedance Fault Detection Based on Signal's High-Frequency Contents," in *IEEE Transactions on Power Delivery*, vol. 33, no. 3, pp. 1398-1407, June 2018.

[27] É. M. Lima, C. M. dos Santos Junqueira, N. S. D. Brito, B. A. de Souza, R. de Almeida Coelho and H. Gayoso Meira Suassuna de Medeiros, "High impedance fault detection method based on the short-time Fourier transform," in *IET Generation, Transmission & Distribution*, vol. 12, no. 11, pp. 2577-2584, 19 6 2018.

[28] T. Cui, X. Dong, Z. Bo and A. Juszczyk, "Hilbert-Transform-Based Transient/Intermittent Earth Fault Detection in Noneffectively Grounded Distribution Systems," in *IEEE Transactions on Power Delivery*, vol. 26, no. 1, pp. 143-151, Jan. 2011.

[29] David Chan Tat Wai and Xia Yibin, "A novel technique for high impedance fault identification," in *IEEE Transactions on Power Delivery*, vol. 13, no. 3, pp. 738-744, July 1998.

[30] T. M. Lai, L. A. Snider, E. Lo and D. Sutanto, "High-impedance fault detection using discrete wavelet transform and frequency range and RMS conversion," in *IEEE Transactions on Power Delivery*, vol. 20, no. 1, pp. 397-407, Jan. 2005.

[31] N. I. Elkalashy, M. Lehtonen, H. A. Darwish, M. A. Izzularab and A. I. Taalab, "Modeling and experimental verification of high impedance arcing fault in medium voltage networks," in *IEEE Transactions on Dielectrics and Electrical Insulation*, vol. 14, no. 2, pp. 375-383, April 2007.

[32] M. Michalik, W. Rebizant, M. Lukowicz, Seung-Jae Lee and Sang-Hee Kang, "High-impedance fault detection in distribution networks with use of wavelet-based algorithm," in *IEEE Transactions on Power Delivery*, vol. 21, no. 4, pp. 1793-1802, Oct. 2006.

[33] W. C. Santos, F. V. Lopes, N. S. D. Brito and B. A. Souza, "High-Impedance Fault Identification on Distribution Networks," in *IEEE Transactions on Power Delivery*, vol. 32, no. 1, pp. 23-32, Feb. 2017.

[34] Chul-Hwan Kim, Hyun Kim, Young-Hun Ko, Sung-Hyun Byun, R. K. Aggarwal and A. T. Johns, "A novel fault-detection technique of high-impedance arcing faults in transmission lines using the wavelet transform," in *IEEE Transactions on Power Delivery*, vol. 17, no. 4, pp. 921-929, Oct. 2002.

[35] A. Ghaderi, H. A. Mohammadpour, H. L. Ginn and Y. Shin, "High-Impedance Fault Detection in the Distribution Network Using the Time-Frequency-Based Algorithm," in *IEEE Transactions on Power Delivery*, vol. 30, no. 3, pp. 1260-1268, June 2015.

[36] Shyh-Jier Huang and Cheng-Tao Hsieh, "High-impedance fault detection utilizing a Morlet wavelet transform approach," in *IEEE Transactions on Power Delivery*, vol. 14, no. 4, pp. 1401-1410, Oct. 1999.

[37] C. J. Kim and B. D. Russell, "Classification of faults and switching events by inductive reasoning and expert system methodology," in *IEEE Transactions on Power Delivery*, vol. 4, no. 3, pp. 1631-1637, July 1989.

[38] B. D. Russell and C. L. Benner, "Arcing fault detection for distribution feeders: security assessment in long term field trials," in *IEEE Transactions on Power Delivery*, vol. 10, no. 2, pp. 676-683, April 1995.

[39] M. Sarlak and S. M. Shahrtash, "High-Impedance Faulted Branch Identification Using Magnetic-Field Signature Analysis," in *IEEE Transactions on Power Delivery*, vol. 28, no. 1, pp. 67-74, Jan. 2013.

[40] B. D. Russell, "Expert system for detecting high impedance faults," U.S. Patent 5 550 751, Aug. 1996.

[41] Yong Sheng and S. M. Rovnyak, "Decision tree-based methodology for high impedance fault detection," in *IEEE Transactions on Power Delivery*, vol. 19, no. 2, pp. 533-536, April 2004.

[42] H. K. Zadeh "ANN-based high impedance fault detection scheme: Design and implementation" Int. J. Emerg. Elect. Power Syst. vol. 4 no. 2 pp. 1-14 2005.

[43] S. R. Samantaray, B. K. Panigrahi and P. K. Dash, "High impedance fault detection in power distribution networks using time-frequency transform and probabilistic neural network," in *IET Generation, Transmission & Distribution*, vol. 2, no. 2, pp. 261-270, March 2008.

[44] M. Michalik, M. Lukowicz, W. Rebizant, S. Lee and S. Kang, "New ANN-Based Algorithms for Detecting HIFs in Multigrounded MV Networks," in *IEEE Transactions on Power Delivery*, vol. 23, no. 1, pp. 58-66, Jan. 2008.

[45] S. Ebron, D. L. Lubkeman and M. White, "A neural network approach to the detection of incipient faults on power distribution feeders," in *IEEE Transactions on Power Delivery*, vol. 5, no. 2, pp. 905-914, April 1990.

[46] A. Soheili and J. Sadeh, "Evidential reasoning based approach to high impedance fault detection in power distribution systems," in *IET Generation, Transmission & Distribution*, vol. 11, no. 5, pp. 1325-1336, 30 3 2017.

[47] M. Sarlak and S. M. Shahrtash, "High impedance fault detection using combination of multi-layer perceptron neural networks based on multi-resolution morphological gradient features of current waveform," in *IET Generation, Transmission & Distribution*, vol. 5, no. 5, pp. 588-595, May 2011.

[48] M. Khani, R. Ghazi and B. Nazari, "Decision support system for optimal location of HIFDs in real distribution network using an integrated EPSO-fuzzy AHP model," in *IET Generation, Transmission & Distribution*, vol. 14, no. 9, pp. 1616-1626, 11 5 2020.

[49] A. H. Etemadi and M. Sanaye-Pasand, "High-impedance fault detection using multi-resolution signal decomposition and adaptive neural fuzzy inference system," in *IET Generation, Transmission & Distribution*, vol. 2, no. 1, pp. 110-118, January 2008.

[50] M. Haghifam, A. R. Sedighi and O. P. Malik, "Development of a fuzzy inference system based on genetic algorithm for high-impedance fault detection," in *IEE*

Proceedings - Generation, Transmission and Distribution, vol. 153, no. 3, pp. 359-367, 11 May 2006.

[51] A. R. Sedighi, M. Haghifam, O. P. Malik and M. -. Ghassemian, "High impedance fault detection based on wavelet transform and statistical pattern recognition," in *IEEE Transactions on Power Delivery*, vol. 20, no. 4, pp. 2414-2421, Oct. 2005.

[52] H. Jabr A. Megahed "A wavelet-FIRANN technique for high-impedance arcing faults detection in distribution systems" *Proc. Int. Conf. Power Systems Transients* (IPST05) pp. 1-6 2005-Jun.

[53] H. Lala and S. Karmakar, "Detection and Experimental Validation of High Impedance Arc Fault in Distribution System Using Empirical Mode Decomposition," in *IEEE Systems Journal*, doi: 10.1109/JSYST.2020.2969966.

[54] S. Nezamzadeh-Ejieh and I. Sadeghkhani, "HIF detection in distribution networks based on Kullback–Leibler divergence," in *IET Generation, Transmission & Distribution*, vol. 14, no. 1, pp. 29-36, 17 1 2020.

[55] S. R. Samantaray and P. K. Dash "High impedance fault detection in distribution feeders using extended Kalman filter and support vector machine," *Eur. Trans. Elect. Power* 2009.

[56] A. A. Girgis, W. Chang and E. B. Makram, "Analysis of high-impedance fault generated signals using a Kalman filtering approach," in *IEEE Transactions on Power Delivery*, vol. 5, no. 4, pp. 1714-1724, Oct. 1990.

[57] C. L. Benner and B. D. Russell, "Practical high-impedance fault detection on distribution feeders," in *IEEE Transactions on Industry Applications*, vol. 33, no. 3, pp. 635-640, May-June 1997.

[58] M. Yang, "Detection of downed conductor in distribution system," Proc. IEEE Power Engineering Society General Meeting 2005 vol. 2 pp. 1107-1114 2005-Jun.

[59] L. Garcia-Santander, P. Bastard, M. Petit, I. Gal, E. Lopez and H. Opazo, "Down-conductor fault detection and location via a voltage based method for radial distribution networks," in *IEE Proceedings - Generation, Transmission and Distribution*, vol. 152, no. 2, pp. 180-184, 4 March 2005.

[60] M. Sedighizadeh "Approaches in high impedance fault detection—A chronological review" *Adv. Elect. Comput. Eng.* vol. 10 no. 3 pp. 114-128 2010.

[61] A. C. Depew, J. M. Parsick, R. W. Dempsey, C. L. Benner, B. D. Russell and M. G. Adamiak, "Field experience with high-impedance fault detection relays," *59th Annual Conference for Protective Relay Engineers, 2006.*, College Station, TX, 2006, pp. 6 pp.

[62] A. M. Cassie, "Theorie Nouvelle des Arcs de Rupture et de la Rigidité des Circuits", CIGRE, Paris, France, Rep.1029, 1939.

[63] O. Mayr, "Beiträge zur Theorie des statischen und des dynamischen Lichtbogens", *Archiv Für Elektrotechnik*, vol. 37, no. 12, pp. 588-608, 1943.

[64] P. H. Schavemaker and L. van der Slui, "An improved Mayr-type arc model based on current-zero measurements [circuit breakers]," in *IEEE Transactions on Power Delivery*, vol. 15, no. 2, pp. 580-584, April 2000.

[65] J. Schwarz, "Dynamisches Verhalten eines Gasbe-blasenen Turbulenzbestimmten Schaltlichtbogens", *ETZ-A*, vol. 92, pp. 389-391, 1971.

[66] S. R. Nam, J. K. Park, Y. C. Kang and T. H. Kim, "A modeling method of a high impedance fault in a distribution system using two series time-varying resistances in EMTP," *2001 Power Engineering Society Summer Meeting. Conference Proceedings (Cat. No.01CH37262)*, Vancouver, BC, Canada, 2001.

[67] IEEE Recommended Practice and Requirements for Harmonic Control in Electric Power Systems," in *IEEE Std 519-2014 (Revision of IEEE Std 519-1992)* , vol., no., pp.1-29, 11 June 2014.

[68] T. Thiringer and J. Luomi, "Comparison of reduced-order dynamic models of induction machines," in *IEEE Transactions on* Power Systems, vol. 16, no. 1, pp. 119-126, Feb 2001.

[69] P. Kundur, Power System Stability and Control. New York: McGraw-Hill, 1994.

[70] B. M. Aucoin and R. H. Jones, "High impedance fault detection implementation issues," in *IEEE Transactions on Power Delivery*, vol. 11, no. 1, pp. 139-148, Jan. 1996.

[71] R. Bhandia, J. d. J. Chavez, M. Cvetković and P. Palensky, "High Impedance Fault Detection Using Advanced Distortion Detection Technique," in *IEEE Transactions on Power Delivery*, vol. 35, no. 6, pp. 2598-2611, Dec. 2020.

CHAPTER 4

EQUIPMENT FAILURE ANTICIPATION

4.1 INTRODUCTION

In this chapter, the implementation of FADS to anticipate equipment failures is presented. The reliable operation of a power system is dependent on the stable operations of the several smaller apparatus, devices and components, which altogether constitute the power system. Any physical apparatus, device or component, which is a part of the power system, can be broadly classified as an equipment of the power system. Underperformance of any of this equipment can lead to loss of stability of the grid operations and might cause blackouts. With the passage of time, power system equipment experience a wide variety of stress, which include mechanical stresses, electrical stresses, thermal phases and other extreme conditions [1]. The origin of this stresses could range from normal wear and tear of equipment to some internal manufacturing defect to damage done by small faults or adverse weather effects. These stresses lead to slow degradation of the equipment, which ultimately leads to the failure of the equipment after a certain time. Majority of the power system equipment have continuous work phase and are installed in the exterior that makes them more vulnerable to damage. An annual report compiled by Dutch DSO Alliander summarizes that 50% of the electricity outage causes in 2018 was due to equipment damage or related issues [2]. There is also an important element of cost factor. It is much more advisable to replace failing equipment in time rather than risk the operations of the entire power grid. Risking operations of the entire grid would prove to be extremely costly to rectify and would cause added inconvenience to the customers. Damaged equipment in some cases might lead to fire hazards, which will lead to safety issues. Hence, it can be summarized that the reliable working operation of a power system calls for strict vigil, continuous monitoring and predictive maintenance of different equipment in the power system.

In order to enforce strict vigilance and monitor signs of equipment damage to achieve predictive maintenance of any power system equipment, there is a need of reliable real time information on health status of the different equipment. A characteristic observed factor for majority of the equipment damage cases are that they do not fail overnight and provide many opportunities for proactive action to be taken such that a catastrophic failure is averted. The signatures of the impending equipment failures can be observed in the pre-failure period usually in the form of minute changes in electrical waveforms. The

Parts of this chapter have been published in Mediterranean Conference on Power Generation, Transmission, Distribution and Energy Conversion (MedPower 2018) [43].

requirement is to detect these signatures of incipient failures in a fast and efficient manner. FADS implementation intends to achieve the same and anticipate an equipment failure. Such anticipation will act as an early warning system and help preserve the stable grid operations.

4.2 STATE-OF-THE-ART

The process of monitoring and identifying changes in equipment parameters to enhance the situational awareness of the grid is generally referred as condition monitoring [3]. As discussed in section 2.2 of Chapter 2, most of the existing incipient failure detection techniques focus solely on anticipating equipment failure and more so on specific equipment failures. The state of art discussion in Chapter 2 was based on the perspective of the techniques used for failure anticipation, so in this section the discussion is based on the perspective of the type of equipment in question.

Underground cables have become an increasingly important medium of electricity distribution, especially in urban places and agglomerates. However, the nature of underground cabling is that often there are issues pertaining to insulation and cable joints. Anticipating cable failure with exact location is of utmost importance since digging entire stretches to locate a failure would be highly undesirable. Incipient failure detection techniques applicable to underground cables have been documented in [4-10]. In [11-12], results from field investigation of cable failure and analysis of failure signatures are documented. Some other techniques working to detect incipient faults in distribution feeders are discussed in [13-14]. Transformers are one of the most expensive and critical equipment in distribution system. Consequently, many incipient failure techniques in [15-19] focus on anticipating failures in transformers. Circuit breakers and insulators are also important for protection actions and stable grid operations. Several incipient failure detection techniques for circuit breakers and insulators are documented in [20-24]. There have been a few techniques to anticipate failure in motors also in [25-26].

Adverse weather conditions are a major source of power system failures and they have tremendous effect on life and property. It is very difficult to predict natural disasters and it is not exactly in the realm of electrical engineering to do so. However, effects of weather events may lead to incipient failures that can be avoided. Some weather events may damage the equipment to the extent that the equipment functions but slowly starts degrading due to the damage. Such damaged equipment will not affect grid operations at that instant immediately but will produce signatures of its impending failure. After a slow degradation over time, the equipment will likely fail. A technique in [27] developed a fire model to estimate the temperature increase of conductors during wildfire to detect a possible equipment failure from weather events. In [28], optimal operation of distribution system has been suggested to build resilience against natural calamities. In [29-30], the insulation discharge characteristics have been used to analyze the effect of adverse weather effects on high voltage transmission lines. An early warning system has been developed in [31] to protect power system from wildfires. In [32-33], an exhaustive review of wildfire management techniques and related issues has been provided.

There have been recent attempts at developing a comprehensive equipment failure anticipation technology in [3], [34-35], whose application is not restricted to the equipment type. DFA developed by EPRI has also been utilized for detecting incipient equipment failures. The application of DFA in real life situations has been documented in [36-38]. A comprehensive summary of equipment failure anticipation techniques through analysis of failure signatures can be found in [39].

4.3 CASE STUDIES

In this thesis, FADS performance evaluation is done by implementing it in different incipient equipment failure scenarios. Since, it was not possible to conduct real field investigations, efforts have been taken to keep the case studies as realistic as possible. In order to create realistic case studies, equipment failure scenarios have been derived from articles documenting real field events. The test systems have been modelled to mimic the event sequences as closely as possible and generate waveform abnormalities similar to the ones observed in real field. Starting from the time of generating initial signatures of incipient failure to complete breakdown of the equipment, it can take form few days to few months. In the course of these months, the rate of deterioration of the equipment increases gradually and more frequent and prominent failure signatures could be observed. In the case studies, the progression of equipment failure with time and the failure signatures associated with it has been divided into multiple phases. Each phase indicates a certain degree or extent of equipment failure and the transient behavior related to it.

The case studies have been chosen such in order to cover major and frequently cited important equipment failure issues. One of the case studies is regarding the FADS implementation in case of a lightning event. The lightning event has been used as a representative of an adverse weather event. Each case study has been divided into three subsections. The first subsection details the field event sequence as documented in real-life; the second subsection explains the laboratory modelling of the same field event and division of the event sequence into multiple phases of different transient behavior patterns. Finally, the third subsection presents the results and observations drawn from it. The measurement points for the benchmark test feeders to be used have been kept fixed as discussed in Chapter 2. Similarly, the reporting interval has been kept fixed at 0.1s.

4.3.1 UNDERGROUND CABLE FAILURE

Underground cables are an important part of utilities. Hence, proactive failure management is necessary to prevent damages. Cable failure occurs mostly due to insulation or cable joint issues. In this case study, the real field cable failure event documented in [11, 39] is utilized.

A. EVENT SEQUENCE

The entire event sequence starting from initial incipient cable failure signatures to a full-fledged fault lasted for around 10 months. The initial signatures were in terms of transients generated by momentary high currents and associated change in voltage profiles. However, the phenomenon lasted barely for 0.22 cycles. Since it was a sub-cycle transient, the conventional relays did not report any outage data. Over the period of 10

months, 140 such sub-cycle transients were recorded with the duration ranging from 0.22-0.47 cycles. As the cable damage worsened, it was observed that the frequency of the occurrences of the sub-cycle transients also increased. Finally, a permanent fault happened leading to a sustained outage.

B. EXPERIMENT MODELLING

Since IEEE-34 node feeder has no nodes or sections interconnected through cables, the IEEE-13 node feeder is used for this case study. In IEEE-13 node feeder, the section between nodes 652 and 684 and section between nodes 675 and 692 are connected via underground cable. The cable failure is simulated between the nodes 675 and 692. As per the real incident, the incipient phase lasted for nearly 10 months, where around four to five different types of transient behavior was observed. Hence, for simplicity and taking into account the long period of actual field event, the modeling of the degradation of the cable is divided in four event sequence phases, indicating the transition from healthy state to total breakdown of the cable. Each of the four phases is associated with a certain frequency of transient occurrence and the duration of the transients in terms of waveform cycle. The phases and the interpretation can be seen in Table 4.1. The first phase has transients appearing every 2s and for a duration of 0.2 cycle. After a simulation run of 50s, the second phase starts with transients appearing every 1.25s for duration of 0.3 cycle and is simulated for 37.5s. Similarly, for the third and fourth event phases, as the cable degradation intensifies, the transients appear more often until the final breakdown happens. The transients generated during the simulation duration are sufficient for FADS analysis.

TABLE 4.1
UNDERGROUND CABLE FAILURE EVENT SEQUENCES

Event Sequence Phase	Sequence Interpretation	Simulation Duration
Phase 1	**Transients observed every 120 phases (2s) for 0.2 cycles**	**50s**
Phase 2	**Transients observed every 75 phases (1.25s) for 0.3 cycles**	**37.5s**
Phase 3	**Transients observed every 37.5 phases (0.6s) for 0.4 cycles**	**24s**
Phase 4	**Transients observed every 15 phases (0.25s) for 0.5 cycles**	**12.5s**

In modelling the simulation, care has been taken to adhere largely to the sub-cycle transient duration limits as observed in the field tests. The total number of transients generated combining all event sequence phases add up to 145, which is comparable to the 140 transients observed in field tests in [11]. The time gap for shifting from the sequence phase 1 to sequence phase 2 is higher than shifting from sequence phase 2 to sequence phase 3 to reflect the incremental equipment failure as the malfunctioning increases. Such

an approach has been kept same for the subsequent study cases. As the transient appearance frequency increases, the effect lasts longer leading to higher number of distorted samples. The sub-cycle transients were generated by injecting certain harmonics for the sequence phase duration. The entire sequence of events for this study case and the subsequent ones discussed in this chapter were simulated in *RTDS* through a batch script execution.

C. RESULTS

The entire simulation runs for 124s from the time of commencement of the first event sequence phase. The interesting snapshots from different time intervals during the entire simulation run showing waveform distortions from each sequence can be seen in Figure 4.1. The waveforms shown in the figure are voltage waveforms of phase C for different measurement points at different nodes. The zoomed version of the voltage waveform distortions is also shown to highlight clearly the sub-cycle transients.

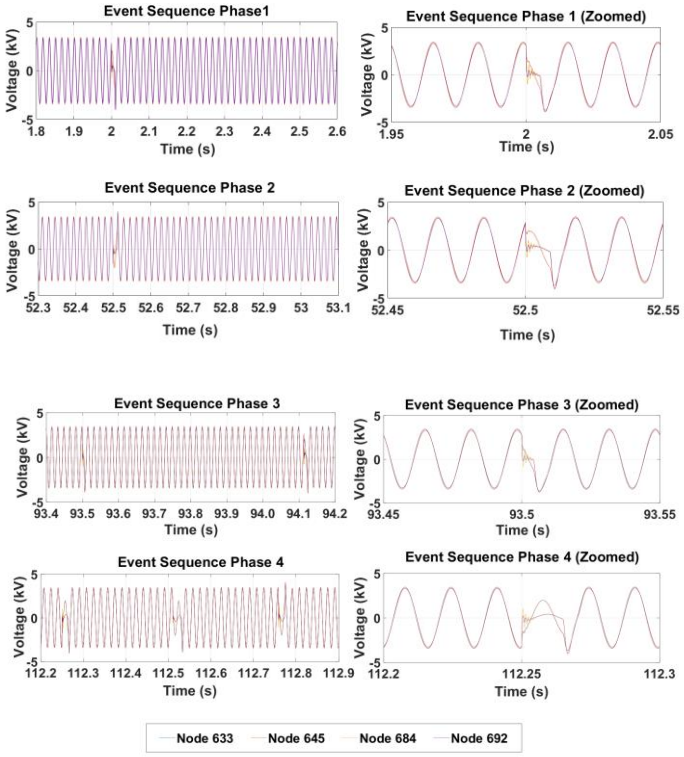

Figure 4.1: Underground cable failure event sequence phases showing sub-cycle voltage waveform distortions for different measurement points (Phase C).

The concise summary of FADS implementation results can be observed from the graphical representation in Figure 4.2. Due to the enormity of the FADS result data generated, the severity ratings across different measurement points for each sequence phase is presented separately. Therefore, for event sequence phase 1, the total simulation

duration of real-time in 50s implies 500 reporting intervals of 0.1s for each measurement point. The total number of different severity rating levels attained by each measurement point and the grid zones in that simulation duration for each event sequence phase is shown in Figure 4.2. This information can then be used by the DSO operators to arrive at a comprehensive conclusion regarding the presence of any potentially harmful event in the grid. Severity rating level 0 is interpreted as normal grid operations. Hence, to keep the graphical representation sharp and refined, the severity rating level 0 instances are not highlighted. This approach to analyze results through graphical representation is kept constant for subsequent case studies in this chapter.

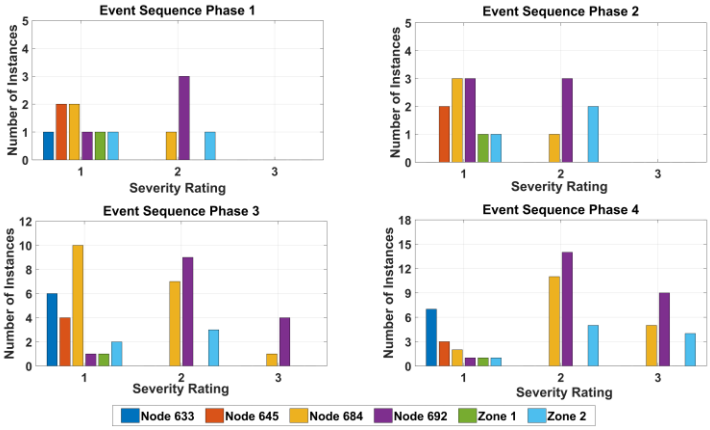

Figure 4.2: Instances of different Severity Rating levels at different measurement points for each event sequence phase during FADS implementation for underground cable failure.

As observed from Figure 4.2, in the first event phase there is no level 3 reporting from any measurement point. Even though the simulation duration of the phase is 50s, the transient appearance frequency of every 2s leads to few level 2 reporting and they are mainly restricted to measurement points at nodes 684 and 692. Considering no level 3 reporting and negligible level 2 reporting in proportion to the simulation duration, it cannot be concluded if event sequence phase 1 indicates presence of any incipient failure in the grid. In phase 2, the simulation duration reduces to 37.5s. There is no level 3 reporting. The level 1 and level 2 reporting stay almost same in number, as phase 1, but the actual interpretation would be a slight proportional increase in the reporting as the simulation duration has decreased. After observing phase 1 and phase 2 reporting, it can be construed that there is some indication of possible issues with the grid operations and maintenance teams maybe kept at standby. In the phase 3 of simulation duration of 24s, first level 3 reporting is observed and the level 2 reporting is proportionately higher. The grid zone result observations also indicate the possible event location in Zone 2. Multiple level 3 reporting should be the trigger to immediately dispatch the standby maintenance teams to Zone 2 to locate the incipient failure before it develops into a fault and cascades into a possible outage. Phase 4 with the smallest simulation duration reports proportionately higher number of level 3 and level 2 severity ratings mainly for Zone 2 measurement points clearly confirming an incipient failure in Zone 2.

In the FADS implementation in real field investigations, the ideal approach would be to take action sometime during sequence phase 3 or possibly at the end of sequence phase 2. The end of sequence phase 2 gives inkling of a possible incipient failure and by end of phase 3, the possibility of incipient failure gets stronger. Since the entire event phase in the real field event (which inspired this case study) stretched around 10 months, FADS implementation results of the simulated case study mapped to that timeline suggests real field FADS implementation could have helped detect incipient failure of the underground cable few months before the ultimate breakdown of the cable. The possible positive effects of such failure anticipation from FADS implementation would include reliable power supply, timely maintenance leading to less frequent outages, overall reduced outage duration and satisfied consumers and utilities.

4.3.2 CAPACITOR BANK SWITCH MALFUNCTION

Capacitor banks are an important asset in distribution feeder and are needed for correcting power factor, providing voltage support etc. A high power factor ensures higher quality of power supply and minimizes losses. Hence, correct operation and maintenance of capacitor banks are a priority. In this case study, we utilize the real field event of capacitor bank switch malfunction documented in [38]. In [38], one of the emerging incipient failure detection methods, DFA, was used to detect the malfunction.

A. EVENT SEQUENCE

The event sequence lasted for a total of 2½ months before the damaged equipment was located and replaced. Initially, the capacitor bank installed in the grid was successfully switched. However, after a while the monitoring systems in substations detected some unexplained transients. These transients however did not cause any alarm and the conventional protection schemes including the state-of-the-art Advanced Metering Infrastructure (AMI) installation did not raise any alert or suspicion. The frequency of appearance of transients increased with time up to twenty-one instances per day, hinting at an equipment damage accelerating towards failure. When the utility took action after 2½ months, around 500 instances of transients were recorded. The cause of the transients was found to be a malfunctioning switch that conducted some current even after it was in the open state leading to an internal damage to the capacitor bank.

B. EXPERIMENT MODELLING

In order to recreate the real field event, the IEEE-34 node feeder was used for the experimental modelling. The capacitor bank was connected at node 854 and the phase C was designed to malfunction. The capacitance is set to 1.9252μF per phase, which is similar to the rating of capacitors connected in the benchmark IEEE-34 node feeder. The capacitor bank is then connected to the grid through a vacuum switch. The vacuum switch is modeled as an ideal switch with a close resistance equal to 0.1Ω and open state of 1e6Ω. The resistance in phase C in open state is designed to change to 250Ω. This results in a small current flowing to the switch even during open condition, leading to small transients. These transients gradually damage the equipment leading to eventual equipment failure, similar to the sequence of events observed in the field investigations in [38].

The sequence of events was planned such that the progressive degradation of the malfunctioning switch can be reflected as it happened in real life. The generation of transients was done through a series of switching actions of the ideal switch. Compared to the last case study where the event sequence lasted for 10 months, the capacitor switch malfunction event lasted for 2½ months. Hence, in the experimental model, the equipment

TABLE 4.2
CAPACITOR BANK SWITCH MALFUNCTION EVENT SEQUENCES

Event Sequence Phase	Sequence Interpretation	Simulation Duration
Phase 1	**Transients observed every 60 cycles (1s simulation time)**	**120s**
Phase 2	**Transients observed every 30 cycles (0.5s simulation time)**	**90s**
Phase 3	**Transients observed every 15 cycles (0.25s simulation time)**	**50s**

damage was achieved through three event sequence phases as seen in Table 4.2. In the first phase, transients are observed every 1s of simulation. After 120s of simulation duration of phase 1, the transients now appear at every 0.5s indicating increased equipment damage. The simulation duration of phase 2 lasts for 90s. Finally, in phase 3, the transients appear every 0.25s for 50s of simulation duration and then the equipment fails, leading to permanent fault and disconnection. The total number of transients generated combining all event sequence phases add up to 500, which is same as the 500 transients observed in field tests in [38].

C. RESULTS

The entire simulation runs for 260s from the time of commencement. The interesting snapshots from different time intervals during the entire simulation run showing waveform distortions from each sequence can be seen in Figure 4.3. The waveforms shown in the figure are voltage waveforms of phase C for different measurement points at different nodes. Since the node 818 is a single phase (phase A) to neutral connected, the waveforms from node 818 are not plotted and no measurements are recorded. Zone 1 recordings are based from common reporting of nodes 812 and 830. The zoomed version of the voltage waveform distortions is also shown to highlight the transients at every switching instant.

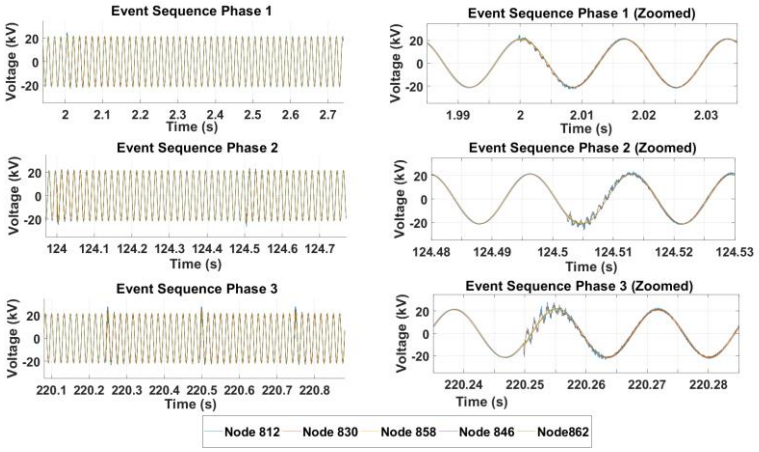

Figure 4.3: Capacitor bank switch malfunction event sequence phases showing voltage waveform distortions for different measurement points (Phase C).

A concise summary of FADS implementation results and instances of severity rating levels at different measurement points and the different zones is presented in Figure 4.4. In phase 1, the transients are appearing every 1s leading to few instances of level 1 severity rating across the grid. Expectedly, the measurement point closest to the event records most instances. Even though there is a single instance of level 2 rating, the observations are largely inconclusive to confirm presence of incipient failure. In phase 2, the transients appear more often and as a result, several instances of level 1 and level 2 ratings spread across different measurement points are observed. The first instance of level 3 reporting is also observed. From the phase 2 observations, the presence of an incipient failure in the grid can be concluded. The Grid Zone severity ratings are inconclusive since instances of ratings of both zones are very similar which makes it difficult to determine in which zone the maintenance teams should be dispatched. In order to locate the event better, the LMD level ratings would have to be used. Since the difference between instances of level 2 ratings for nodes 830 and 858 far outnumber that of other measurement points, the search area priority could be the segments between nodes 830 and 858. In the phase 3, it becomes clearer that incipient failure is somewhere between the nodes 830 and 858 as they together report most instances of level 2 and level 3 severity ratings.

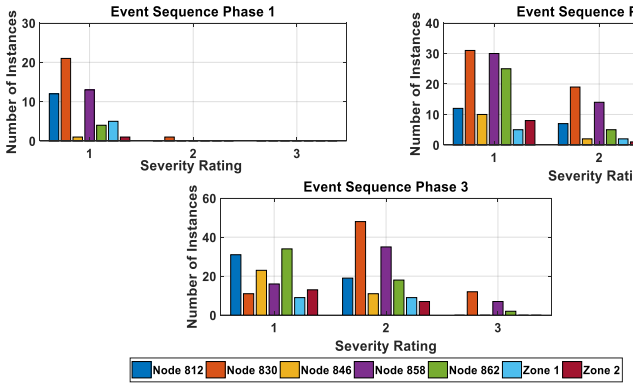

Figure 4.4: Instances of different Severity Rating levels at different measurement points for each event sequence phase during FADS implementation for capacitor bank switch malfunction.

In the FADS implementation in real-field investigations for this case study, phase 2 seems the ideal time to take action. However, in this case study, the underperformance of grid zoning concept is evident and the fallback option of LMD severity ratings have to be used to locate accurately the incipient failure. Even though this case study highlights the need of implementing optimization tools for better execution of grid zoning concept, the overall FADS performance would not be affected much due to inbuilt failsafe feature of two-tier severity rating system in FADS. Mapping the phase 2 timeline to real field event occurrence, FADS implementation would help to detect the incipient failure few weeks before the eventual equipment breakdown happens.

4.3.3 TRANSFORMER INTERNAL FAILURE

Transformers are one of the most important assets in AC distribution system. A transformer is very expensive equipment and is generally build to work for decades. The long work phase of the transformers expose it to stress generated from different distribution system faults over years. This weakens the transformers over time and makes them more susceptible to failure. Failure of critical equipment like transformer will have a significant negative effect on the distribution system and will lead to large stretches of area without electricity. Hence, adequate protection and care of transformers is always desired and necessary. This case study is partly based on the real field event of transformer bushing damage leading to internal failure documented in [40].

A. EVENT SEQUENCE

In the field event, the initial transients from the incipient failure indicated voltage sag on phase B. As the incipient failure accelerated towards failure, a fuse on the primary side of the transformer blew out leading to some transients also on the phase A and B. However as no large currents were drawn, the conventional protection systems did not raise any alarm and there was no tripping action. Finally, after a span of around 25

minutes, a permanent fault occurred and the transformer was disconnected via means of the tripping of conventional relays. It was found out that the bushing o the transformer was damaged either from a previous fault like condition or normal ageing, which led to water seeping inside and damaging the insulation windings of the transformer. This insulation damage then quickly developed into a permanent fault.

TABLE 4.3
TRANSFORMER INTERNAL FAILURE EVENT SEQUENCES

Event Sequence Phase	Sequence Interpretation	Simulation Duration
Phase 1	**Transients observed every 60 cycles (1s simulation time)**	**90s**
Phase 2	**Transients observed every 30 cycles (0.5s simulation time)**	**60s**

B. EXPERIMENT MODELLING

The IEEE-13 node feeder is used for simulating the transformer failure event. The transformer located between the nodes 633 and 634 is utilized for the purpose. It is assumed that the bushing damage has already taken place due to some internal factors. As a result, it is considered that the moisture seeping inside is damaging the winding insulation. In order to model the internal damage, the leakage inductance in the *RTDS* model is varied after every phase. The phase B is designed to be internally damaged, similar to as observed in [40].

In real life, the event lasts for just 25mins. Hence, in the simulation only two event sequence phases is considered as seen in Table 4.3. In the first event sequence phase, the equipment damage is simulated by increasing the leakage inductance to make the transformer less efficient such that the transients appear every 1s of simulation. The duration of the simulation of first phase is kept at 90s. In the second phase, the equipment is supposed to be more severely damaged. Hence, leakage inductance is increased to double of the last value to reflect the increased damage. Hence, the transients now appear every 0.5s and the duration of simulation for second phase is kept at 60s. The end of event sequence phase 2 is considered as the final breakdown of transformer leading to permanent fault.

C. RESULTS

The entire simulation runs for 150s from the time of commencement. The interesting snapshots from different time intervals during the entire simulation run showing waveform distortions from each sequence can be seen in Figure 4.5. The waveforms shown in the figure are voltage waveforms of phase C for different measurement points at different nodes. The zoomed version of the voltage waveform distortions is also shown to highlight the transients at every switching instant.

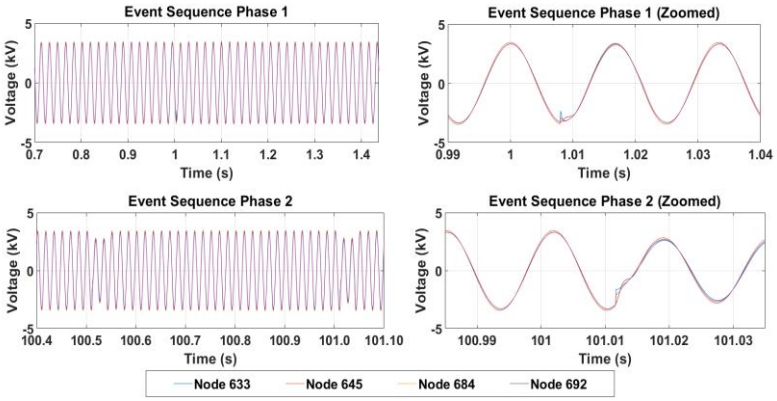

Figure 4.5: Transformer internal failure event sequence phases showing voltage waveform distortions for different measurement points (Phase B).

The FADS implementation results summary for the instances of severity ratings at different measurement points and the zones can be seen in Figure 4.6. In the first phase, transients appear every 1s for the simulation duration of 90s. The high number of instances of level 1 reporting from nodes 633 and 645 indicate to an incipient failure in the system. The lower number of instances for nodes 684 and 692 and the corresponding grid zone severity ratings mainly points to an existence of incipient failure in Zone 1.

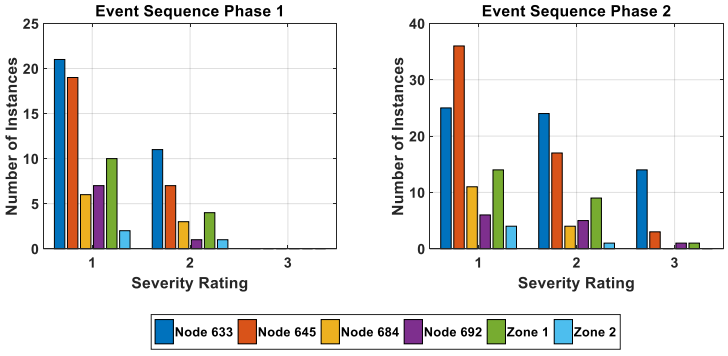

Figure 4.6: Instances of different Severity Rating levels at different measurement points for each event sequence phase during FADS implementation for transformer internal failure event.

Moreover, the comparatively high instances of level 2 ratings in ratio of total transients generated in that event sequence phase should be the trigger for utilities to dispatch the maintenance teams to Zone 1. In the second phase, the instances of level 1 and level 2 ratings across different measurement points at different nodes clearly confirms the presence of incipient failure in Zone 1. Another major observation that can be made here is that the difference between the nodes 633 and 645 for the instances of the dangerous, level 3 severity ratings, indicate that the incipient failure location is closer to node 633. Hence, the search priority could be the regions near to node 633 before moving to other areas of Zone 1.

In the FADS implementation in real-field investigations for this case study, ideally the phase 1 itself raises numerous red flags to consider immediate dispatch of maintenance teams. During phase 2, the multiple instances of level 3 ratings confirm the presence of incipient failure event. Mapping the phase 1 timeline to real field occurrence, FADS implementation would detect the incipient failure several minutes before the permanent fault. Even though grid zone reporting is accurate in phase 2, the LMD reporting help to further refine the data to deduce that the event is closer to node 633. Hence, with FADS implementation, the search area for the maintenance teams could be further reduced and prioritized leading to quicker and efficient response.

4.3.4 LIGHTNING EVENT

Adverse weather effects ranging from lightning to a broken tree branch to normal vegetation growth interfering with conductors have great potential to cause equipment damage leading to outages. Weather prediction and related studies can constitute a reasonable approach so that a proactive action can be taken to prevent equipment damage but since it requires high-level coordination and cooperation among different agencies, it is outside the scope of this thesis. In the earlier case studies, FADS performance was already evaluated in case of equipment failures that might or might not be due to adverse weather effects. In this case study it is evaluated if FADS implementation can help in sudden adverse weather conditions like a lightning strike, which is accompanied by fast transients.

A. EVENT SEQUENCE

Lightning is a short duration event accompanied with very fast travelling transients. These transients can cause high magnitude voltage surges. These voltage surges can significantly damage equipment and cause outages. Conventional protection schemes use expensive surge arrestors to limit the magnitude of the voltage surges originating from lightning event. Surge arrestors are effective in limiting the damage but not all damage can be prevented. Around 20% of all lightning strikes still lead to permanent faults and sustained outages [41]. Hence, it is important to detect those incipient failures signatures emanating out of damaged equipment and conduct proactive maintenance before a complete breakdown of the equipment takes place in future.

The lightning event with its fast transients travelling almost at the speed of light makes it highly unlikely to predict. FADS is not designed to be able to track such fast transients and it can be considered one of the shortcomings of FADS functionality. Currently, there

is a lack of standardized tracking techniques for such fast transients. Hence, FADS implementation here aims to rather detect waveform distortions caused by lightning to assess the damage caused and indicate the area of event so that a quick predictive maintenance can take place to identify and isolate the possible damaged equipment.

B. EXPERIMENT MODELLING

A standard lightning event has a fast rise followed by a slow decay. A typical lightning surge voltage waveform has a rise time of 1.2µs and a decay of 50µs. The waveform can be represented by the eqn. (4.1) as described in [42]. The trace of the lightning voltage surge waveform can be seen in Figure 4.7.

$$v(t) = V_o\left(e^{-t/t_b} - e^{-t/t_a}\right) \tag{4.1}$$

Here

- $v(\mathrm{t})$ is the voltage of the lightning strike
- V_o is the initial voltage
- t is the time
- t_a and t_b are time to reach 30% and 90% of the peak value
- $t_a = 71\mu s$ and $t_b = 0.2\mu s$

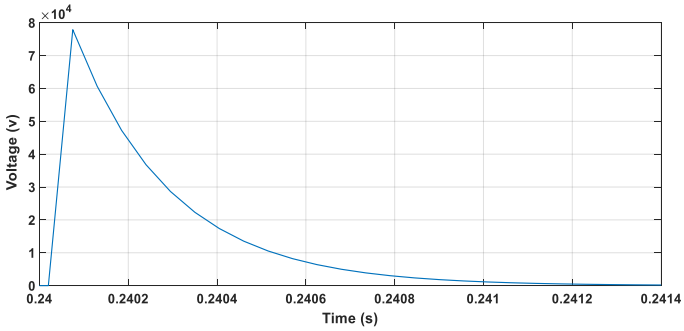

Figure 4.7: Lightning Surge Voltage Behavior

The long IEEE-34 node feeder is used to simulate the lightning event. The node chosen to simulate the lightning is node 832. The choice of node is influenced by the fact it is closest to one of the most expensive equipment in a distribution grid, the transformer. Since lightning is such a fast event, there is no sequence of phases. The FADS performance is evaluated after the event strikes.

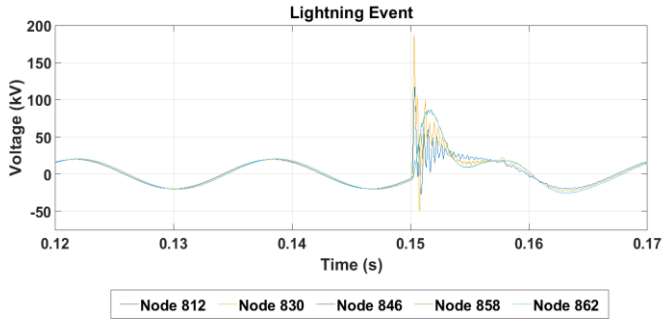

Figure 4.8: Distorted voltage waveforms across different measurement points after lightning strike at $t = 0.15s$ (Phase C)

C. RESULTS

The lightning strikes at phase C at $t = 0.15s$. The voltage waveforms from all the measurement points can be seen at Figure 4.8. The breach of thresholds and the corresponding severity level ratings for 0.8s divided into 8 reporting intervals (T1→ T8) can be seen in Figure 4.9. Since, the reporting intervals are comparatively less in number; the severity rating interval for every measurement point can be displayed for each interval. As the lightning strike event is modelled to affect phase C, the measurement at node 818 is not taken into account. It can be observed that just after lightning strike, the measurement points at nodes 858, 846 and 830 indicate severity rating level 3 while nodes at 812 and 862 indicate level 2. With time, as the lightning event dies out, the nodes 858 and 846 maintain level 3 for next three and two reporting intervals respectively and then they both move down to level 2. Node 862 maintains level 2 throughout while node 830 stays at level 3 for one more reporting interval and then moves to level 2. Node 812 moves to level 0 immediately after the event. The fact that node 830 maintains level 3 for a lesser duration than node 858 can be possibly attributed to the fact there is a presence of voltage regulator between the nodes 830 and 832. Similarly for zonal ratings, Zone 2 indicates level 2 throughout while Zone 1 (including only nodes 812 and 830) indicates level 1 initially and then moves to zero.

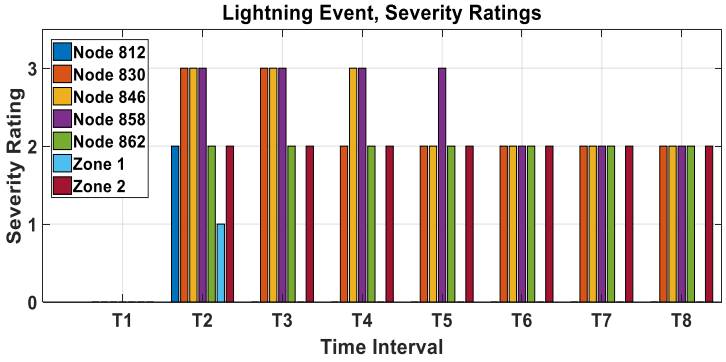

Figure 4.9: Instances of different Severity Rating levels at different measurement points for each event sequence phase during FADS implementation for lightning event.

It can be concluded from the observations that initially it seemed that a very harmful event has occurred between nodes 858 and 846. However, with time it was observed that the level 2 was reported throughout among the nodes 830, 858, 846 and 862 for multiple time intervals. The reasonable conclusion that can be drawn is that a harmful event has occurred somewhere between those nodes. In order to locate the event by maintenance teams and look for damage, the priority can be accorded to the areas encompassed by measurement points at nodes 830, 846 and 858 as they combined report highest level 3 severity ratings. Hence, even if it is practically impossible to anticipate where the lightning would strike, FADS implementation can give a fair idea of the lightning location and the areas most affected. Such an exercise will help in early identification and replacement of probable damaged equipment and components in that area. This will eventually result in preventing failures or interruptions in future.

4.4 CONCLUSIONS

In this chapter, FADS was implemented to anticipate equipment failures. The case studies comprised several failure scenarios involving different equipment. All the failure scenarios were based on real-field occurrences where the initial occurrence of transients was not enough to trigger the conventional protection schemes and after a while, permanent fault took place. The event sequences and transient appearance patterns of the case studies were modelled to mimic the observations in real-field cases. FADS implementation successfully detects the incipient failure signatures and anticipates the equipment failure well before the eventual equipment breakdown or occurrence of a permanent fault would have happened. The two-tier severity rating scale results of different event sequence phases provides information to quantify the accelerating deterioration of equipment condition and provides actionable input on possible event location. This information helps to determine when to take action and where to dispatch the maintenance teams.

FADS performance evaluation comprised implementing FADS to anticipate equipment failure in case studies with timelines varying from 10 months to 25 minutes. FADS performance was also evaluated in a case study regarding effects and possible negative aftermath of adverse weather event. The results obtained for those case studies clearly highlight the comprehensiveness and efficacy of FADS and how it can complement the working of conventional protection schemes. Hence, the main contribution of this chapter is to display the effectiveness of FADS as a failure anticipation tool/technology. FADS can be also combined with the different proven approaches as discussed in section 4.2 to develop a comprehensive tool for anticipating equipment failure.

Since in some case studies, the underperformance of grid zoning concept was observed, the concept of special observation zones was suggested for critical equipment's like transformer or critical connected loads like hospitals or railways. Special observation zones might come at a certain cost but would lead to better monitoring of those zones and make FADS implementation more efficient. Further studies involving other power distribution system components needs to be conducted to better evaluate FADS performance and systematically improve FADS.

REFERENCES

[1] C. L. Benner and B. D. Russell, "Investigation of incipient conditions leading to the failure of distribution system apparatus," *IEEE PES Power Systems Conference and Exposition, 2004.*, New York, NY, 2004, pp. 703-708 vol.2.

[2] Annual Report 2018. Alliander N.V. 2018. [Online]. Available: https://www.alliander.com/content/uploads/dotcom/Alliander_Annual_Report_2018.pdf

[3] G. W. Chang, Y. Hong and G. Li, "A Hybrid Intelligent Approach for Classification of Incipient Faults in Transmission Network," in *IEEE Transactions on Power Delivery*, vol. 34, no. 4, pp. 1785-1794, Aug. 2019.

[4] M. Jannati, B. Vahidi and S. H. Hosseinian, "Incipient Faults Monitoring in Underground Medium Voltage Cables of Distribution Systems Based on a Two-Step Strategy," in *IEEE Transactions on Power Delivery*, vol. 34, no. 4, pp. 1647-1655, Aug. 2019.

[5] A. Hamel, A. Gaudreau and M. Cote, "Intermittent arcing fault on underground low-voltage cables," in *IEEE Transactions on Power Delivery*, vol. 19, no. 4, pp. 1862-1868, Oct. 2004.

[6] T. S. Sidhu and Z. Xu, "Detection of Incipient Faults in Distribution Underground Cables," in *IEEE Transactions on Power Delivery*, vol. 25, no. 3, pp. 1363-1371, July 2010.

[7] T. Ghanbari, "Kalman filter based incipient fault detection method for underground cables," in *IET Generation, Transmission & Distribution*, vol. 9, no. 14, pp. 1988-1997, 5 11 2015.

[8] W. Zhang, X. Xiao, K. Zhou, W. Xu and Y. Jing, "Multiphase Incipient Fault Detection and Location for Medium Voltage Underground Cable," in *IEEE Transactions on Power Delivery*, vol. 32, no. 3, pp. 1450-1459, June 2017.

[9] S. Kulkarni, S. Santoso and T. A. Short, "Incipient Fault Location Algorithm for Underground Cables," in *IEEE Transactions on Smart Grid*, vol. 5, no. 3, pp. 1165-1174, May 2014.

[10] B. Kasztenny, I. Voloh, C. G. Jones, G. Baroudi, "Detection of incipient faults in underground medium voltage cables", Proc. 61st Annu. Conf. Protect. Relay Eng., pp. 349-366, Apr. 2008.

[11] R. Moghe, M. J. Mousavi, J. Stoupis and J. McGowan, "Field investigation and analysis of incipient faults leading to a catastrophic failure in an underground distribution feeder," *2009 IEEE/PES Power Systems Conference and Exposition*, Seattle, WA, 2009, pp. 1-6.

[12] K. L. Butler, "An expert system based framework for an incipient failure detection and predictive maintenance system," in Proc. 1996 Intelligent System Application to Power Systems Conf., Jan. 1996, pp. 321-326.

[13] S. Ebron, D. L. Lubkeman and M. White, "A neural network approach to the detection of incipient faults on power distribution feeders," in *IEEE Transactions on Power Delivery*, vol. 5, no. 2, pp. 905-914, April 1990

[14] C. J. Kim, Seung-Jae Lee and Sang-Hee Kang, "Evaluation of feeder monitoring parameters for incipient fault detection using Laplace trend statistic," in *IEEE Transactions on Industry Applications*, vol. 40, no. 6, pp. 1718-1724, Nov.-Dec. 2004.

[15] T. S. Sidhu and M. S. Sachdev, "Online identification of magnetizing inrush and internal faults in three-phase transformers", *IEEE Trans. Power Delivery*, vol. 7, pp. 1885-1891, Oct. 1992.

[16] Q. Su, C. Mi, L. L. Lai and P. Austin, "A fuzzy dissolved gas analysis method for the diagnosis of multiple incipient faults in a transformer," in *IEEE Transactions on Power Systems*, vol. 15, no. 2, pp. 593-598, May 2000

[17] Hang Wang and K. L. Butler, "Modeling transformers with internal incipient faults," in *IEEE Transactions on Power Delivery*, vol. 17, no. 2, pp. 500-509, April 2002.

[18] P. A. Venikar, M. S. Ballal, B. S. Umre and H. M. Suryawanshi, "A Novel Offline to Online Approach to Detect Transformer Interturn Fault," in *IEEE Transactions on Power Delivery*, vol. 31, no. 2, pp. 482-492, April 2016.

[19] D. R. Morais and J. G. Rolim, "A hybrid tool for detection of incipient faults in transformers based on the dissolved gas analysis of insulating oil," in *IEEE Transactions on Power Delivery*, vol. 21, no. 2, pp. 673-680, April 2006.

[20] V. Demjaneko, "A noninvasive diagnostic instrument for power circuit breakers", *IEEE Transactions. Power Delivery*, vol. 7, pp. 656-663, Apr. 1992.

[21] S. E. Habib and M. Khalifa, "A new monitor for pollution on power line insulators", *Proc. Inst. Elect. Eng.*, vol. 133, no. 2, pp. 24-30, Mar. 1986.

[22] C. J. Kim, "A study on the characterization of the incipient failure behavior of insulators in power distribution line", *IEEE Trans. Power Delivery*, vol. 14, pp. 519-524, Apr. 1999.

[23] C. J. Kim, J. A. Momoh and H. J. Lee, "Phase-time analysis of the leakage impulse current of unhealthy line-post insulators", *IEEE Trans. Power Delivery*, vol. 18, pp. 323-328, Jan. 2003.

[24] W. Bassi, H. Tatizawa, "Early prediction of surge arrester failures by dielectric characterization", *IEEE Elect. Insul. Mag.*, vol. 32, no. 2, pp. 35-42, Mar./Apr. 2016.

[25] B. Akhil Vinayak, K. Anjali Anand and G. Jagadanand, "Wavelet-based real-time stator fault detection of inverter-fed induction motor," in *IET Electric Power Applications*, vol. 14, no. 1, pp. 82-90, 1 2020.

[26] C. Wang, X. Liu and Z. Chen, "Incipient Stator Insulation Fault Detection of Permanent Magnet Synchronous Wind Generators Based on Hilbert–Huang Transformation," *in IEEE Transactions on Magnetics*, vol. 50, no. 11, pp. 1-4, Nov. 2014.

[27] E. I. Koufakis, P. T. Tsarabaris, J. S. Katsanis, C. G. Karagiannopoulos and P. D. Bourkas, "A Wildfire Model for the Estimation of the Temperature Rise of an Overhead Line Conductor," in *IEEE Transactions on Power Delivery*, vol. 25, no. 2, pp. 1077-1082, April 2010.

[28] D. N. Trakas and N. D. Hatziargyriou, "Optimal Distribution System Operation for Enhancing Resilience Against Wildfires," in *IEEE Transactions on Power Systems*, vol. 33, no. 2, pp. 2260-2271, March 2018.

[29] T. Wu, K. Liu, T. Liu, B. Xiao, Y. Peng and Z. Su, "Investigation on simulation method of gaps discharge characteristic under forest fire conditions", *Proc. 12th IET Int. Conf. AC DC Power Transmiss.*, pp. 1-6, 2016.

[30] T. Wu *et al*., "Insulation property of wire-plane gap under fire condition: Effects of vegetation flame conductivity," *2015 5th International Conference on Electric Utility Deregulation and Restructuring and Power Technologies (DRPT)*, Changsha, 2015, pp. 1600-1605.

[31] S. Dian et al., "Integrating wildfires propagation prediction into early warning of electrical transmission line outages", *IEEE Access*, vol. 7, pp. 27586-27603, 2019.

[32] S. Jazebi, F. de León and A. Nelson, "Review of Wildfire Management Techniques—Part I: Causes, Prevention, Detection, Suppression, and Data Analytics," in *IEEE Transactions on Power Delivery*, vol. 35, no. 1, pp. 430-439, Feb. 2020.

[33] S. Jazebi, F. de León and A. Nelson, "Review of Wildfire Management Techniques—Part II: Urgent Call for Investment in Research and Development of Preventative Solutions," in *IEEE Transactions on Power Delivery*, vol. 35, no. 1, pp. 440-450, Feb. 2020.

[34] B. Li, Y. Jing and W. Xu, "A Generic Waveform Abnormality Detection Method for Utility Equipment Condition Monitoring," in *IEEE Transactions on Power Delivery*, vol. 32, no. 1, pp. 162-171, Feb. 2017.

[35] S. Tao, Y. Chai and N. Q. Vi, "Incipient fault online estimation based on Kullback-Leibler Divergence and fast moving window PCA," *IECON 2017 - 43rd Annual Conference of the IEEE Industrial Electronics Society*, Beijing, 2017, pp. 8065-8069.

[36] K. Manivinnan, C. L. Benner, B. D. Russell and J. A. Wischkaemper, "Automatic identification, clustering and reporting of recurrent faults in electric distribution feeders," *2017 19th International Conference on Intelligent System Application to Power Systems (ISAP)*, San Antonio, TX, 2017, pp. 1-6.

[37] B. D. Russell and C. L. Benner, "Intelligent Systems for Improved Reliability and Failure Diagnosis in Distribution Systems," in *IEEE Transactions on Smart Grid*, vol. 1, no. 1, pp. 48-56, June 2010.

[38] J. A. Wischkaemper, C. L. Benner, B. D. Russell and K. Manivannan, "Application of Waveform Analytics for Improved Situational Awareness of Electric Distribution Feeders," in *IEEE Transactions on Smart Grid*, vol. 6, no. 4, pp. 2041-2049, July 2015.

[39] IEEE Working Group on Power Quality Data Analytics, Tech. Rep. 73: Electrical signatures of power equipment failures. Dec 2019. [online] Available: http://grouper.ieee.org/groups/td/pq/data/.

[40] DPQ Event: Cracked Bushing Leads to Tranformer Bank Failure. Tech. Rep. 1012435, 2003. Electrical Power Research Institute (EPRI), USA. [Online]. Available: https://www.epri.com/research/products/000000000001017225/

[41] T. A. Short, "*Electrical Power Distribution Handbook*", 2nd Ed., CRC Press, 2014.

[42] P. F. Ribeiro, C. A. Duque, P. M. da Silveira, and A. S. Cerqueira, "Power Systems Signal Processing for Smart Grids" John Wiley & Sons, 2013.

[43] R. Bhandia, M. Cvetković, J. J. Chavez and P. Palensky, "Incipient equipment failure assessment and avoidance through robust detection technqiue," *Mediterranean Conference on Power Generation, Transmission, Distribution and Energy Conversion (MEDPOWER 2018)*, Dubrovnik, Croatia, 2018, pp. 1-6.

CHAPTER 5

EFFECT ON RELIABILITY INDICES

5.1 INTRODUCTION

Reliability indices are a set of metrics widely used by DSO's and power utilities to measure the reliability of power supply to the end consumers. Reliability indices are generally used for distribution systems as the distribution systems account for roughly 80%-95% of the failure events [1]. Reliability indices serve as the key performance indicators of any DSO or power utility. In broad terms, reliability indices give us information on the total outages, frequency of outages, total customers affected, total duration of customers affected and time taken to recover the power supply. This information is critical to DSO's as they use it to improve their reliability. In order to achieve improved reliability index measurement, DSO's spend significant amount of time and money on planning and resource allocation to achieve a fast and efficient response to any outage in the grid. The reliability indices also help in identifying problematic feeders and DSO's use this information to determine their capital expenditure on future infrastructural investments in a bid to fix such problems.

Reliability indices need to be taken seriously, as unreliable power supply also has major economic costs attached to it. An estimate calculated by the energy company *Eneco* as part of their internal optimization study shows that reduction of even 1% in their supply recovery time would yield a saving of around €1.4 Million per year [2]. The yearly benchmarking report by CEER has also stated the need to have regulations on improving quality of energy supply to achieve optimum efficiency of implemented investments [3]. Several regulatory commissions determine regulatory limits based on average values and standard deviations of yearly reliability indices [4-5]. Hence, reliability evaluation has become an important task for both DSO's and power utilities [6]. Based from the observations made in this section, it can be easily concluded that improvement of reliability indices is important, as it would translate into significant savings for utilities while guaranteeing reliable power supply to its consumers.

In this chapter, the main reliability indices are introduced first, followed by the discussion on the limitations of current DSO practices for improving reliability indices. A literature review is done to document the existing techniques and methods developed for application in this area of research. Subsequently, the possible advantage in

Parts of this chapter have been accepted for publication in Innovative Smart Grid Technologies Conference (ISGT 2020).

improvement of reliability indices by anticipating and locating a failure via means of FADS implementation is highlighted.

5.2 RELIABILITY INDICES

The main reliability indices used in distribution systems as described in the IEEE Standard in [7] are:

- *SAIDI: System Average Interruption Duration Index*
- *SAIFI: System Average Interruption Frequency Index*
- *CAIDI: Customer Average Interruption Duration Index*
- *CAIFI: Customer Average Interruption Frequency Index*
- *MAIFI: Momentary Average Interruption Frequency Index*

SAIDI and SAIFI are the most commonly used indices for sustained interruptions to benchmark reliability and quality regulations [8-9]. Hence, in this chapter we limit our studies to evaluate the effect of FADS implementation in improvement of SAIDI and SAIFI. The indices SAIDI and SAIFI can be defined as [7, 10]:

$$SAIDI = \frac{\sum U_i N_i}{N_T} \tag{5.1}$$

$$SAIFI = \frac{\sum N_i}{N_T} \tag{5.2}$$

Here:

- U_i is the annual outage time for location i
- N_i is the number of customers in location i
- N_T is the total number of customers

SAIDI is measured as reliability of the of the distribution system in terms of average duration of interruptions of one consumer per year while SAIFI is measured as average frequency of interruptions for one consumer per year. SAIDI is generally expressed in minutes or hours while SAIFI is unit-less. As observed from eqns. (5.1) and (5.2), a low value of SAIDI and SAIFI reflects reduced duration and frequency of interruptions, which implies higher quality and reliability of the power supply.

5.3 STATE-OF-THE-ART

The traditional DSO approach to improve reliability is to conduct periodic maintenance, which would entail inspection of distribution grid components to identify damage and fix it before outage occurs. The practice has disadvantages, as any device damage just after maintenance work will not be detected for a long time [11]. In addition, for distribution systems that are spread over wide geographic areas with thousands of components, the current practices have limited effectiveness. In the report compiled by Dutch DSO, Alliander, it is stated that traditional approaches took very long time to fix a cascading blackout, significantly pushing up its average outage duration [12]. DSO's are working

on developing new techniques but there is still a considerable lack of grid data analytics tools, which can utilize the existing grid monitoring infrastructure of the DSO's for providing better observability of grid operations.

In [13], modern techniques like FDIR and AMI have been used to improve grid reliability while shunt circuit breaker has been used in [14] for improving reliability of underground systems. Evaluation of the possible improvement of reliability indices is done by optimization of interrupter switch placement in [15] and by dividing the network in sections, with each section as a function of parameters in [16]. Severe weather related constraints have been considered in [9, 17] to gauge the effect on reliability indices and to plan improvements. Techniques like fault incidence matrix determination in [6], weighted-consecutive-system estimation in [18], data driven approach for estimating failure modes in [19] and network automation in [20] have been used to better evaluate the reliability of the system to find deficiencies. Monte-Carlo simulation based methods have been used in [4, 8, 21-25] and Markov models have been used in [26] to better evaluate the reliability of the distribution system for improved predictive maintenance.

The functionality of most of the techniques and methods discussed above does not take into the account the effect of failure anticipation on improvement of reliability indices. As the famous adage goes, *prevention is better than cure*, FADS implementation also aims to improve reliability indices by preventing failures. The two most critical characteristics for any technique used for improving reliability indices are *early detection* and *accurate localization*. FADS implementation in earlier chapters has highlighted both of the above-mentioned characteristics. In this chapter, the use of these characteristics for the possible improvement of reliability indices is demonstrated on the numerous test cases simulated in Chapter 3 and Chapter 4 of this thesis.

5.4 POSSIBLE IMPROVEMENT OF RELIABILITY INDICES

In this section, the extent of possible improvements in the reliability indices via FADS implementation is estimated and calculated. In order to provide a better overview of FADS effectiveness, an attempt has been made to quantify the improvements in reliability indices due to FADS implementation. Apart from helping to anticipate failures, FADS also helps to reduce the search area for locating the event causing waveform distortions. The search area reduction helps in reducing the span of the grid the maintenance teams would have to scan to locate the event. Hence, the time saved can be utilized by the maintenance teams to conduct preventive maintenance and reduce overall outage duration. Identifying the zone where the event causing distortions is located will help in isolating the consumers in other zones. Hence, early warning of impending failure in a system also helps DSO to limit the number of customers suffering from disconnection of electricity. The two features of outage duration and number of customers affected are directly proportional to SAIDI and any reduction in the value of these features will result in proportionate reduction in SAIDI.

Effective preventive maintenance based on accurate inputs from FADS operation would also help in reducing the frequency of outages in long term, which would eventually help in improving SAIFI. However, it is practically impossible to know how

frequent interruptions would have occurred because of non-anticipation of failures. Hence, the improvement in SAIFI cannot be quantified as such in this thesis. Nevertheless, it can be safely assumed that early detection or anticipation in test cases where conventional protection systems underperform will result in reducing the number of outages, which would imply that a reduction of SAIFI could be achieved.

Practically, SAIDI is calculated after the failure has led to an outage and the time taken to fix the outage has been calculated. Hence, the calculation of SAIDI is not possible when the outage is yet to occur but the anticipation of failure by FADS would help in preventive maintenance and restricting the interruption of electricity to few consumers. However, it can be easily assumed that for the majority of cases the time needed for preventive maintenance and the consumers affected would be much less than that of an outage.

In order to estimate the impact of FADS on indices, the search area reduction is quantified in terms of percentage of total length of the distribution grid. However, search area reduction will not always translate to similar reduction in outage time duration as limited interruption of electricity would be needed to conduct preventive maintenance. Similarly, it is difficult to estimate the accurate number of consumers affected. Hence, to translate better the search area reduction to SAIDI reduction, a *Weighting Factor* is used to calculate a realistic positive effect of FADS implementation on SAIDI.

5.4.1 Length and Loading of Benchmark Systems

As mentioned before, in this thesis the benchmark distribution systems, IEEE-13 and IEEE-34 node test feeders [27] have been used. As detailed in [27-28] and also listed in detail in Appendix A of this thesis, the total length of IEEE-13 node feeder is 8200 feet. Converting it to metric system would give us approximately 2.5km of length. The figure was arrived at by summing up the length between different nodes. Similarly, for the long distribution system of IEEE-34 node feeder, the length is calculated to be 308,114 feet or 93.91km. Similarly, the total active power loads in IEEE-13 node feeder combining the spot and distributed loads for all the three phases can be calculated at 3466kW. The estimation total active power loads for all the three phases of IEEE-34 node feeder is calculated at 1769kW.

5.4.2 Weighting Factors

The literature survey conducted during the research work yielded very limited information on comprehensive and validated techniques, which can help to quantify accurately the correlation of search area reduction to reduction in SAIDI. Hence, FADS employs novel parameters called weighting coefficients to effectively correlate and quantify search area reduction to SAIDI reduction. The two main factors governing SAIDI are the number of consumers affected and the duration of the outage. Hence, to estimate the effect of search area reduction on the two governing factors of SAIDI, the weighting factors are divided in two categories, WF_C and WF_T. WF_C is weighting factor to estimate the reduction in number of consumers affected and WF_T is for estimating the savings in outage time duration. The weighting factors are based on certain assumptions and are limited to the test cases discussed in this thesis.

Two assumptions are made for estimation of WF_C. The first assumption is that sectionalizer switches are positioned according to the grid zoning proposed in FADS. Sectionalizer switch is used as a protective device to isolate a section of the distribution system. Therefore, if a failure happens downstream in single feeder radial systems, the upstream section of the distribution system can be isolated and need not be de-energised. Hence, if sectionalizer switches are placed in the distribution grids discussed in this thesis, it would be easy to isolate the consumers in affected section and reduce the numbers of consumers affected. For example, in both IEEE-13 and IEEE-34 node test feeders, Zone 2 can be isolated without affecting Zone 1 but since both IEEE-13 and IEEE-34 are single feeder radial systems, Zone 1 cannot be isolated without affecting Zone 2. As per grid zoning proposed in this thesis, the sectionalizer for IEEE-13 node feeder will lie at the exact middle of the distance between the nodes 632 and 671. For IEEE-34 node feeder, the sectionalizer will lie in middle of distance between the nodes 830 and 858. As per the length calculated from data in Appendix A, the sectionalizer will lie between nodes 854 and 852.

The second assumption made for WF_C is that the active power loads are evenly distributed among all the consumers. This will help in simplifying the calculation of affected consumers. For example, any reduction in search area from FADS implementation will help us to identify the zone, which needs to be isolated for preventive maintenance. Identifying the zone helps us to calculate the active power loading in that zone, which will be affected by power interruption. The active power loading in the affected zone can be calculated as percentage of the total active power loading of the particular distribution grid. Now, considering the earlier assumption that active power loads are evenly distributed among consumers, the percentage of active power loads affected can be directly correlated to percentage of consumers affected.

The assumption for WF_T is used to quantify the reduction in outage time. As discussed before, the preventive maintenance would invariably consume less time than an actual outage but there is little data to quantify such reduction. A study in [26] highlights that for 50% reduction in repair time for different equipment, the SAIDI savings were in the range of 0%-17%. The highest SAIDI reduction achieved in [26] was when the repair time of a critical equipment like transformer was reduced by 50%. Search area reduction would reduce time taken to locate event and consequently reduce the time taken to conduct preventive maintenance. Hence, for the test cases in this thesis, it is assumed that WF_T for outage time reduction would be 0.90 times the search area reduction (*implying a 10% reduction in outage time due to FADS*) for cases not involving damage to transformer and 0.85 for cases involving transformer.

The estimation of weighting factors are rudimentary in nature and used to get a realistic idea of SAIDI improvement in relation to search area reduction. Further studies, field investigations and cooperation with DSO's and utilities would be required to determine an accurate value for the weighting factors. Possibilities of false positive detection also needs to be considered for a balanced analysis of weighting factor and overall effectiveness of FADS in reduction of SAIDI. The main objective of the analysis conducted in this chapter along with the assumptions and considerations is not to claim

generality on the value of SAIDI reduction achieved due to FADS but instead to highlight that FADS would invariably help in improving reliability indices, mainly SAIDI.

5.4.3 FADS EFFECT ON RELIABILITY INDICES

In this section, it would be discussed how search area reduction achieved due to FADS implementation in the earlier chapters of this thesis can be used to estimate possible SAIDI reduction. Four test cases are discussed in detail, two simulation cases from Chapter 2 and two case studies from Chapter 4. The possible SAIDI reduction for the rest of the test cases discussed in this thesis is summarized and presented altogether in Table 5.1. The data from Table 5.1 is then used to calculate an overall average value of the possible SAIDI reduction achieved due to FADS implementation for the test cases in this thesis.

A. SIMULATION CASE II, SCENARIO B (*CHAPTER 3, HIF EVENT*)

This short transient simulation case and scenario discussed in detail in Chapter 3 had events of HIF, capacitor switching and load switching at close proximity in an IEEE-34 node feeder. It is important to distinguish the HIF event location from that of other events. In Table 3.2, it can be observed that the HIF is simulated at node 834 while the load and capacitor switching occurs at nodes 836 and 854 respectively in the IEEE-34 node feeder.

FADS along with the grid zoning managed to locate the event in Zone 2, which is between the area covered by the nodes 846, 858 and 862. Hence, in such a case, the length between the node segments 858 to switch position between nodes 854 and 852, 832 to 890, 858 to 864, 858 to 834, 834 to 848, 834 to 860 and 836 to 838 would have to be scanned by the maintenance teams of the DSO or utility. If the length encompassed between these nodes is summed up, the length is calculated to be 67,395 feet, which is approximately 20.54km. The search area reduction is around 78%. This reduced search area is in zone 2; hence, consumers in Zone 1 can be isolated. The total active power loading in zone 2 is around 1424kW, which is 80.5% of the total active power loads of the entire IEEE-34 node feeder. Therefore, based on assumption that active power load is equally distributed among consumers; around 80.5% of the consumers would be affected by preventive maintenance. Hence, the WF_C can be estimated at 0.805. Since, transformer damage is not considered, the WF_T is assumed at 0.9. Using these weighting factors, the possible SAIDI reduction is estimated at 10.5%. The quick detection of HIF in this case will prevent further damage and possible cascading into sustained outage that will reduce the frequency of interruption and help improve SAIFI.

B. SIMULATION CASE IV, SCENARIO A (*CHAPTER 3, HIF EVENT*)

This short transient simulation case and scenario discussed in detail in Chapter 3 has events of HIF, capacitor switching and load switching spaced out from each other in an IEEE-13 node feeder. As observed in Table 3.2, the HIF occurs at node 675 while the load and capacitor switching takes place at nodes 646 and 634 respectively in the IEEE-13 node feeder. Based on the FADS implementation results, it was concluded that a potentially harmful event has occurred in zone 2 between the areas covered by nodes 684 and 692.

According to FADS, the area to be searched by the maintenance teams would comprise of node segments 611 to 684, 684 to 652, 684 to 671, 671 to 680, 671 to 692, 692 to 675 and half the length between nodes 632 and 671. Summing up, the total length is calculated at 3900 feet or 1.18km. The search area reduction is calculated as 53%. This reduced search area is in Zone 2; hence, consumers in zone 1 can be isolated. The total active power loading in Zone 2 is around 2466kW, which is 76.9% of the total active power loads of the entire IEEE-13 node feeder. Therefore, based on assumption that active power load is equally distributed among consumers; around 76.9% of the consumers would be affected by preventive maintenance. Hence, the WF_C can be estimated at 0.769. WF_T is estimated at 0.9. Hence, the possible reduction in SAIDI is estimated at 30.5%.

C. CAPACITOR BANK SWITCH MALFUNCTION (CHAPTER 4, *EQUIPMENT FAILURE*)

This equipment failure event discussed in detail in Chapter 4 had a malfunctioning switch in a capacitor bank. The malfunctioning switch was the source of transients. The case study was inspired from a real-life equipment failure event. The manifestation of the transients was divided in three phases with the frequency of transient appearance increasing in each cycle. The event sequence can be seen in Table 4.2. The capacitor bank is connected at node 854 in IEEE-34 node feeder.

Unlike the previous simulation cases, this case study highlights the apparent underperformance of grid zoning concept of FADS. The event location leads to inconclusive reports from grid zoning results, which would make it difficult for the maintenance teams to determine which zone should be prioritized for searching. However, the LMD severity ratings in phase 2 of event sequence clearly indicates that the event location could be between the node segments monitored by measurement points at node 830 and node 858. The length of all node segments between nodes 830 and 858 would add up to 104040 feet or approximately 31.7km, which would translate to search area reduction of around 66%. However, as per assumptions, the sectionalizer are placed as per grid zoning. Since, the area between the nodes 830 and 858 are not earmarked exclusively in one zone in the thesis, it would entail that electricity would have to be interrupted to all consumers for preventive actions. Accordingly, WF_C would be 1 and WF_T would be 0.9. These weighting factors would entail a possible 10% reduction in SAIDI.

One major observation that can be drawn from this case study is that the grid zoning of IEEE-34 node does not exactly define the zone classification for area covered between nodes 830 and 858. Hence, LMD level severity ratings need to be utilized, when an event occurs in such areas. Therefore, it can be concluded that DSO's should be more careful how they interpret the LMD and Grid Zone severity ratings and frame some guidelines for that.

D. TRANSFORMER INTERNAL FAILURE (CHAPTER 4, *EQUIPMENT FAILURE*)

This equipment failure event discussed in detail in Chapter 4 was regarding an internal fault developing in the transformer over time due to moisture seeping from a damaged

bushing. The incipient failure starts generating transients and within a span of 25 minutes, a permanent fault takes place. The case study was inspired from a real-life equipment failure event. The manifestation of the transients was divided in two phases with the frequency of transient appearance increasing in each cycle. The event sequence can be seen in Table 4.3. The transformer between nodes 633 and 634 of IEEE-13 node feeder is modelled as damaged for this case study.

FADS implementation along with the grid zoning managed to locate the event in Zone 1 from the reporting of the first event sequence phase. The reporting's from phase 2 helps in further search area reduction to locate the incipient failure event but since phase 1 reporting's are meant to be the trigger to dispatch maintenance teams, the area spanned by zone 1 needs to be considered. Hence, in this case study, the maintenance teams would have to focus in the area between the node segments 646 to 645, 645 to 632, 632 to 650, 632 to 633, 633 to 634 and half the length between nodes 632 and 671. The area adds up to be 4300 feet, which is approximately 1.3km. That would entail to search area reduction of 48%. However, as the failure has happened upstream, there is no way consumers downstream can be supplied electricity. Hence, WF_C would be 1. In this case study, the FADS implementation helps to detect the incipient failure in a transformer. Hence, WF_T would be 0.85. Accordingly, the possible SAIDI reduction is calculated at 15%. An observation that can be made is that the zones containing expensive equipment like the transformer can be given special attention or designation for improved reliability of grid operations.

TABLE 5.2
POSSIBLE SAIDI REDUCTION ACHIEVED FOR SELECTED CASES (*SUMMARY*)

Simulation Case/ Case Study	Search Area Reduction	WF_C	WF_T	Possible SAIDI Reduction
Simulation Case II, Scenario A (*Chapter 3, HIF event*)	**63.7%**	**1.0**	**0.9**	**10%**
Simulation Case II, Scenario B (*Chapter 3, HIF event*)	**78%**	**0.805**	**0.9**	**27.5%**
Simulation Case IV, Scenario A (*Chapter 3, HIF event*)	**53%**	**0.769**	**0.9**	**30.5%**
Simulation Case IV, Scenario B (*Chapter 3, HIF event*)	**53%**	**0.769**	**0.9**	**30.5%**
Simulation Case V, Motor Starting (*Chapter 3, HIF event*)	**53%**	**0.769**	**0.9**	**30.5%**
Simulation Case VI, Feeder Energization (*Chapter 3, HIF event*)	**53%**	**0.769**	**0.9**	**30.5%**
Underground Cable Failure (*Chapter 4, Equipment Failure*)	**53%**	**0.769**	**0.9**	**30.5%**
Capacitor Bank Switch Malfunction (*Chapter 4, Equipment Failure*)	**66.2%**	**1.0**	**0.9**	**10%**
Transformer Internal Failure (*Chapter 4, Equipment Failure*)	**48%**	**1.0**	**0.85**	**15%**
Lightning Event (*Chapter 4, Equipment Failure*)	**63.7%**	**1.0**	**0.9**	**10%**

AVERAGE POSSIBLE SAIDI REDUCTION → *22.50%*

5.4.4 OBSERVATIONS

The test cases discussed in this thesis involving HIF detection and equipment failure anticipation included varied failure conditions, simultaneous switching events, different time frames and distribution networks. Based on the assumptions made, the summary of possible SAIDI savings for all the test cases in this thesis due to FADS implementation is estimated at an average value of 22.50%. Such a considerable reduction in SAIDI would greatly enhance the reliability of power supply and provide economic benefits. The use of weighting factor and special considerations of certain equipment adds more realism to the achieved SAIDI reduction value.

The real field SAIDI reduction achieved due to FADS implementation will be affected due to field conditions and constraints, which cannot be emulated in laboratory conditions but overall conclusive observations can be made that FADS implementation would eventually lead to lower SAIDI values. Considering the savings attributed to even 1% reduction in SAIDI value in [2], it can be said that FADS implementation would possibly lead to a more reliably power supply and considerable cost savings. The average reduction in SAIDI value achieved in the analysis conducted in this chapter maps closely to the marked improvement of SAIDI values shown in Figure 1.2 of Chapter 1. The marked improvement in the Figure 1.2 was seen as a positive effect of a technological jump. Hence, it can be said that FADS implementation provides for such a technological jump, which is also the aim of this thesis.

5.5 CONCLUSIONS

In the previous chapters, the utility of FADS as failure anticipation tool was highlighted in detecting HIF event and anticipating equipment failure cases where conventional protection schemes failed. One major need to anticipate failures is to prevent interruptions and outages and maintain reliable power supply. Hence, in order to quantify and better evaluate the tangible benefits of FADS implementation, the analysis of possible realistic improvement in the reliability indices is necessary. The main contribution of this chapter is to conduct such analysis and quantify the possible FADS implementation benefit in context of improvement of reliability indices.

The effect on grid operations from failures in different sections of the grid would vary based on a host of factors. Hence, in order to have a realistic analysis, weighting factors were used. The weighting factors were correlated to active power load in the grid and the perceived reduction in outage time duration with few assumptions and considerations. The results obtained show that a considerable reduction in SAIDI can be achieved due to FADS implementation. Anticipating failures or identifying undetected harmful events in the grid helps to reduce unwanted interruptions and outages, which would also significantly improve SAIFI. Even though further studies and optimization approaches would be needed to better quantify the impact of FADS on reliability indices, the analysis conducted in this chapter clearly highlights the beneficial effect on reliability indices.

REFERENCES

[1] R. Allan and R. Billinton, "Probabilistic assessment of power systems," in *Proceedings of the IEEE*, vol. 88, no. 2, pp. 140-162, Feb. 2000.

[2] M. Kruithof, J. Hodemaekers and R. Van Dijk, "Quantitative risk assessment; A key to cost-effective SAIFI and SAIDI reduction," *CIRED 2005 - 18th International Conference and Exhibition on Electricity Distribution*, Turin, Italy, 2005, pp. 1-5.

[3] 6th CEER Benchmarking Report on the Quality of Electricity and Gas. Supply Ref: C16-EQS-72–03 CEER Brussels July 2016. [Online]. Available: https://www.ceer.eu/eer_publications/annual_reports/

[4] N. Balijepalli, S. S. Venkata, C. W. Richter, R. D. Christie and V. J. Longo, "Distribution system reliability assessment due to lightning storms," in *IEEE Transactions on Power Delivery*, vol. 20, no. 3, pp. 2153-2159, July 2005.

[5] California Public Utilities Commission, Decision 96-09-045, Sep. 4, 1996. [Online]. Available: https://docs.cpuc.ca.gov/publishedDocs/

[6] C. Wang, T. Zhang, F. Luo, P. Li and L. Yao, "Fault Incidence Matrix Based Reliability Evaluation Method for Complex Distribution System," in *IEEE Transactions on Power Systems*, vol. 33, no. 6, pp. 6736-6745, Nov. 2018.

[7] IEEE Guide for Electric Power Distribution Reliability Indices," in IEEE Std 1366-2012, vol., no., pp.1-43, 31 May 2012.

[8] G. T. Heydt and T. J. Graf, "Distribution System Reliability Evaluation Using Enhanced Samples in a Monte Carlo Approach," in *IEEE Transactions on Power Systems*, vol. 25, no. 4, pp. 2006-2008, Nov. 2010.

[9] K. Alvehag and L. Soder, "A Reliability Model for Distribution Systems Incorporating Seasonal Variations in Severe Weather," in *IEEE Transactions on Power Delivery*, vol. 26, no. 2, pp. 910-919, April 2011.

[10] A. Sundaram, "Distribution Reliability Trends and Correlations," EPRI, Tech. Rep. TR-1010658, Nov. 2005.

[11] J. A. Wischkaemper, C. L. Benner, B. D. Russell and K. Manivannan, "Application of Waveform Analytics for Improved Situational Awareness of Electric Distribution Feeders," in *IEEE Transactions on Smart Grid*, vol. 6, no. 4, pp. 2041-2049, July 2015.

[12] Annual Report 2018. Alliander N.V. 2018. [Online]. Available: https://www.alliander.com/content/uploads/dotcom/Alliander_Annual_Report_2018.pdf

[13] Y. P. Agalgaonkar and D. J. Hammerstrom, "Evaluation of Smart Grid Technologies Employed for System Reliability Improvement: Pacific Northwest Smart Grid Demonstration Experience," in *IEEE Power and Energy Technology Systems Journal*, vol. 4, no. 2, pp. 24-31, June 2017.

[14] M. Gonzalez, "Improvement of SAIDI and SAIFI reliability indices using a shunt circuit-breaker in ungrounded MV networks," *22nd International Conference and Exhibition on Electricity Distribution (CIRED 2013)*, Stockholm, 2013, pp. 1-4.

[15] R. Billinton and S. Jonnavithula, "Optimal switching device placement in radial distribution systems," in *IEEE Transactions on Power Delivery*, vol. 11, no. 3, pp. 1646-1651, July 1996.

[16] G. Levitin, S. Mazal-Tov, and D. Elmakis, ‘‘Reliability indices of a radial distribution system with sectionalizing as a function of network structureparameters,’’*Electr. Power Syst. Res*., vol. 36, no. 2, pp. 73–80, 1996.

[17] Y. Zhou, A. Pahwa and S. -. Yang, "Modeling Weather-Related Failures of Overhead Distribution Lines," in *IEEE Transactions on Power Systems*, vol. 21, no. 4, pp. 1683-1690, Nov. 2006.

[18] K. K. Kamalja and K. P. Amrutkar, "Computational Methods for Reliability and Importance Measures of Weighted-Consecutive-System," in *IEEE Transactions on Reliability*, vol. 63, no. 1, pp. 94-104, March 2014

[19] H. A. Khorshidi, I. Gunawan and M. Y. Ibrahim, "Data-Driven System Reliability and Failure Behavior Modeling Using FMECA," in *IEEE Transactions on Industrial Informatics*, vol. 12, no. 3, pp. 1253-1260, June 2016.

[20] H. Hajian-Hoseinabadi, M. Hasanianfar and M. E. H. Golshan, "Quantitative Reliability Assessment of Various Automated Industrial Substations and Their Impacts on Distribution Reliability," in *IEEE Transactions on Power Delivery*, vol. 27, no. 3, pp. 1223-1233, July 2012.

[21] Z. Shu, P. Jirutitijaroen, A. M. Leite da Silva and C. Singh, "Accelerated State Evaluation and Latin Hypercube Sequential Sampling for Composite System Reliability Assessment," in *IEEE Transactions on Power Systems*, vol. 29, no. 4, pp. 1692-1700, July 2014.

[22] R. Billinton and Peng Wang, "Teaching distribution system reliability evaluation using Monte Carlo simulation," in *IEEE Transactions on Power Systems*, vol. 14, no. 2, pp. 397-403, May 1999.

[23] L. Goel, "Monte Carlo simulation-based reliability studies of a distribution test system", *Elect. Power Syst. Res.*, vol. 54, no. 1, pp. 55-65, Apr. 2000.

[24] N. Balijepalli, S. S. Venkata and R. D. Christie, "Modeling and analysis of distribution reliability indices," in *IEEE Transactions on Power Delivery*, vol. 19, no. 4, pp. 1950-1955, Oct. 2004.

[25] R. Billinton and W. Li, Reliability Assessment of Electric Power Systems Using Monte Carlo Methods, New York: Plenum, 1994.

[26] M. Al-Muhaini and G. T. Heydt, "A Novel Method for Evaluating Future Power Distribution System Reliability," in *IEEE Transactions on Power Systems*, vol. 28, no. 3, pp. 3018-3027, Aug. 2013.

[27] K. P. Schneider *et al*., "Analytic Considerations and Design Basis for the IEEE Distribution Test Feeders," in *IEEE Transactions on Power Systems*, vol. 33, no. 3, pp. 3181-3188, May 2018.

[28] IEEE PES AMPS DSAS Test Feeder Working Group. [Online]. Available: https://site.ieee.org/pes-testfeeders/resources/

CHAPTER 6

FIELD DATA ANALYSIS

6.1 INTRODUCTION

It is imperative for any failure anticipation technology to be tested and validated on real field data. However, access to field data is often restricted and not readily available. In light of such limitations, FADS validation studies in previous chapters are conducted by implementing FADS on test cases simulated in real time environment. The test cases were designed such that the realism of transient occurrences and phenomena are preserved as observed in real field data documented in various articles. However, field data analysis became possible as Stedin B.V; one of the leading DSO in the Netherlands provided failure data recorded by its IEDs in different sections of the grid. In this chapter, the field data is analyzed where conventional protection system operated very late and could not prevent an incipient failure from developing into a permanent fault. The objective of this chapter is to highlight how FADS implementation would have prevented a permanent failure in real-field application.

6.2 FIELD DATA ANALYSIS

The field data provided for FADS implementation is from a 10kV feeder network from a section of the distribution grid located near Utrecht in the Netherlands. The incipient failure develops over a short time to a permanent fault triggering a conventional relay.

6.2.1 DATA CONSTRAINTS

The conventional monitoring practice for recording fault data depends mainly on the relay setting done by the user. Usually, a relay can record disturbance in waveforms when the starting function is activated. Depending upon relay settings, relays can record for some time before the failure occurs like for a relay setting of 5s and 20% steady- state, the relay would record 60ms pre-failure. However, most utilities lack a comprehensive failure anticipation mechanism and relay settings are not utilized for recording pre-failure events. Hence, utilities are interested to know how quick and efficient the relay performed after it picked up the fault. Even with advent of IEDs, which have a greater recording and monitoring potential, utilities barely use it for failure anticipation purposes. In the data available from Stedin relays, there is a sequence of recordings in which the relay picks up some abnormal behavior and after a few milliseconds, the trip action takes place. Since, the relay picks up some abnormalities before actual trip, few milliseconds of incipient failure recording is available where relay still did not trip even though the

The data for this chapter was provided by Stedin B.V.

signatures of incipient failure were there. It can be easily stated that the signatures of incipient failure would have ideally existed for a longer timeline but since there is no current policy to record them, FADS implementation in this thesis for field data analysis would be limited to the few milliseconds of incipient failure signatures available.

6.2.2 ADAPTING FADS PARAMETERS

Since it was not possible to conduct threshold determination studies on the real feeder network, an attempt was made to extrapolate FADS thresholds by corresponding it with voltage rating. As observed in Chapter 2, the threshold values increased slightly for IEEE-34 node feeder in comparison to IEEE-13 node feeder. The logical assumption for such an occurrence could be that the voltage rating of IEEE-34 node feeder is almost six times of that of IEEE-13 node feeder. Higher voltage levels might be more sensitive to interruptions leading to higher and sustained distortions. Since the voltage level of 10kV is almost in middle of the voltage ratings of IEEE-13 and IEEE-34 node test feeders, the threshold parameter for FADS has been modified to the mean value of the difference between the thresholds of the two test feeders. Hence, the LMD level threshold becomes around 5.6% of samples distorted in one cycle when the waveform is sampled at 128 samples per cycle. Since, we have data recording from only one IED, we do not consider the DS-Grid Zone level thresholds. The severity rating table remains the same with no new addition of alert levels.

6.2.3 FIELD EVENT SEQUENCE

The evolvement of incipient failure to permanent fault is explained in three consecutive data sequences as available from field recordings. The line-to-line voltage recordings are mainly used for FADS implementation as they are the least distorted of the all the signals recorded. The choice of the voltage recordings for FADS implementation follows the approach used in the thesis to have stringent test of FADS performance. In order to correlate the voltage distortions with current magnitude changes, the line-to-line current signals are also shown. The first data sequence can be seen in Figure 6.1. The line voltage and current waveforms are observed with a timeframe of 0.35s. The changes in current magnitude and the visible distortions of voltage waveforms indicate abnormalities. The relay actions below indicate that the relay does sense and picks up some abnormalities but there is no fulfillment of the rest of the actions in order to trigger the tripping command. In Figure 6.2, the next sequence of recordings can be observed. The timeframe is around 0.5s. There are still visible distortions in both the current and voltage waveforms indicating signs of incipient failure. At a certain juncture towards the end of the current waveforms, the current magnitude goes down briefly to rise again. Such an occurrence could be the intermittence characteristic of a HIF. The relay again picks up the abnormalities but it is not sufficient to force a trigger action. The next and last sequence of recordings can be seen in Figure 6.3 in sequence 3. The timeframe of this sequence is around 1.3s. It can be observed that current magnitude increases dramatically indicating that the incipient failure has developed into a permanent fault. The increase in current magnitudes leads the relay to finally trip.

The entire sequence of events lasts for approximately 2.15s. As observed in this constrained dataset, the two-second duration of incipient failure signatures are from the

end stage of pre-failure period as the relay trips around 2s and a permanent fault occurs. The relay action analysis shows that relay was able to sense some abnormalities but the relay tripped only after the permanent fault occurred.

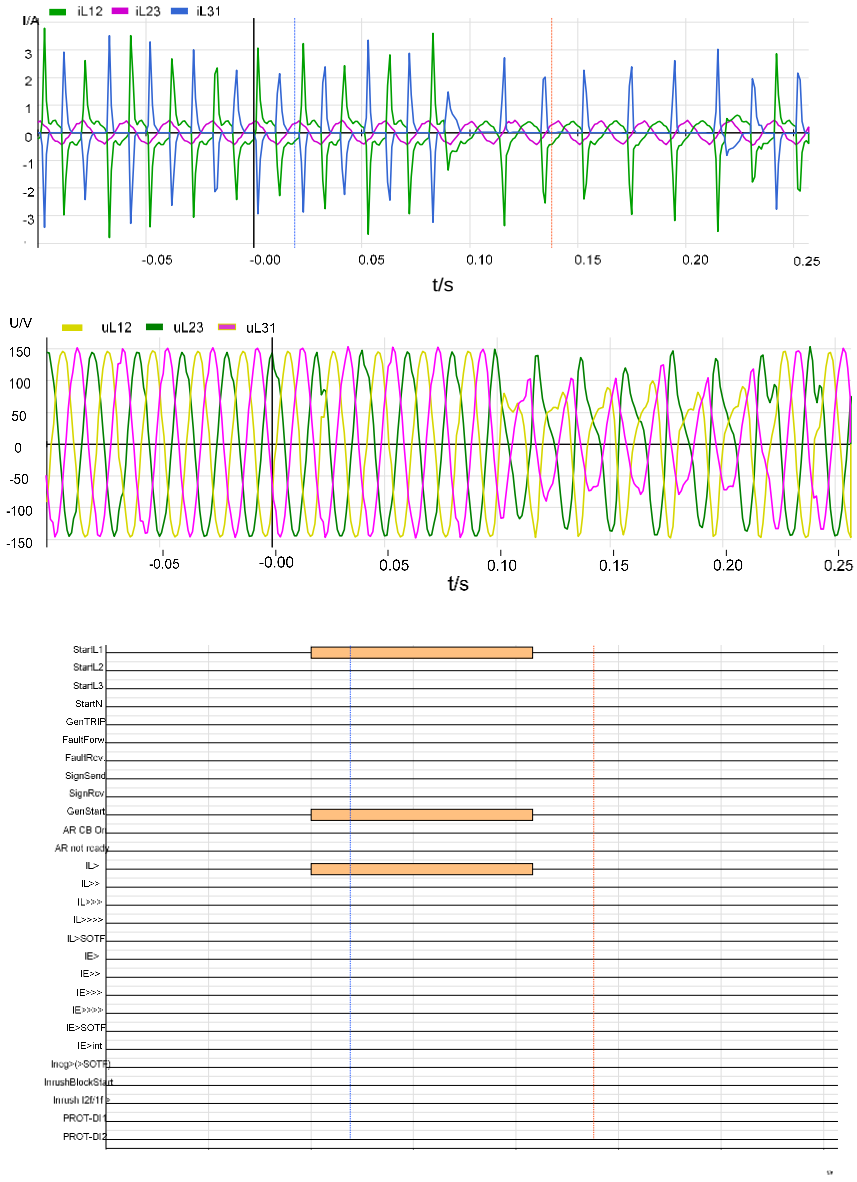

Figure 6.1: Field data voltage and current waveform distortions with associated relay actions - *Sequence -1*

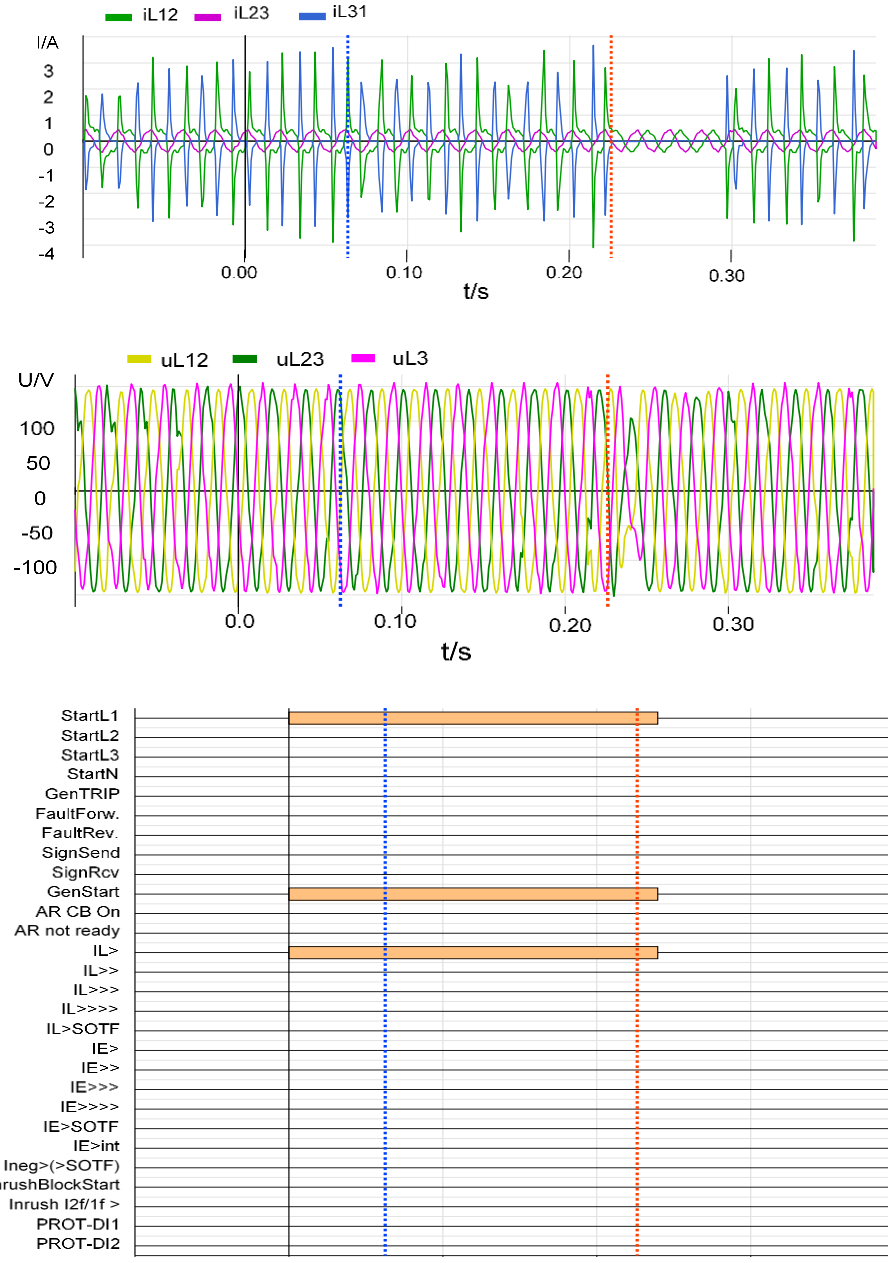

Figure 6.2: Field data voltage and current waveform distortions with associated relay actions - *Sequence -2*

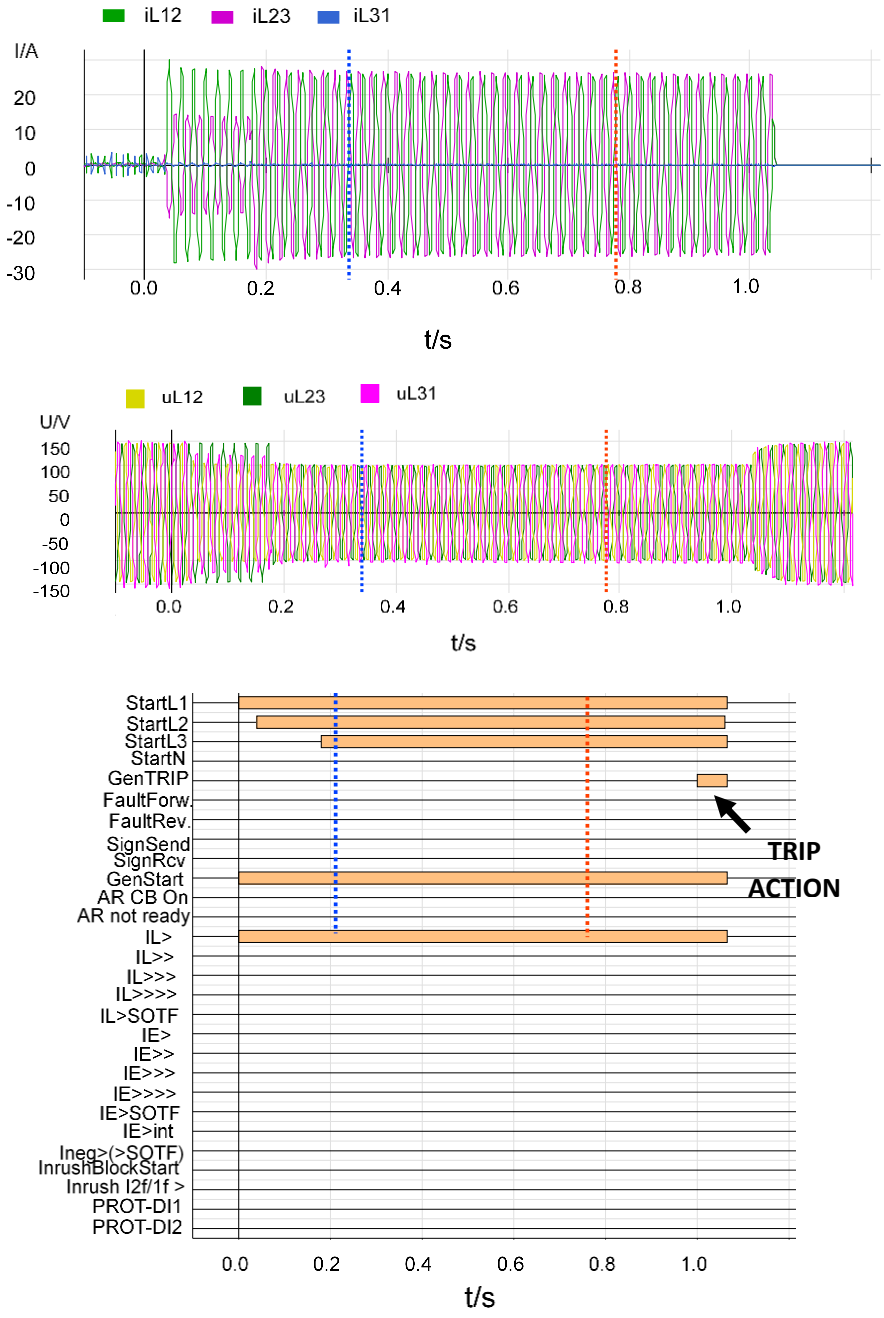

Figure 6.3: Field data voltage and current waveform distortions with associated relay actions - *Sequence -3*

6.2.4 FADS ANALYSIS

The entire voltage waveform consisting of the different sequences with duration of around 2.15s can be seen in Figure 6.4. Using the 0.1s as the reporting interval, as used for other simulation cases, there would be roughly 22 reporting periods with FADS implementation. However, for sake of clarity and representation, we divide the severity rating also in three sequences as observed previously. Accordingly, sequence 1 would have four reporting periods, sequence 2 would have five reporting periods, and sequence 3 will have thirteen reporting periods. The FADS analysis is done for all line-to-line voltages of phases A–B, B-C and C-A. The instances of severity ratings for different live voltages for each of the field data sequences can be observed in Figure 6.5.

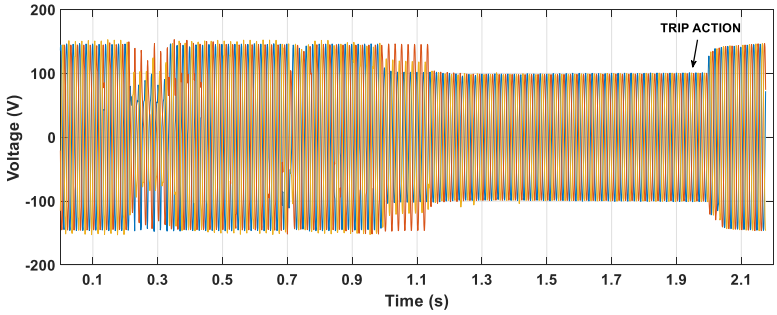

Figure 6.4: Continuous Line-to- Line voltage waveform combining all the three field data sequences from Stedin (*Phase B-C*).

The FADS implementation results for the field data show that there is single level 2 reporting for the phase B-C in sequence 1 while for other line voltages there is single reporting for level 1 each. In sequence 2, all the three line voltages have level 1 reporting only but phase B-C has two instances of it while in sequence 3, phase B-C has the single level 1 reporting. Even though primality it looks like that the information is not sufficient to draw definitive conclusions, it can be said that something is amiss in phase B. The single level 2 reporting should be reason enough for caution. The stable nature of line voltages is one reason why distortions are low and even a single level 2 reporting should be taken more seriously. Even though the duration is few seconds before the relay actually trips, taking sequence 1 level 2 severity rating alert as primary indicator, the incipient failure might have been mitigated or controlled before the trip action.

The data available for this analysis was the last few seconds of the pre-failure period. It can be said that with a greater duration of incipient signatures, more refined information could have been obtained from FADS implementation. Nonetheless, the FADS implementation results on the field data can be taken as a practical proof of concept of how real time FADS implementation can help in detecting incipient failures where conventional protection schemes underperform.

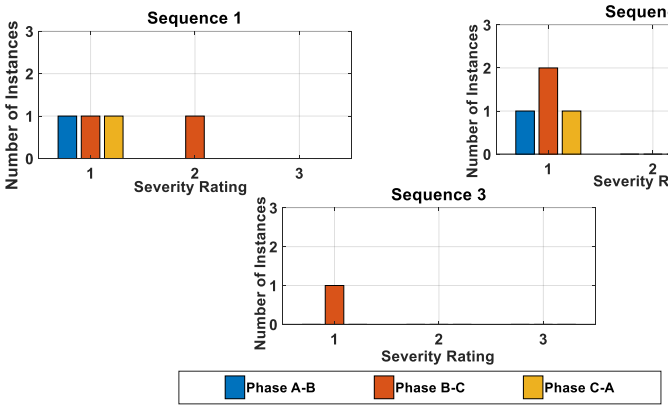

Figure 6.5: Instances of different Severity Rating levels for different sequences of field data analysis.

6.3 CONCLUSIONS

In this chapter, the result of FADS implementation on field data is discussed. Even though the data had some constraints and FADS parameters could not be normalized to the actual grid system in question, results indicate that FADS manages to sense and raise a cautionary alarm that the grid might be affected by some harmful event in the grid. The availability of continuous data during online FADS deployment would have helped FADS to better assess the distortions and raise appropriate severity levels for efficient response by maintenance teams.

The analysis conducted in this chapter provides a basic but fundamental proof of FADS applicability in real field situations. FADS performance is comparable to the results obtained in previous chapters. However, the available field data is not enough to draw a generalized conclusion of FADS effectiveness in real-field situations. Numerous further field data based investigations are needed across different situations and conditions so that FADS parameters can be modified and adapted to the utility needs and requirements before FADS can be adopted as an industry standard for detecting incipient failures.

CHAPTER 7

CONCLUSIONS AND RECOMMENDATIONS

7.1 THESIS CONCLUSIONS

The importance of reliable power supply for both utilities and consumers has been highlighted in the first chapter of this thesis. The current protection schemes are able to achieve reliability requirements to a large extent but the world is moving fast to more complex and interconnected power systems, bringing with it new challenges and technological and operational requirements. Reliability is rooted in the fact that there are no unwanted interruptions or fluctuations. In order to ensure fewer interruptions, there is a need to move a step forward from the current practice of reacting to a failure to anticipating a failure. Taking a step forward in realistic terms would require innovative approaches and intelligent algorithms, which can significantly improve our situational awareness of grid operations. Improved situational awareness will help to anticipate failures and act faster to preserve the reliability of power supply. The research work conducted in this thesis provided for foundation of such an innovation by proposing FADS as a failure anticipation technology to be implemented in distribution systems. The various properties and technological requirements of any comprehensive failure anticipation technology should usually include affordability, flexibility, ease of installation and wide application across different test cases. These properties and requirements are modelled as research objectives for FADS to fulfill in order to prove itself as a comprehensive failure anticipation technology.

As cited by several articles, there is currently a lack of comprehensive failure anticipation technology. Some available technologies are either not sufficient or too restricted in their application. The FADS presented in Chapter 2 aims to fills this research gap. The use of waveform distortions in electrical signals is motivated as the prime indicator of any abnormality in the grid operations. The various functionalities and data analysis process of real time FADS implementation is divided in different stages so that raw measurements from grid can be refined systematically to extract actionable knowledge from it. The waveform distortion detection functionality of FADS is based on certain mathematical approaches, which contributes to its efficiency and robustness. The use of such mathematical approaches as explained in Chapter 2, to detect incipient failure signatures are novel and were not implemented before the research work of this thesis. Several new concepts and terminologies backed by studies like Monte-Carlo trials are

introduced in data processing stages of FADS to make the entire process simpler, faster yet robust in nature. The data processing stage combines several observations like threshold violations, coordinated monitoring and impact indicators as means to improve observability and understanding of power system transients. This enhanced understanding of power system transients eventually helps to detect and locate incipient failures. The low computational burden of FADS implies less resource cost. Additionally FADS is designed as such that it can be easily programmed in commercial digital relays or IEDs already installed in the for grid monitoring. These features emphasize the affordability and ease of installation aspects of FADS. The novel concepts and parameters used in data processing are easy to calculate and implement and are largely dependent on certain user requirements. Hence, FADS functionalities can be adapted as per the user need, which proves the flexibility aspect of FADS.

The application of FADS in realistic test cases in this thesis commences with use of FADS to detect HIF in Chapter 3. HIF is typically a low current failure event that remains mostly undetected by conventional protection schemes. Even though HIF phenomenon is a result of an already occurred failure, from detection perspectives, the HIF event has considerable overlaps with incipient failure. FADS application included stringent evaluation of its performance in detecting and locating HIF events across different scenarios involving simultaneous occurrences of normal grid events. FADS was found to be robust enough to differentiate and detect HIF for both small transient and long transient events. FADS was also found to be robust to false positives and false negatives. Sensitivity test of FADS performance to different HIF patterns further highlighted the consistency of FADS performance. Overall, it can be claimed that FADS was able to avoid false flags and detect HIF in all test cases. However, some underperformance of the grid zoning concept was observed in few test cases but the overall veracity of several other novel concepts of the data processing feature of FADS was established by successful detection of HIF events along with accurate indications of severity and location of the event.

The next stage of FADS performance evaluation involved application in equipment failure scenarios in Chapter 4. Equipment failure scenarios were based on real life incidents where failure to detect an accelerating equipment failure finally led to a permanent fault. The test cases were designed to mimic the nature and frequency of transient appearances as observed in real life. FADS was applied to detect those incipient failure signatures and provide actionable input before the ultimate breakdown of the equipment. In all cases, FADS implementation managed to provide actionable inputs for probable action by maintenance teams much earlier than the eventual equipment breakdown would have happened. FADS performance was consistent throughout for all the test cases with differing timelines and phenomena. Similar to observations in Chapter 3, the grid zoning concept was found to be slightly affecting the FADS performance but overall the inbuilt failsafe features helped to FADS perform at expected levels.

The positive results of FADS implementation in different test cases needed to be translated in actual benefits in context of reliability of power supply to evaluate better FADS implementation benefits. In Chapter 5, the savings in time to locate the event occurrence due to input from FADS results are used to estimate the possible improvement

of reliability indices. Weighting factors regulated by realistic assumptions and considerations is introduced and used to convert FADS performance results into probable realistic improvement in SAIDI. The results obtained indicate an average reduction of 22.5% in SAIDI values. Such a reduction would lead to considerable improvement in reliability indices. If these probable savings are extrapolated, they will closely resemble the red curve shown in Figure 1.2 of Chapter 1. The red curve in that image quantifies the possible positive effect of technological jump on reliability of power supply. Hence, it can be concluded that FADS implementation would act as an enabler of such a technological jump direly needed for stable operations of modern power distribution systems.

Finally, in Chapter 6, the FADS is implemented on field data obtained from a DSO. Even with the restrictions and constraints involved with the data analysis, the results obtained highlight the perceived FADS implementation advantages in practical real field conditions. The analysis conducted in Chapter 6 is very crucial to emphasize that FADS is effective not only in laboratory-based simulations but can be also implemented in field conditions with positive results.

The primary objective of the research work done in this thesis was to develop a comprehensive failure anticipation technology. The effectiveness of FADS was validated through different test cases and calculation of probabilistic improvements in power supply reliability. The results from field data analysis further enhance the reliability of FADS as a comprehensive failure anticipation technology that can be adopted as a standard. Designing FADS architecture and functionalities was a major challenge since FADS is intended to be easily adaptable to the utility environment without much material effort or incurrence of high costs. The use of waveform distortions for detecting incipient failure helped to develop resource efficient mathematical approaches to identify incipient failure signatures. The next set of challenges comprised of designing and modeling the various stages of data processing of FADS implementation. The stages were incorporated with different parameters and indicators in order to be comprehensive and to robust in approach. The different stages are designed to be implemented at device and control room levels, making it easy to adapt FADS.

The results obtained from FADS implementation confirm that the research objectives were fulfilled by the research work conducted in this thesis. However, certain shortcomings and underperformance of FADS was also observed. The shortcomings were from the perspective of grid zoning, which in few test cases did not produce the desired result. However, further optimization studies and collaboration with utilities can lead to systematic improvement in FADS. Even though in recent times considerable research work has been directed towards failure anticipation, FADS presents itself as a major failure anticipation technology aiming to fulfill a large research gap.

7.2 SCIENTIFIC CONTRIBUTIONS

The research work conducted in this thesis led to the following main scientific contributions:

- The thesis provided the framework and structure of a comprehensive failure anticipation technology in power distribution systems (FADS). The proposed use of different functional blocks provided a guideline to effectively transform raw grid measurements to meaningful information based on which specific actions could be taken to maintain grid reliability.

- The fundamental feature of incipient failure signatures was identified and a mathematical approach to leverage the waveform distortions to detect such signatures was determined.

- A set of novel parameters including impact indicators, thresholds and severity rating scales were determined to apply during data processing in order to correctly evaluate the damage intensity and impact potential in case the incipient failure develops into a permanent fault.

- The concept of grid zoning was proposed for better observability and monitoring of grid operations. The advantage of using grid zoning to accurately determine the locating of incipient failure was also demonstrated.

- FADS implementation for HIF detection and equipment failure anticipation in realistic test cases helped to evaluate and investigate the impact on stable grid operations. The potential underperformance of grid zoning in few cases was also identified.

- Application of FADS implementation results helped in quantifying possible improvement of reliability indices. The analysis helped to evaluate the positive effects of the proposed technological jump provided by FADS.

7.3 ANSWERS TO RESEARCH QUESTIONS

The research questions related to the research objectives of this thesis can be answered as follows:

Q1. *Would a shift towards development of innovative, intelligent and proactive protection schemes to anticipate failures lead to improvement in reliability of power supply?*

A1. Yes, based on the research work conducted in this thesis, it can be observed that FADS led to improvement in reliability of power supply. The analysis in Chapter 5 documents the positive effect of FADS on reliable power supply in the test cases discussed in this thesis. The possible improvement in reliability indices due to FADS for selected test cases is estimated at around 22.5%.

The development of FADS as presented in Chapter 2 is motivated by the need to develop innovative protection schemes to anticipate failures. The recent advancements in protection technology also further validate the point made in the research question as the global research focus has shifted to development of intelligent proactive protection schemes. In this thesis, through means of several varied test cases, it has been highlighted how FADS implementation helps in avoiding cascading failures and improving the reliability of power supply. Chapter 3 provides example of how HIF event, which goes mostly undetected normally, is detected by FADS in different conditions. Several examples of real world equipment failures has been provided in Chapter 4 to highlight how reactionary approach fails to detect incipient failures and act before the equipment breakdown occurs in contrast to FADS application results. Chapter 5 quantifies improvement in reliability of power supply for the different test cases and shows how significant improvement in reliability can be achieved with FADS implementation. The FADS implementation results of field data analysis of Chapter 6 further cements the fact that an innovative, intelligent and proactive protection scheme like FADS is the need of the hour.

Q2. *Can incipient failures be accurately detected in distribution grids in real time by applying waveform analytics in pre-failure period?*

A2. Yes, as observed in the test cases discussed in this thesis, FADS was able to successfully detect incipient failures and be insensitive to false positive and negatives. FADS functionalities technically rely on advanced waveform analytics and FADS utilizes the pre-failure period for its operation.

The state-of-the-art discussion in Chapter 2 shows how recent research has focused on detecting incipient failures with varying degree of success. Efforts have been made to either focus on specific equipment specific failure signatures or classify the signatures as PQ disturbances but a comprehensive technique was missing. Since, the incipient failure signatures do not usually lead to over-voltages or overcurrent, the failure anticipation techniques documented in literature rely on leveraging certain changes or variations in waveforms or phase angles. Analytical approach is the best way to implement such techniques. Similarly, in the FADS developed in this thesis, fundamental aspects of AC sinusoids have been identified and the violation of fundamental aspects has been linked to the waveform distortions. The mathematical approach to detect the distortions and subsequent data processing constitutes the waveform analytics. In Chapters 3, 4 and 5 the waveform analytics based approach of FADS implemented in pre-failure period accurately detects incipient failure events in real time.

Q3. *Which parameters, thresholds or ratings should waveform analytics leverage for a fast and accurate detection and economical implementation?*

A3. In order to detect accurately the incipient failures, the data processing feature of FADS takes help of several elements. As discussed in Chapter 2, the first stage of data processing after detection of the distortion involves comparing the distortions detected in a certain time interval to the thresholds determined by Monte-Carlo studies. The thresholds have been determined by factoring-in the effects of normal switching events in the grid. Hence, violation of thresholds would invariably indicate some abnormalities.

To enhance further the situational awareness of grid operations, the concept of coordinated monitoring was proposed which involved a two-tier grid monitoring system. The underlying factor behind such an approach was to take into account the non-uniform effect of events on grid operations. The two tier monitoring system complemented each other and helped to locate the event. A severity scale was proposed to further rate the severity of the impact of any event on grid operations. The severity scale helped to refine further the knowledge obtained from threshold violations. The different parameters, thresholds and ratings proposed in this thesis together worked in combination for fast and accurate detection of incipient failures. The robustness of the elements chosen and validation of the performance is evident from the implementation results in the Chapter 3-6. The user flexibility of all the elements so that FADS can adapt to any grid design or requirements lends additional credibility to FADS as a failure anticipation technology.

The distortion detection technique is based on mathematical approach of low computational burden and can be easily implemented/ programmed in current IEDs. Additionally, FADS does not require installation of new devices or hardware. FADS also does not cross-reference any database for its functioning that eliminates the need to collect data and manage the database. The current protection and monitoring infrastructure is enough to support FADS implementation. Hence, with minimal startup and running costs involved, FADS is highly economical in its implementation.

Q4. *Can such a failure anticipation technology help also to locate the event area for quicker response and mitigation and subsequent improvement in reliability indices?*

A4. The severity rating scale helps to rate the damage potential of any event affecting grid operations. The LMD level and DS-Grid Zone based severity ratings further helps to identify which areas or sections of the grid are affected the most. Hence, based on those inputs, the search area for maintenance teams to locate the exact point of event occurrence reduces considerably. This reduction in search area would help in better planning of coordinated mitigation strategies without losing time on scanning the entire grid to locate the event. The FADS implementation results in Chapter 3, 4, and the associated analysis in Chapter 5 further highlights these points.

The FADS acts as an early warning system by providing specific inputs on the severity and location incipient failures. Acting on this information, proactive actions can entirely mitigate the incipient failure before either it develops into a fault or the number of consumers getting affected by the fault can be reduced. Achieving the former would help

in reducing overall number of interruptions occurring in the grid, which will improve the SAIFI index. Achieving the reduction in number of consumers getting affected will help in reducing the customer minutes lost to outage and proactive actions possible due to FADS implementation will result in overall reduction in outage duration. Both of these reductions will help in improving the reliability indices of SAIDI and CAIDI. The results obtained in Chapter 5 clearly highlight the potential improvements in reliability indices due to FADS implementation.

Q5. *Can such a failure anticipation technology be validated across different test cases so that it can be adopted as a novel and comprehensive protection scheme to complement the conventional protection schemes?*

A5. The FADS was implemented in different tests cases and various challenging scenarios. Chapter 3 dealt with FADS application on HIF detection. HIF event often go undetected and can cause severe disruptions. FADS implementation involved detecting HIF in multitude of scenarios. The results indicated that FADS was successful in detecting HIF in exhaustive set of complex scenarios involving simultaneous switching events and for both small and long transients. Similarly, in Chapter 4 the FADS implementation was successful in detecting incipient failure signatures and identifying the event location for equipment failure scenarios of different types of equipment and with varying timelines. The test cases were simulated in two standard distribution systems with distinct properties, which further highlights the consistency of FADS implementation.

In summary, it can be claimed that the FADS proposed in this thesis has been evaluated across different stringent test cases. The results obtained validate the use of several novel concepts and parameters in FADS. These aspects along with the ease of implementation firmly puts FADS as an innovative and comprehensive failure anticipation technology, which can be seamlessly, integrated with conventional protection systems and complement their functioning. FADS in its entirety serves to establish as a template for development of future failure anticipation technologies.

7.4 RECOMMENDATIONS FOR FUTURE RESEARCH

The research work done conducted in this thesis to establish FADS as a foundation for further development of failure anticipation technologies has led to identification of several topics on which the future research should be based on so that systematic improvement of FADS can be achieved:

1. Further improvement of FADS novel concepts and identification of new parameters via additional field tests:

The determination of FADS thresholds via means of Monte-Carlo trials sets an important precedent for future failure anticipation technologies. However further work

should involve taking into consideration other normal grid events or phenomena while determining the thresholds. In FADS development in this thesis, the difference between thresholds determined for IEEE-13 and IEEE-34 node feeders were quite small. Future research should conduct studies on different distribution systems to investigate how the thresholds are proportionately dependent on voltage values, length of grid, number of feeders, sampling rate etc. so that a standardized system of thresholds determination could be achieved. The optimization of the length of time frame according to specific real field requirements is also important since a too small or too large time frame might compromise the detection sensitivity of FADS. The future work should also consider creating a provision for a error margin or allowance according to different field conditions to make FADS more comprehensive in its application. The severity rating scale proposed in this thesis is basic in nature. In collaboration with utilities, further research and field tests should be conducted to add new alert levels and sub-levels to streamline the process of adequate response planning by maintenance teams. Lastly, further research should also help in identifying and integrating new parameters deemed useful to augment the efficiency of FADS implementation but care must be taken to preserve the core FADS properties of low computational burden, wide applicability and ease of implementation.

2. Optimization studies for smart placement of measurement points:

In FADS, the concept of grid zoning helped to achieve better situational awareness of the grid. Grid zoning results helped in narrowing down the search area, which will expedite maintenance and support actions. However, as observed in some test cases, grid zoning was not always as effective as desired. Even though the efficacy of the concept of grid zoning is visible, further exhaustive optimization studies are needed, which can determine the exact placement of measurement points according to the grid topology for best observability. Such studies are resource intensive and require input from utilities. Future research can focus on such optimization studies to devise a strategy for smart placement of measurement points according to grid design and other requirements. However, one of the priority areas of such optimization study should be to strike a reasonable balance between possible costs incurred and balanced data collection.

3. FADS application in distribution grids with DER penetration:

In this thesis, FADS application studies for distribution grid with Distribution Energy Resource (DER) penetration could not be included mainly as it was outside the scope of the thesis. However, the world is steadily moving towards adopting renewable energy sources. The renewable energy sources have very different characteristics in comparison to conventional sources, which necessitates the use of inverters and rectifiers. However, the use of such power electronic devices brings with it new set of challenges and phenomena which can affect FADS performance. FADS should be thoroughly investigated in different types of distribution grids with varying percentages of DER penetration to identify what changes have to be made to make FADS into a universal failure anticipation technology.

4. Resiliency to Cyber-Security threats:

In recent times, cybersecurity threats have emerged as a major risk to power grid operations with several examples of blackouts caused by cyber-attacks. Most of the cybersecurity threats tends to avoid detection by conventional protection schemes in order to cause outages. A solution to defend against such cybersecurity threats would be to make the working of protection schemes dependent on several interdependent parameters. In such a scenario, even if one of the parameter functionality is compromised by cyber-attack, the dependency on other parameters will ensure that the system does not collapse. FADS has few layers of security attributed to strong interdependency of several parameters before a final judgement on the event causing distortions is made but further research could focus on making FADS more resilient to cybersecurity attacks. Collaboration with cybersecurity experts would be required to modify FADS to be more effective against cyber-attacks. Separate system of alert levels even if one of the parameter seems compromised so that entire grid does not fail can be one of the proactive steps.

5. Towards automated mitigation strategies:

A missing piece of FADS comprehensiveness is the associated mitigation strategies whenever an incipient failure is detected. However, it can be attributed to the fact that often the realistic mitigation strategies have to be based on certain ground realities and information on resources available. In absence of such information, any mitigation strategy will not be effective. Future research should focus on devising such strategies with utilities and try creating an automated approach for mitigation of incipient failures. The chain of actions would involve using the input of FADS to detect and locate the event and then automated decisions would determine what actions to take in order to mitigate the failure without human involvement. Such a practice can work well for less severe cases while in very severe cases, the DSO operator can be the fallback option for planning adequate mitigation strategy. Such future technological advancement will make FADS very independent, comprehensive and efficient failure anticipation and mitigation technology.

APPENDIX A

BENCHMARK TEST SYSTEMS

A.1 INTRODUCTION

The IEEE benchmark distribution test systems are used throughout all the chapter of this thesis for FAD implementation and evaluation of results. These benchmark test system comprise of IEEE-13 Node and IEEE-34 Node test feeders. The configuration data of these test feeders are explained in detail in this Appendix as documented by IEEE PES Distribution System Analysis (DSA) Subcommittee in [1].

A.2 IEEE-13 NODE TEST FEEDER

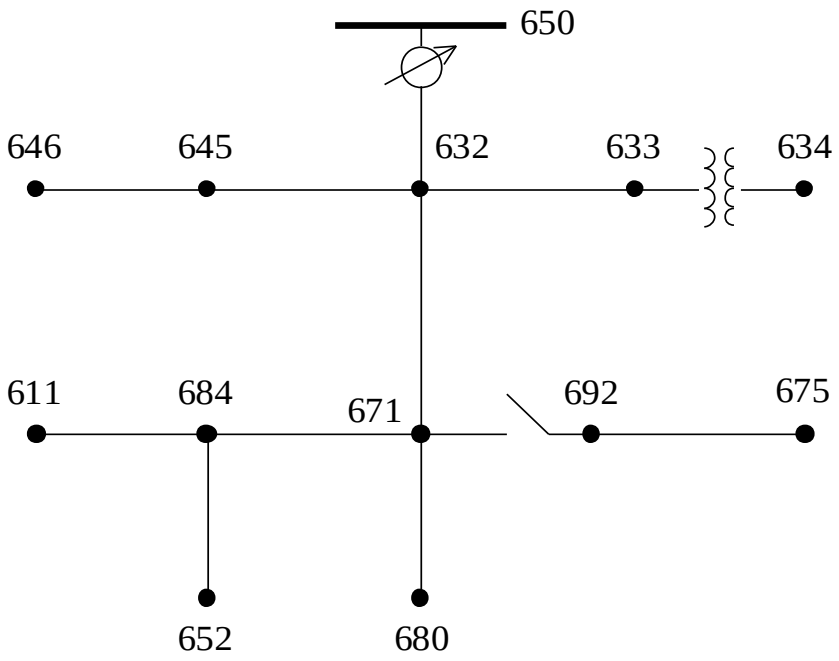

Figure A.1: IEEE-13 Node Test Feeder Layout

Table A.2.1: Overhead Line Configuration Data

Config.	Phasing	Phase	Neutral	Spacing
		ACSR	ACSR	ID
601	B A C N	556,500 26/7	4/0 6/1	500
602	C A B N	4/0 6/1	4/0 6/1	500
603	C B N	1/0	1/0	505
604	A C N	1/0	1/0	505
605	C N	1/0	1/0	510

Table A.2.2: Underground Line Configuration Data

Config.	Phasing	Cable	Neutral	Space ID
606	A B C N	250,000 AA, CN	None	515
607	A N	1/0 AA, TS	1/0 Cu	520

Table A.2.3: Line Segment Data

Node A	Node B	Length(ft.)	Config.
632	645	500	603
632	633	500	602
633	634	0	XFM-1
645	646	300	603
650	632	2000	601
684	652	800	607
632	671	2000	601
671	684	300	604
671	680	1000	601
671	692	0	Switch
684	611	300	605
692	675	500	606

Table A.2.4: Transformer Data

	kVA	kV-high	kV-low	R - %	X - %
Substation:	5,000	115 - D	4.16 Gr. Y	1	8
XFM -1	500	4.16 – Gr.W	0.48 – Gr.W	1.1	2

Table A.2.5: Capacitor Data

Node	Ph-A	Ph-B	Ph-C
	kVAr	kVAr	kVAr
675	200	200	200
611			100
Total	200	200	300

Table A.2.6: Spot Load Data

Node	Load	Ph-1	Ph-1	Ph-2	Ph-2	Ph-3	Ph-3
	Model	kW	kVAr	kW	kVAr	kW	kVAr
634	Y-PQ	160	110	120	90	120	90
645	Y-PQ	0	0	170	125	0	0
646	D-Z	0	0	230	132	0	0
652	Y-Z	128	86	0	0	0	0
671	D-PQ	385	220	385	220	385	220
675	Y-PQ	485	190	68	60	290	212
692	D-I	0	0	0	0	170	151
611	Y-I	0	0	0	0	170	80
	TOTAL	1158	606	973	627	1135	753

Table A.2.7: Distributed Load Data

Node	Node	Load	Ph-1	Ph-1	Ph-2	Ph-2	Ph-3	Ph-3
A	B	Model	kW	kVAr	kW	kVAr	kW	kVAr
632	671	Y-PQ	17	10	66	38	117	68

A.3 IEEE-34 NODE TEST FEEDER

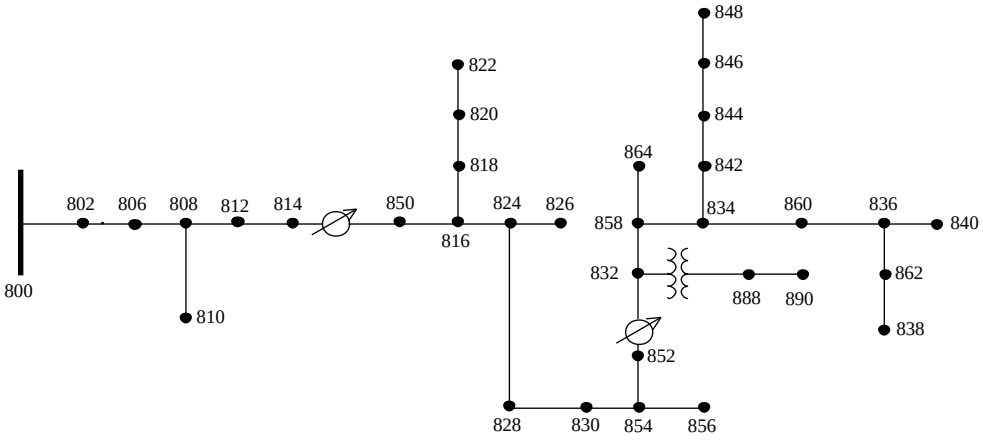

Figure A.2: IEEE-34 Node Test Feeder Layout

Table A.3.1: Overhead Line Configuration Data

Config.	Phasing	Phase	Neutral	Spacing
		ACSR	ACSR	ID
300	B A C N	1/0	1/0	500
301	B A C N	#2 6/1	#2 6/1	500
302	A N	#4 6/1	#4 6/1	510
303	B N	#4 6/1	#4 6/1	510
304	B N	#2 6/1	#2 6/1	510

Table A.3.2: Line Segment Data

Node A	Node B	Length(ft.)	Config.
800	802	2580	300
802	806	1730	300
806	808	32230	300
808	810	5804	303
808	812	37500	300
812	814	29730	300
814	850	10	301
816	818	1710	302
816	824	10210	301
818	820	48150	302
820	822	13740	302
824	826	3030	303
824	828	840	301
828	830	20440	301
830	854	520	301
832	858	4900	301
832	888	0	XFM-1
834	860	2020	301
834	842	280	301
836	840	860	301
836	862	280	301
842	844	1350	301
844	846	3640	301
846	848	530	301
850	816	310	301
852	832	10	301
854	856	23330	303
854	852	36830	301

858	864	1620	302
858	834	5830	301
860	836	2680	301
862	838	4860	304
888	890	10560	300

Table A.3.3: Transformer Data

	kVA	kV-high	kV-low	R - %	X - %
Substation:	2500	69 - D	24.9 -Gr. W	1	8
XFM -1	500	24.9 - Gr.W	4.16 - Gr. W	1.9	4.08

Table A.3.4: Capacitor Data

Node	Ph-A	Ph-B	Ph-C
	kVAr	kVAr	kVAr
844	100	100	100
848	150	150	150
Total	250	250	250

Table A.3.5: Spot Load Data

Node	Load	Ph-1	Ph-1	Ph-2	Ph-2	Ph-3	Ph-3
	Model	kW	kVAr	kW	kVAr	kW	kVAr
860	Y-PQ	20	16	20	16	20	16
840	Y-I	9	7	9	7	9	7
844	Y-Z	135	105	135	105	135	105
848	D-PQ	20	16	20	16	20	16
890	D-I	150	75	150	75	150	75
830	D-Z	10	5	10	5	25	10
Total		344	224	344	224	359	229

Table A.3.6: Distributed Load Data

Node A	Node B	Load Model	Ph-1 kW	Ph-1 kVAr	Ph-2 kW	Ph-2 kVAr	Ph-3 kW	Ph-3 kVAr
802	806	Y-PQ	0	0	30	15	25	14
808	810	Y-I	0	0	16	8	0	0
818	820	Y-Z	34	17	0	0	0	0
820	822	Y-PQ	135	70	0	0	0	0
816	824	D-I	0	0	5	2	0	0
824	826	Y-I	0	0	40	20	0	0
824	828	Y-PQ	0	0	0	0	4	2
828	830	Y-PQ	7	3	0	0	0	0
854	856	Y-PQ	0	0	4	2	0	0
832	858	D-Z	7	3	2	1	6	3
858	864	Y-PQ	2	1	0	0	0	0
858	834	D-PQ	4	2	15	8	13	7
834	860	D-Z	16	8	20	10	110	55
860	836	D-PQ	30	15	10	6	42	22
836	840	D-I	18	9	22	11	0	0
862	838	Y-PQ	0	0	28	14	0	0
842	844	Y-PQ	9	5	0	0	0	0
844	846	Y-PQ	0	0	25	12	20	11
846	848	Y-PQ	0	0	23	11	0	0
Total			262	133	240	120	220	114

REFERENCES

[1] K. P. Schneider *et al.*, "Analytic Considerations and Design Basis for the IEEE Distribution Test Feeders," in *IEEE Transactions on Power Systems*, vol. 33, no. 3, pp. 3181-3188, May 2018.

GLOSSARY

LIST OF ABBREVIATIONS

AC	Alternating Current
AMI	Advanced Metering Initiative
ANN	Artificial Neural Network
CAIDI	Current Average Interruption Duration Index
CAIFI	Current Average Interruption Frequency Index
DER	Distributed Energy Resource
DFA	Distribution Fault Anticipation
DGA	Dissolved Gas Analysis
DS	Distribution System
DSAS	Distribution System Analysis Subcommittee (*part of IEEE PES*)
DSO	Distribution System Operator
EPRI	Electrical Power Research Institute
FADS	Failure Analysis and Diagnosis Scheme
FDIR	Fault Detection, Isolation and Restoration
GE	General Electric
GOOSE	Generic Object Oriented Substation Event
HIF	High Impedance Fault
IED	Intelligent Electronic Device
IEEE	Institute of Electrical & Electronics Engineers
KLD	Kullback-Liebler Divergence
LMD	Local Measurement Device
MAIFI	Momentary Average Interruption Frequency Index
PES	Power and Energy Society (*part of IEEE*)
PQ	Power Quality
PQM	Power Quality Monitor

PSRC	Power System Relaying Committee
RTDS	Real Time Digital Simulator
SAIDI	System Average Interruption Duration Index
SAIFI	System Average Interruption Frequency Index
SEL	Schweitzer Electric Laboratories
SOM	Self-Organizing Map
UFLS	Under Frequency Load Shedding
UVLS	Under Voltage Load Shedding
TSO	Transmission System Operator
WAMS	Wide Area Measurement System
WF_C	Weighting Factor for reduction in consumers affected
WF_T	Weighting Factor for reduction in outage time

LIST OF SYMBOLS AND NOTATIONS

Chapter 2

A	Base window for smallest dataset
a_{base}	Initialization time instant for base window
a_r	Initialization time instant for dataset S_r
b_{base}	End time instant for base window
b_r	End time instant for dataset S_r
C_r	Data container
d_k	Distortion detection data at f^{th} sample
e	Base of natural logarithm
$g[k]$	Difference of sampled values at samples at k and $k-1$
h	Sample spacing interval
j	Imaginary unit
k	Sample number
N	Samples per cycle
m	Total number of IEDs

S_r	Dataset containing instances of distortions detected for r^{th} IED
$\widetilde{S_r}$	Curtailed dataset within size limits of base window
t	Time *(in seconds)*
t_k	Time stamp of f^{th} sample
T	Sinusoidal waveform time period
ω	Angular frequency (*in radians per second*)

Chapter 4

t	Time *(in seconds)*
t_a	Time constant to reach 30% of peak voltage value due to lightning
t_b	Time constant to reach 90% of peak voltage value due to lightning
$v(t)$	Voltage of the lightning strike
V_o	Initial voltage

ACKNOWLEDGEMENTS

The entire Ph.D. journey was one of the biggest learning experiences of my life. The journey had its fair share of ups and downs but it was a great opportunity to work with some of the most talented professionals. Working with them not only helped to improve my thesis work but also instilled in me an enhanced sense of professionalism. I met some wonderful colleagues during my time, some of whom have become lifelong friends. Without them, it would have been very difficult to face the tougher times of the journey. Finally, I dedicate this thesis to my parents. Their unwavering support and love kept me motivated throughout the journey.

The journey started with my promoter, Prof. Peter Palensky, offering me this wonderful opportunity in one of the best technological universities in the world. I cannot thank him enough and my deepest gratitude to him for having faith in my capabilities. His straightforward approach towards work and clarity of thinking always inspired me. Prof. Palensky was always very receptive of innovative ideas and his feedback was key to giving the final shape to my research work. The autonomy given by him helped me to become a better researcher. I would like to thank profusely my co-promoter, Dr. Milos Cvetkovic, whose consistent guidance and constant support helped me to improve my research work and publish innovative articles. The motivation and confidence provided by Dr. Cvetkovic helped me to face resolutely the difficulties encountered during research. My sincerest gratitude to my colleague, Jose Chavez Muro, without whom this thesis would not have been a reality. I will never forgot the endless hours we put together to combine our ideas and skills to produce some of the best research work. I have great admiration for Jose's humility and simplicity. I would like to thank Dr. Simon Tindemans for his time and valuable advice, which helped to improve key elements of my thesis. I would also like to thank Dr. Marjan Popov and Dr. Jose Rueda Torres for their help. I would like to thank all members of my doctoral examination committee members for their time and effort to evaluate the thesis. Their comments and feedback further enriched the quality of this thesis. It was a great honor to have my thesis reviewed by them. Finally, I would like to thank our superb departmental secretaries. Thank you Ellen, for being extremely kind and friendly in your approach towards many difficult issues. Ph.D. life was made considerably easier with Ellen's excellent and solid administrative support. I would like to thank Sharmila for always helping me out whenever I asked. I would also like to thank Carla for her help with all my recent dissertation formalities. I would like to extend my thanks to Diane and Margot for their timely approvals and clearances to all administrative issues. My special gratitude to Remko for bringing the much needed discipline and order in the RTDS lab. It was fun to interact with him.

During my Ph.D. journey, I was involved in the European Commission funded project, ERIGrid. It was a great learning experience and I met many academia and industry veterans. I would like to thank them all and especially, Thomas Strasser, for his exemplary project management. In TU Delft, I worked in the project alongside my colleague, Arjen. I would like to thank him for his help and support. Certain sections of the thesis were possible due to data provided by Stedin B.V. I would like to thank Ron Eerhard, Arjan

Voorden, Peter Buys and Marko Kruithof for their generous help and support for facilitating the collaboration with Stedin B.V.

This wonderful journey would not have been possible without friends and colleagues. Big cheers and thanks to Swasti, who has been a huge support for me in Delft. I have great memories of many fun moments we have shared together and he is someone, I can always rely on. Our inside jokes on old Indian television shows will never get old. Life in Delft would have been bland without his wisecracks. Great thanks to Yildiz who has been a great advisor and provider of delicious cakes during my thesis writing. Thanks for always encouraging me. I will miss our long gossip sessions on several evenings. My gratitude to Lian, my first office mate. Thanks for answering my umpteen questions. He is one of the most grounded person I have met. Lynn, it was a great pleasure knowing you. I am a big admirer of your sense of humor. Hossein, the Gent, has been a very dear friend. It was fun to spend time with him, especially discussing our stock market investments. Matija and Tina, it was a great experience to attend your wedding and my best wishes to young Mark. Matija has been a great friend and I would like to thank him for his suggestions during thesis writing. Katy, you are one of the most fun person I have met. Vinay, you are a great friend and your professionalism has always inspired me. Thanks for all your help, advices and especially, for translating the summary. Nakisa, I have great admiration for your determined fight against all odds, which always motivates me. Kaikai, your discipline and determination is something I try to emulate every day. Digvijay is one of the coolest colleague, I have ever met. It is difficult to see him not smiling, even when tensed. My two officemates, Arun and Claudio; life at TU Delft would have been boring without them. Arun, you are a very kind person and wish you all the success for future. Claudio, I will miss our long discussions on current affairs. Umer has been a great friend and a knowledgeable person to discuss complex world politics. My special thanks to Bart, Mario, Hazem, Aihui, Chenguang, Aleksander, Saeed, Nidarshan, Zameer, Arcadio, Ilya, Ajay, Aditya, Geetha and Prashant. The Ph.D. journey was made memorable by my two master students, Vetrivel and Kiran. They both have great potential and it was an absolute pleasure to guide them. I cannot wait to attend Vetrivel's defense ceremony soon.

The Ph.D. journey was complemented by many leadership positions held by me in different organizations. I will sorely miss my friends in the Ph.D. council, Yuki, Jacopo, Franziska, Chirag, Joeri, Christine and Sobhan. Jacopo, heartfelt thanks for proofreading my mathematical equations. It was a great learning experience in IEEE student branch and was fun working with Belma, Mladen and Shea. My thanks to colleagues in Young CIGRE: Luis, Aniket, Maui, Harish, Siddharth and Nikoleta.

Even though not present in Delft, my friends from different parts of the world have been a great source of confidence and emotional support for me. My brother from another mother, Animesh, has always helped me see things in perspective. His work ethics are pure class and his passion, wisdom and innovative spirit always keeps me motivated. Deepa, your effortlessness in doing the most complex things in the world inspires me a lot. Sky is the limit for you. Words cannot express the admiration I have for Meriem. A thorough professional, the way you have faced all odds is commendable. Thanks for being my rock in tough times and best wishes for young Rali. Amine, I wish we had met before. Never met such a calm, composed and sorted person in my life. Elena, you are the most pure and wonderful soul, I have ever met. Bassel, you were a constant source of positive energy for me. I could not have asked for a better friend. Rami, I had a great time with you and miss those intense political discussions we had during long walks. Mona, I have

never met such a cheerful girl in life. Your smile and optimism has infectious positive energy. Amardeep, my buddy since ages, I cannot thank you enough. Tanuj, your conviction and discipline is legendary and very inspiring. Anil, I will never forget some of our long conversations. I learnt some unique and logic defying truths about life from you. Teesta, it was great fun knowing you. Keep that energy alive. Salma, your intelligence and maturity belies your age. Good luck for future. Karim, thanks for being such a responsible and wonderful host at your sister's wedding. Hariharan, our bitcoin and political discussions will never end. Thanks for encouraging my stand-up comedy instincts. Zineb, it was great fun interacting with you, especially during the pandemic. Salman, cannot thank you enough for our intellectual and philosophical discussions. Hamada, even from Belgium your actions keep motivating me. Kartick, memories of your mimicries have kept me smiling on gloomy days. Avik, you are one person, whose guts I admire a lot. I had great fun with you. Abhinav bhaiya, you have been a constant source of inspiration from my undergraduate days. Thank you Benedetta for the great cover design. I would like express my sincerest appreciation and thanks to countless other people who have been in some form or way, instrumental to my Ph.D. journey.

Last but not the least, special thanks to my birth city of Kolkata (*formerly Calcutta*). The great intellectual spirit, sense of social justice, cultural diversity and political awareness of the city had a great effect on my upbringing. My scientific temperament has been largely shaped by the varied experiences and observations in the city. I would like to credit a great deal of my success to my beloved city of Kolkata.

Rishabh Bhandia
Delft, January 2021

BIOGRAPHY AND PUBLICATIONS

Rishabh Bhandia was born in Kolkata, India in 1989. He received his B.Tech degree in electrical and electronics engineering from Sikkim Manipal University, Sikkim, India in 2011 and his M.S. degree in smart grid and buildings from Grenoble Institute of Technology, Grenoble, France in 2015. January 2016 onwards, he started pursuing his Ph.D. degree at the Electrical Sustainable Energy department in Delft University of Technology, the Netherlands. During his Ph.D., he was also involved in the European Commission financed project, ERIGrid and collaborated with 18 other research institutions and universities in Europe.

His research interests include development of intelligent algorithm for failure anticipation and diagnosis in power distribution systems via real-time monitoring.

PH.D. PUBLICATIONS

1. **R. Bhandia**, J. d. J. Chavez, M. Cvetković and P. Palensky, "High Impedance Fault Detection Using Advanced Distortion Detection Technique," in *IEEE Transactions on Power Delivery*, vol. 35, no. 6, pp. 2598-2611, Dec. 2020.

2. **R. Bhandia**, J. J. Chavez, M. Cvetković and P. Palensky, "High Impedance Fault Detection in Real-Time and Evaluation Using Hardware-In-Loop Testing," *IECON 2018 - 44th Annual Conference of the IEEE Industrial Electronics Society*, Washington, DC, 2018, pp. 182-187.

3. **R. Bhandia**, M. Cvetković and P. Palensky, "Improved Grid Reliability by Robust Distortion Detection and Classification Algorithm," *2018 IEEE PES Innovative Smart Grid Technologies Conference Europe (ISGT-Europe)*, Sarajevo, 2018, pp. 1-6.

4. **R. Bhandia**, M. Cvetković, J. J. Chavez and P. Palensky, "Incipient equipment failure assessment and avoidance through robust detection technqiue," *Mediterranean Conference on Power Generation, Transmission, Distribution and Energy Conversion (MEDPOWER 2018)*, Dubrovnik, Croatia, 2018, pp. 1-6.

5. **R. Bhandia**, J. J. Chavez, M. Cvetković and P. Palensky, "Towards Improved Reliability Indices using Waveform Distortions in Distribution System," *2020 IEEE PES Innovative Smart Grid Technologies Europe (ISGT-Europe)*, The Hague, Netherlands, 2020, pp. 227-231.

OTHER PUBLICATIONS

1. Strasser, T.I., Pröstl Andrén, F., Widl, E. *et al.* An integrated pan-European research infrastructure for validating smart grid systems. *Elektrotech. Inftech.* **135,** 616–622 (2018).

2. S. Vogel *et al*., "Improvements to the Co-simulation Interface for Geographically Distributed Real-time Simulation," *IECON 2019 - 45th Annual Conference of the IEEE Industrial Electronics Society*, Lisbon, Portugal, 2019, pp. 6655-6662.

3. A. A. van der Meer *et al*., "Towards Scalable FMI-based Co-simulation of Wind Energy Systems Using PowerFactory," *2019 IEEE PES Innovative Smart Grid Technologies Europe (ISGT-Europe)*, Bucharest, Romania, 2019, pp. 1-5.

4. R. Bhandia et al., "D-JRA2.3 Smart Grid simulation environment", *The ERIGrid Consortium Deliverable D8.3*, Dec. 2018. [online] Available: https://erigrid.eu/dissemination/.

5. A. A. van der Meer, R. Bhandia, P. Palensky, M. Cvetković, E. Widl, V. H. Nguyen, ... & K. Heussen, (2020). Simulation-Based Assessment Methods. In *European Guide to Power System Testing* (pp. 35-50). Springer, Cham, 2020.

6. M. Cvetković, K. Pan, C. David López, R. Bhandia and P. Palensky, "Co-simulation aspects for energy systems with high penetration of distributed energy resources," *2017 AEIT International Annual Conference*, Cagliari, 2017, pp. 1-6.

7. M. Cvetkovic, H. Krishnappa, C. D. López, R. Bhandia, J. R. Torres, and P. Palensky. "Co-simulation and dynamic model exchange with consideration for wind projects." In *Berlin Wind Integration Workshop*, pp. 1-6. 2017.

8. P. H. Divshali, M. Laukkanen, R. Bhandia, A. A. Van der Meer, E. Widl, C. Steinbrink, A. Kulmala, and K. Mäki. "Smart Grid Co-Simulation by Developing an Fmi-Compliant Interface for Pscad." In *Proceedings of the 25th International Conference on Electricity Distribution (CIRED 2019)*, pp. 3-6. 2019.

9. E. Widl et al., "D-JRA2.1 Simulator coupling and Smart Grid libraries", *The ERIGrid Consortium Deliverable D8.1*, Apr. 2017, [online] Available: https://erigrid.eu/dissemination/.

10. T. I Strasser, E. C. W. de Jong, M. Sosnina, J. E. Rodriguez-Seco, P. Kotsampopoulos, D. Babazadeh, K. Mäki, R. Bhandia et al. "Achievements, experiences, and lessons learned from the European research infrastructure ERIGrid related to the validation of power and energy systems." *e & i Elektrotechnik und Informationstechnik* 137, no. 8 (2020): 502-508.